DETERMINATION OF PILLAR STRENGTH FROM KAMOTO ROOM AND PILLAR COLLAPSE BY NUMERICAL APPROACH

Nzenga Kongolo

A project report submitted to the Faculty of Engineering, University of the Witwatersrand, Johannesburg, in partial fulfilment of the requirements for the degree of Master of Science in Engineering.

Johannesburg, 1998.

DECLARATION

I declare that this project report is my own, unaided work. It is being submitted for the Degree of Master of Science in Engineering in the University of the Witwatersrand, Johannesburg. It has not been submitted before for any degree or examination in any other university.

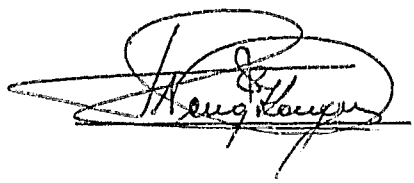

12nd day of MARCH 1998

DECLARATION

I declare that this project report is my own, unaided work. It is being submitted for the Degree of Master of Science in Engineering in the University of the Witwatersrand, Johannesburg. It has not been submitted before for any degree or examination in any other university.

_____

_____ day of _____ 1998

ABSTRACT

In September 1990, a section of Kamoto mine where two thick and superimposed ore bodies were being mined, using the room and pillar mining method operating in isolated blocks, experienced a large scale collapse. Pillars 15 meters long, 10 meters wide and 12 meters high in the upper ore body and 14 meters high in the lower ore body were left during mining of a block with 15 meter-wide-rooms. Due to the unstable nature of some pillars within the first mined blocks, a decision was taken to fill, partially or totally, the mined area with uncemented backfill. Unfortunately, this decision did not incorporate a re-evaluation of pillar strength in terms of rock mass classification encountered during the development stage of that mining method, hence the need to determine the pillar strength from the Kamoto room and pillar collapse.

This back-analysis of Kamoto pillar strength assessment involved a combination of several approaches in rock engineering such as the rock mass classification, rock mass strength and pillar stresses, and strength. The Bieniawski's geotechnical rock mass classification (1976) has been used to determine the Geological Strength Index (GSI) for each layer of the ore bodies. This concept, combined with the strength of intact rock and the Hoek-Brown failure criterion have been exploited to assess the rock mass properties, such as the strength, elastic modulus, Poisson's ratio, cohesion, friction angle and Hoek-Brown constants. These estimates are used as input data in the Kamoto room and pillar model.

The strength values of pillar have been determined by analytical method and numerical modelling. In the first approach, the strength of a cubical specimen of Kamoto rocks has been separately assessed by the procedure proposed by Ryder

and Ozbay (1990) and by the Rock Mass Index (RMI) developed by Palmstöm (1997). The modified Salamon's formula and Obert-Duvall formula for pillar design in the hard rock have been employed to assess the strength of pillar in the study area. In the second approach, an elastic boundary code named MinsimW has been performed to generate the elastic model of Kamoto room and pillar area from the real mine plans edited before the collapse, and to compute the mining induced stresses acting on the pillars. Under conditions assumed during this work, the numerical analysis reveals that the ultimate average stresses acting on the pillar edge at the beginning of the large scale failure mechanism are estimated at 35 MPa and 43 MPa in the upper ore body and the lower ore body respectively. It has been noticed that these values are abcut 2.7 times greater than those calculated by Salamon's formula and about 1.3 times greater than the strength values from Obert-Duvall formula.

To my family

ACKNOWLEDGEMENTS

This project achievement might not be possible if the following assistance was not available:

- I wish to thank the management of the company " La Générale des Mines et Carrières" (GECAMINES) for sponsoring my tertiary education.
- I thank Prof. M.U Ozbay, my supervisor for the orientation of this project and his endless encouragement.
- I am grateful to Mr Roger Johnson from CSIR / Miningtek for his advice in running the MinsimW program.

CONTENTS PAGE

PAGE

PAGE

PAGE

LIST OF FIGURES PAGE

LIST OF TABLES **PAGE**

LIST OF ABBREVIATIONS

ABS: Absolute value
σ_1 or SIG1: major principal stress
σ_2 or SIG2: intermediate principal stress
σ_3 or SIG3: minor principal stress
BOMZ: Black Ore Mineralised Zone
CAF: Cut And Fill mining method
Coh: Cohesion
CORxOBx: Coarse sheet On Reef [number] Ore Body [type]
CSIR: Council for Scientific and Industrial Research
D.Strat: Stratified dolomite (Dolomites Stratifiées)
FORxOBx: Fine sheet On Reef [number] Ore Body [type]
H/W: Hangingwall
F/W: Footwall
GCM: Générale des Carrieres et des Mines de la Républiique Démocratique du Congo
GSI: Geological Strength Index
IRS or Sigci: Intact Rock material Strength
Ktn: Kilotons
MinsimW: Mine simulation programme for Windows
MPa: Mega Pascal
NGI: Norwegian Geotechnical Institute
OBI: Lower ore body
OBS: Upper ore body
Phi: Friction angle
RAP: Room And Pillar mining method
RAT: Argillaceous dolomitic siltstone (Roches Argilo-Talqueses)
RGS: Dolomitic and argillaceous silstones (Roches Grésceuse Supérieures)

RMR: Rock Mass Rating system

RMR_{76}: Bieniawski's 1976 Rock Mass Rating

RQD: Rock Quality Designation

RSC: Massive dolomite (Roches Silceuses Cellulaires)

RSF: Silecous laminated dolostones (Roches Silicieuses Feuilletées)

SD: Dolomitic shales (Shales Dolomitiques)

SDB: Lower dolomitic shales (Shales Dolomitiques)

SF: Safety factor

Sigcm: Rock mass strength

SLC: Sub Level Caving mining method

SS: Upper dolomite (Shistes Supérieurs)

TXXH: Hangingwall stress in ore body strike direction

TYYH: Hangingwall stress in ore body dip direction

TZZH: Hangingwall stress in the direction normal to the ore body

UCS: Uniaxial Compressive Strength

CHAPTER 1

INTRODUCTION

1.1 Background

Kamoto mine is one of the underground mines that belong to the Congolese (ex-Zairian) State Company named "LA GENERALE DES CARRIERES ET DES MINES DU CONGO". It is located in the western part of the Shaba province (ex- Katanga / Zaire) about 10 Km from the town of Kolwezi. Access works were started in 1958 and real mining production (Copper 3.5 - 4.5 % and Cobalt 0.3 %) commenced in 1970, using Sub-level caving (SLC) and Cut and Fill mining (CAF) methods. The Room and Pillar (RAP) mining method was introduced in 1979 in order to mine the flat part of the ore-bodies. Trends in mining methods are shown in Fig.1.1 and Appendix A. From the beginning, Kamoto Mine thrived until September 1990, when large-scale instability occurred in the full-mechanised room and pillar workings below 465 m ... the two orebodies. This collapsed area is shown in Fig 1.2. Although there were no fatalities, the collapse caused severe damage and production losses.

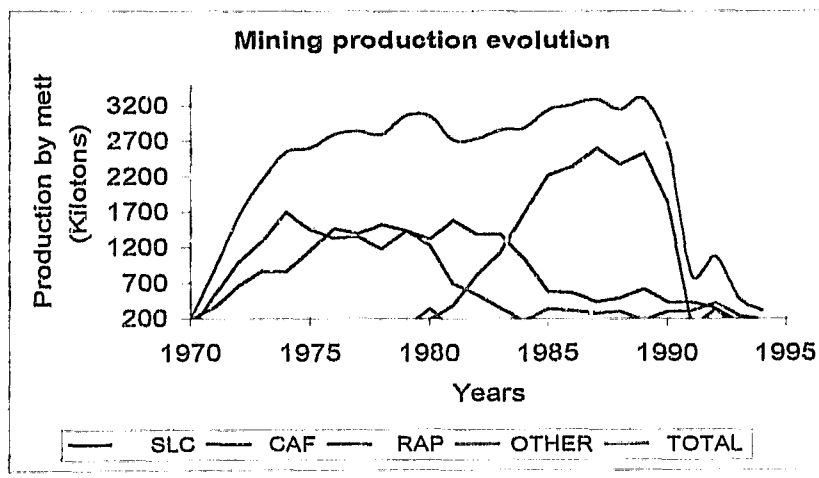

Fig. 1.1 Production by mining method

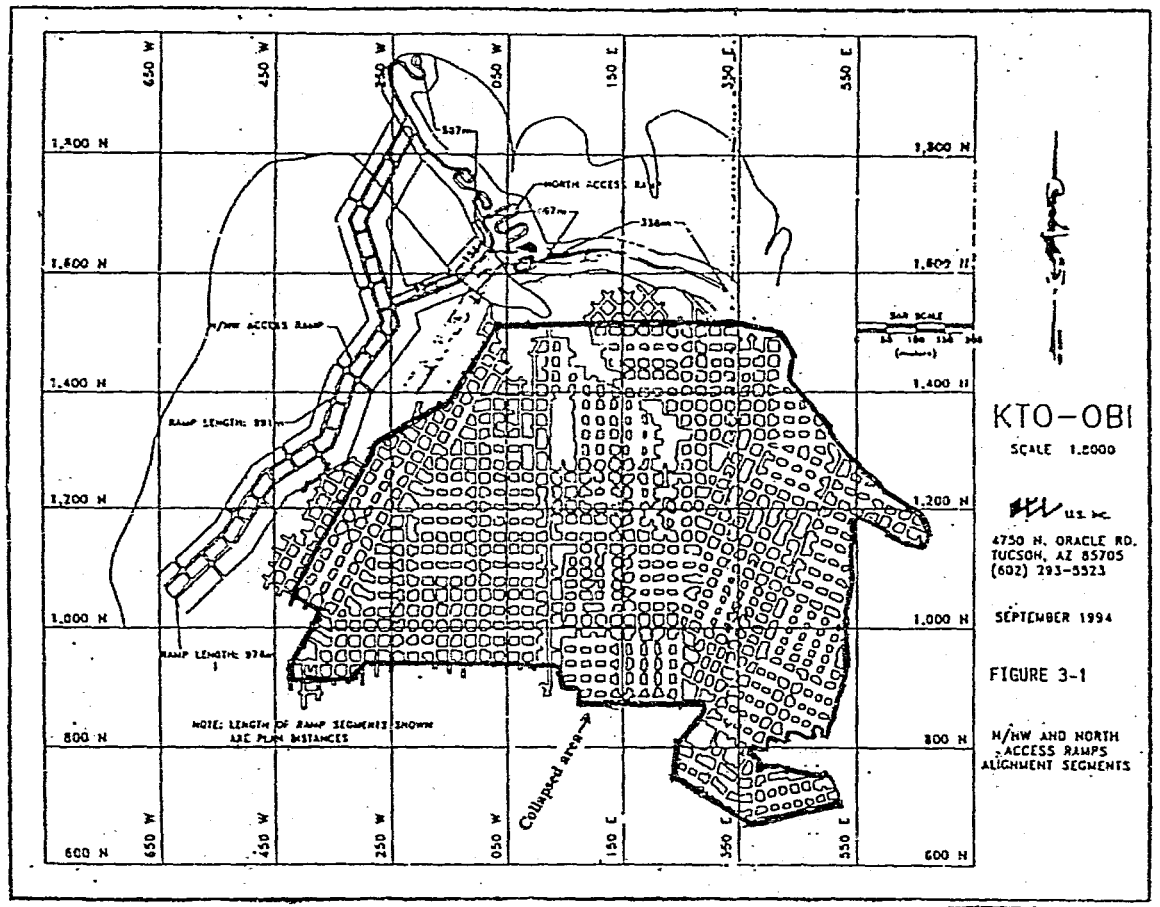

Fig.1.2 Kamoto collapsed area

The current room and pillar mining layout used at Kamoto mine appeared to have provided regional stability, although in 1990 the management noticed that all the area mined using the room and pillar method had been affected by instability. There were occurrences of intense seismic activity, pillar splitting and rockfalls. Furthermore, it was observed that some damage had occurred to service excavations, such as the underground crusher site and tne access ramps.

1.2 Purpose of the work

Provisional mine planning shows that in the near future, 80% of the available geological reserves will be mined by transverse cut and fill (59%) and room and pillar (21%) methods. Both these mining methods involve the design of pillars. Therefore, the main aim of this work is to determine the rock mass and pillar strength values from the collapse of the Kamoto Room and Pillar area in 1990. The approach adopted is to examine the system of pillar loading during the mining process in order to assess the failure strength of pillars at the time approaching the collapse. This empirically based value will be used for the future design of mining methods.

1.3 Methodology

In order to achieve the objective given above, the following methodology has been applied:

a) Literature of rock mass classification in general and review of Kamoto rock mass characteristics of the area of interest.

b) Review of pillar design methodologies as means to determine a natural stope support system in shallow depth mines.

c) Use of numerical modelling technique to simulate the mining process in space and time and to analyse the pillar loading system before the failure.

d) Determination of pillar strength values from analytical method and numerical analysis.

CHAPTER 2

LITERATURE SURVEY

2.1 Introduction

Many research attempts have been undertaken, in the laboratory, in situ and on historic collapse cases, to evaluate the strength of pillars. The objective was to define an efficient and safe size of pillar, taking into account the ground conditions. Despite these various efforts, more theoretical and experimental studies are still needed, particularly with respect to specific geological conditions, to understand the pillar behaviour and to establish rational pillar strength estimation. This chapter gives successively a succinct review of relevant literature concerning rock mass classification, pillar strength theory and numerical modelling techniques.

2.2 Rock Mass Classification

The quality of mine design and thus the stability of underground excavations depend on the accuracy of geological and geomechanical properties of rocks used for the design. However, the determination of these properties remains one of the most difficult topics in rock mechanics. ~~Different~~ empirical methods and techniques to classify rocks and rock masses are described in the literature cited at the end of this document. The most frequently used of geotechnical classifications for a variety of mine engineering purposes have been developed by different authors (Deere, 1964, Bieniawski, 1974 and 1976, Barton et al.1974, Laubscher, 1977). The purpose of this chapter is only to highlight in the following sections the most relevant elements of rock mass classification.

2.2.1 The NGI Tunnelling Quality Index or Q-Classification.

Barton et al. (1974) of the Norwegian Geotechnical Institute (NGI) developed a tunnelling rock mass classification scheme to estimate the quality of a rock mass (Appendix B). A relevant summary of this cumulative rating system is as follows:

a) **Rock Quality Designation (RQD)**: as developed by Deere (1964) to describe rapidly and quickly the rock quality from borehole cores. The rating changes between zero (very poor) and 100 (excellent).

b) **Joint Structure Number (Jn)**: this parameter describes the persistence of discontinuities in a rock mass. The rating changes between 0.5 (massive) and 20 (crushed rock)

c) **Joint Roughness Number (Jr)**: this number defines the discontinuity roughness. The rating changes between 0.5 (slickensided, planar) and 4 (discontinuous joints)

d) **Joint Alteration Number (Ja)**: this parameter describes the nature of filling material between the adjacent rock walls of discontinuities. The rating changes between 0.75 and 12.0 as shown in appendix .

e) **Joint Water Reduction Factor (Jw)**: this factor expresses the influence of groundwater pressure on the quality of rocks. Therefore, the rating changes from 1.0 (dry excavation or minor inflow) to 0.05 (exceptionally high inflow or pressure continuing without decay.)

f) **Stress Reduction Factor (SRF)**: this parameter describes the influence of weakness zones intersecting excavation and in situ

rock stresses which may cause loosening of the rock mass when tunnel is excavated. The rating varies from 2.5 to 20.0.

The overall of the above values gives the tunnelling quality index Q used for the classification:

$$Q = (RQD/Jn).\ (Jr/Ja).\ (Jw/SRF)$$

Tunnelling Quality index	Classification
< 0.01	- Exceptionally poor
0.01 - 0.1	- Extremely poor
0.1 - 1	- Very poor
1 - 4	- Poor
4 - 10	- Fair
10 - 40	- Good
40 - 100	- Very good
100 - 400	- Extremely good
> 400	- Exceptionally good

More recently, Palmström (1997) has developed the Rock Mass Index (RMI) to characterise the strength of a rock mass for rock engineering purposes. This concept is based on the Q-Classification system. It includes some parameters such as the joint roughness factor (Jr) and the joint alteration factor (Ja) as defined in the above rock mass classification. These parameters are shown in Appendix B. Nevertheless, in this concept the block volume represents the structure and the block size of the rock mass instead of the RQD and the joint set number (Jn). The uniaxial compressive strength of the rock mass is, therefore, expressed as follows:

$$RMI = \sigma_c \,.\, JP$$

Where σ_c is the uniaxial compressive strength of the intact rock,

JP is the jointing parameter that expresses the resulting effect of the joints in a volume of rock. It is calculated by this equation

$$JP = 0.2\,(JC)^{0.5}.\ V_b^{\alpha}$$

Where $\alpha = 0.37JC^{-0.2}$,

JC = JL . JR/JA,

JR is the joint roughness factor,

JA is the joint alteration factor and

JL is the joint size and continuity.

V_b is the volume of the rock block (m^3)

2.2.2 Bieniawski's Geomechanics Classification

Bieniawski (1976) modified his geomechanics classification for a jointed rock mass system from civil engineering data in sedimentary rocks, as shown in Appendix C. The basic classification parameters are:

a) **Strength of intact rock material**: the rating changes between 15 (UCS> 200 MPa) and 0 (UCS = 1-3 MPa) according to the ranges of uniaxial compressive strength values.

b) **Rock Quality Designation (RQD)**: as defined by Deere (1964) for the quality of core recovery by diamond drilling: the rating changes depending on the redefined ranges of values , between 20 (RQD = 90 -100%) and 5 (RQD< 25%).

c) **Spacing of joints (Js)**: this parameter describes all the discontinuities and the rating varies from 30 (Js > 3m)to 5 (Js < 0.05m) in function of the given ranges of joint spacing .

d) **Condition of joints (Jc)**: this parameter takes into account some geomechanical properties of discontinuities (aperture, roughness, wall condition, persistence and the nature of filling). The rating changes from 25 (very rough surface, not continuous, no separation, hard joint wall rock) to 0 (soft gouge > 5mm thick or joints open > 5mm, continuous joints).

e) **Groundwater condition:** this parameter gives the influence of water on the stability of an underground excavation. The rating changes from 10 (completely dry) to 0 (severe water problems).

The overall Rock Mass Rating (RMR) is given by the sum of the rating values assessed for each parameter. In relation to discontinuities' orientation (strike and dip), the RMR value can be adjusted. The adjustment rating for tunnels is between 0 (very favourable joints orientation) through minus 12 (very unfavourable joints orientation). From the RMR values, the Rock mass classes can be determined using the chart below:

Ratings	Class No	Description
100 - 81	I	Very good rock
80 - 61	II	Good rock
60 - 41	III	Fair rock
40 - 21	IV	Poor rock
< 20	V	Very poor rock

From this classification, Bieniawski (1976) gives approximate stand-up time of an unsupported excavation for each class.

2.2.3 Laubscher's Geomechanics Classification

For the purpose of mining applications, Laubscher (1977) up-dated Bieniawski's geomechanics classification in order to develop the mining rock-mass rating (MRMR) classification system. He used the same five

classification parameters as defined by Bieniawski, but he changed the range and rating systems of intact rock strength and the evaluation of joint spacing and condition of joint parameters. He divided each of the five rock mass classes into two sub-classes.

Before applying the rating values of the five basic parameters, an adjustment is carried out, taking account of the mining environment affecting the rock mass such as weathering, mining induced stresses, joint orientation and blasting effects (Table 2.1). It must be stressed that the adjustment procedure is empirical and requires a background based on numerous observations in the field.

Table 2.1 Summary of adjustments

Parameter	Possible adjustment
Weathering	30 - 100 %
Orientation of blocks	63 - 100 %
Induced stresses	60 - 120 %
Blasting	80 - 100 %

It is not unusual in mining practice to arrive at the situation that all the geotechnical data required for rock mass classification are not available due to technical or economic reasons. Under such circumstances, the different parameters for classification can be assessed in reference to a similar ground condition case. Consequently, the level of confidence should reflect the situation.

2.2.4 Discussion on rock mass classification systems

The aim of each rock mass classification is to provide a better understanding of the overall rock mass by providing a quantitative assessment of ground conditions. Each rock mass classification system described in this section was

successfully applied in the past for specific applications. However, the recent trend would be to establish correlation between different classification systems and to develop from their basic concept, new methods for evaluating of the rock mass strength for mining purposes.

The Q-classification, initially developed for rock mass classification for tunnels has recently provided a basis of the Rock Mass Index (RMI) for characterisation of the strength of rock mass. The Bieniawski's Rock Mass Rating (RMR) currently and widely used in civil engineering has been successfully practised in mining applications. The new concept of Geological Strength Index (GSI) for evaluating of the strength rock mass has been derived from the RMR system. The Q-Classification and the RMR systems use closely the similar parameters for evaluating the relative effects of geology and geometry of the rock mass for support requirements. The main differences between these systems are based on the weighted numerical values for each parameter and the use of compressive strength in the RMR system as a parameter.

Laubsher's geomechanics classification has been derived from Bieniaswski's classification in order to provide a Mining Rock Mass Rating system (MRMR). The differences between these two systems are the division of classes defined by Bieniaswki into subclasses, the evaluation of different parameters and the influence of mining environment. These differences give further advantages to this system in specific mining applications such as excavation support, stability of open stopes, fragmentation, ground cavability and mining methods.

2.2.5 Influence of geology on pillar stability

A number of authors emphasise the role of geological discontinuities or rock structure on pillar performance. The more the discontinuities the lower the pillar bearing ability. Subsequently, the most widely used rock mass

classification systems, described in this section, include some parameters with high rating values to describe discontinuities in the rock mass.

Brady and Brown (1985) stated that at shallow depth and in de-stressed areas the ground discontinuities might be the prime concern in excavation design. Jeremic (1987) reported similar observations in which pillar strength can decrease up to 50 % with the increase of continuous and discontinuous structural defects. Roberts and Jager (1993) found that, according to the size, the geological discontinuities weaken the pillar. Therefore, the correction factor can range between 0.2 and 0.5 of the laboratory uniaxial compressive strength. Hoek *et al.* (1995) confirmed that the behaviour of pillars depend on the characteristics of both the rock material and the discontinuities in the rock mass.

2.3 Pillar Strength Theories in Shallow Depth Mines

2.3.1 Categories of mine pillars in shallow mines

In coal or hard rock mining at shallow depth, pillars are used either as the main support for the roof strata or to protect surface structures.

According to Ozbay et al. (1994), there are four types of pillars having different stress / strain characteristics and these are shown in Fig. 2.1. A brief discussion on each of these pillar types is presented below:

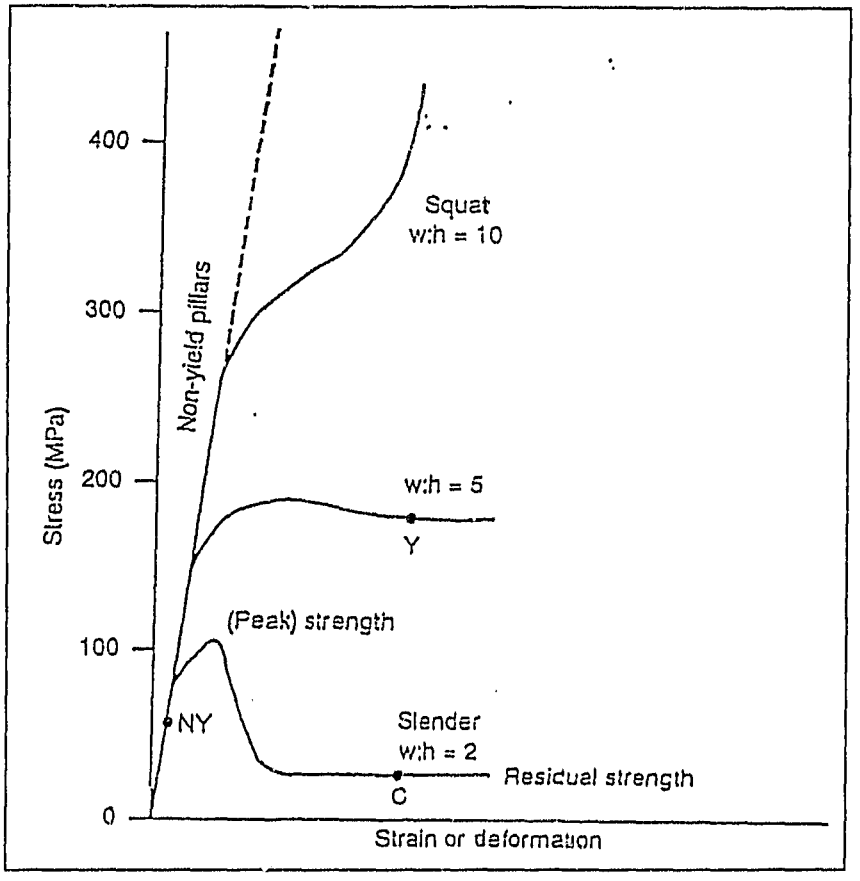

Fig. 2.1 Categories of mine pillars

a) **Non - yield pillars**: these pillars are supposed to remain intact and elastic during the life of the mine. This assumes that the strength of pillar should be higher than the average pillar stress due to the weight of country rocks. Esterhuizen (1993) indicated that the factors of safety of 1.3 to 2.0 are typically used in the hard rock pillar design.

b) **Squat or Barrier pillars**: these pillars with a width to height ratio of about 10, are essentially protective and used to provide a regional support of structures and mining

workings. Hence, they should remain stable during the mine life.

c) **Yield pillars**: these pillars are designed to be initially intact, but can yield in a stable manner as loaded beyond their peak strength as the mining progresses.

d) **Slender or Crush pillars**: these pillars with a small width to height ratio are designed to crush while either they are still part of the face or in the back area at shallow mining depth. Their post-peak residual strength provides sufficient support resistance to the immediate hangingwall.

2.3.2 Pillar strength and design

In the past, the rock mechanics research effort in the design of pillars was focused on coal mines. In pillar design, the most complex task is to estimate the rock mass strength, and thus the pillar strength due to the variability of the properties of rocks. It had been noticed at the earlier stage of rock mechanics that the uniaxial compressive strength of the intact rock was not enough to express the rock mass strength. Nevertheless, it remains one of the most important parameters in the majority of rock mass classification and pillar strength. Correlation of laboratory measured strengths to in situ values is important, because most design criteria are based on the rock strength. Unfortunately, in general terms, no single design approach or pillar strength formula has been accepted as reliable in hard rock pillar design.

This literature survey examines some empirical formulae:

- Evans and Pomeroy (1958), and Evans *et al.* (1961) found that the crushing strengths of coal cubes of various side lengths decrease with the side length of the cube. A mathematical expression of this relationship is as shown below:

$$\sigma_s = Ka^{\alpha}$$

Where σ_s : crushing strength

K: constant

α : 0.17 - 0.32 for various coals

- Protodiakonov (1964) proposes the following relation:

$$\sigma_d/\sigma_r = [(d/b) + m] / [(d/b) + 1]$$

Where σ_d : strength of a cubical specimen

σ_r : in situ strength of the rock mass

d : side length of a cubical specimen

b : average spacing of discontinuities in the rock mass

m : strength reduction factor. This value is selected as shown below:

σ_d	compression	tension
> 75 Mpa	2< m < 5	5< m < 15
< 75 Mpa	5 < m < 10	15 < m < 30

- Obert and Duvall (1967) derived the following formula from laboratory tests on hard rock and elasticity considerations for width to height ratio of 0.25 to 4.0:

$$\sigma_p = K (0.778 + 0.222 .w/h)$$

Where σ_p is the pillar strength,

K is the uniaxial compressive strength of a cubical specimen,

w is the pillar width and

h is the pillar height.

- Salamon and Munro (1967), after conducting a survey of stable and unstable pillars in South African coal mines, came up with the formula shown below to estimate the strength of coal pillar:

$$\sigma_s = Kh^{\alpha}w^{\beta}$$

Where σ_s: pillar strength

h : pillar height

w : pillar width

α and β : constants depending on the nature of coal deposits.

For South Africa Coal Fields, the statistical values are as follows:

α= -0.66 and β= 0.46

K: constant depending on the geostructure of the material.

- Subsequent work by Hedley and Grant (1972) recommended the above formula with α = - 0.75 and β = 0.5 for the most common hard rock pillar design.

- Laubscher (1990) proposed to use the Design Rock Mass Strength (DRMS) for constant K, in cases where a rock mass classification has been carried out. The DRMS is the strength of unconfined rock mass adjusted to the specific mining environmental conditions such as weathering, orientation of joints, mining in situ induced stresses, blasting effects.

- Hardy and Agapito (1977) took into account the scale effect between the laboratory specimen and the rock mass by using the following formula:

$$\sigma_p/\sigma_c = (V_e/V_p)^{0.118}\,[(L_p/H_p)(H_e/L_e)]^{0.833}$$

Where σ_p : pillar strength

σ_c : uniaxial compressive strength

V_p : volume of pillar

V_e : volume of laboratory specimen

L_p : pillar width

H_p : pillar height

L_e : specimen width (specimen diameter)

H_e : specimen length

- Ryder and Ozbay (1990) proposed a methodology for designing pillar layouts for shallow mines and introduced the correction factors to be applied to the laboratory value of UCS:

$$\sigma_s = UCS*f_1*f_2*f_3*f_4*f_5*f_6$$

Where UCS : Uniaxial compressive strength .

f_1 : size effect ; expressing the weakening effect of discontinuities' features. Experimental results from tests on rock have shown that there is, a strength reduction with increase from small size to critical size at which the strength values can be directly applicable to full size pillars (Fig 2.2). A size correction factor has been assessed at a value of 0.4 of the uniaxial compressive strength.

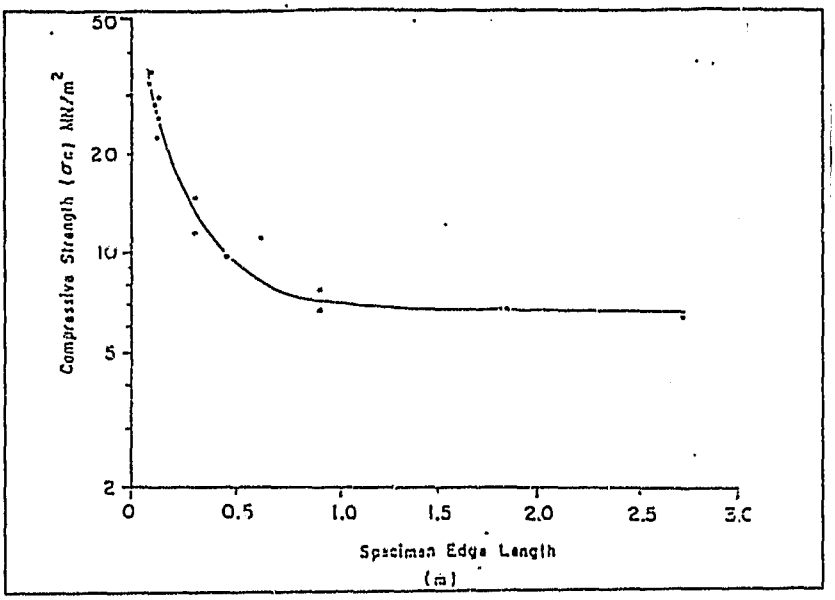

Fig. 2.2 Size effect on rock strength

f_2 : shape effect factor: 1-1.3 depending on length (l) x width (w)

l x w	f2
1 x 1	1.0
2 x 1	1.1
4 x 1	1.2
∞ x 1	1.3

f_3 : cubic strength conversion factor :1.3

f_4 : correction factor due to weight(w) / height(h) ratio

w/h	f3
1	1.0
2	1.2
3	1.4
4	1.6

f_5 : foundation strength effect in case of a brittle pillar on weak or plastic foundations, or the punching /shearing/ heave of pillar system in the foundations. For shallow mines, the conventional value of f_5 is equal to 1.

f_6 : creep effect : 1 for hard rock

- For estimating the triaxial strength of rock materials, Murrell (1965) proposed the following equation:

$$\sigma_1 = F\,(\sigma_3)^A + \sigma_c$$

Where σ_1 : major principal stress

σ_3 : minor principal stress

σ_c : uniaxial compressive strength

A and F are constants

Moreover, Hoek (1968) proposed these empirical failure criteria:

$$(\tau_m - \tau_o)/\,\sigma_c = B(\sigma_m/\sigma_c)^c$$

Where τ_m is the maximum shear $= (\sigma_1 - \sigma_3) / 2$,

σ_m is the mean normal stress $(\sigma_1+\sigma_3) / 2$ and

B, C are constants.

For practical purposes τ_o = Uniaxial tensile strength.

- Some mine designers apply the Hoek and Brown (1980a) rock mass strength failure criterion given the following empirical formula:

$$\sigma_1 = \sigma_3 + (m\sigma_c\sigma_3 + \sigma_c^2\, s)^{1/2}$$

Where σ_1 : major principal stress at the failure

σ_3 : minor principal stress or confining stress

σ_c: uniaxial compressive strength

m and s :material constants depending on the properties of the rock and the extent to which it has been fractured, being subjected to principal stresses σ_1 and σ_3.

For rock mass, Priest and Brown (1983) proposed the following estimates:

$$m = mi * \exp^{[(RMR-95)/13.4]}$$

$$s = \exp^{[(RMR-100)/6.3]}$$

Where RMR: rock mass rating from the Geomechanics Classification (after Bieniawski, 1976).

mi : empirical constant for intact rock

According to Bieniawski (1984), this empirical strength criterion for rock and rock masses is the most promising in rock engineering.

After having conducted some studies in South African mines Ozbay, Ryder and Jager (1995) found out that an acceptable unconfined rock mass strength for 'good quality' rock ($\sigma 3 = 0$ and $s = 0.1$) is of the following form:

$$\sigma_1 = 0.32\sigma_c$$

Where σ_1 is the major principal stress at failure, and σ_c is the uniaxial compressive strength of intact rock.

From the above formulae, it is clear that the pillar strength depends on the size (height and width), shape (square, rectangular, circular or irregular) and material property (uniaxial compressive strength, nature of discontinuities, anisotropy and pore water pressure).

2.3.3 Pillar loading system

In general, the assessment of pillar load in mining applications is a complex issue. However, some available theories are described in the literature. One of the major available approaches for expressing the pillar loading system is the tributary area (Fig 2.3). This method is simple and practical for regular pillar system.

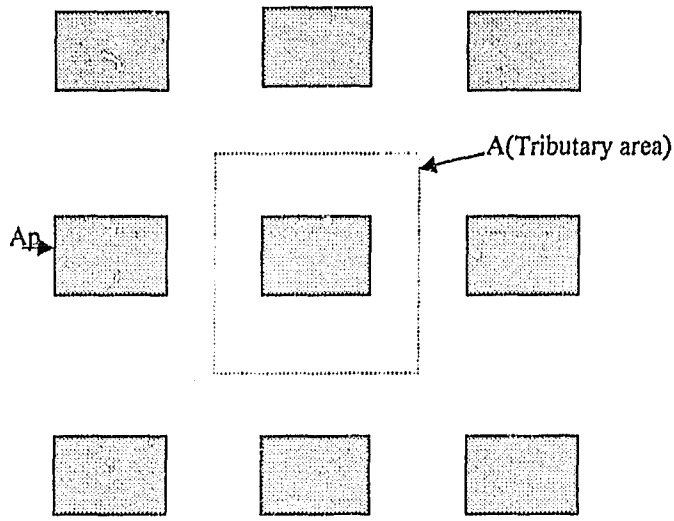

Fig.2.3 Tributary area approach for pillar loading

The general expression for pillar load is given as follows:

$$\upsilon_p = \gamma H (A / Ap) \qquad (1)$$

$$A = Ap + Am$$

Where A: Total area (m^2)

Ap: Pillar area (m^2)

Am: Mined area (m^2)

γ : Unit weight of the overburden (N/m^3)

H: Depth below surface (m)

σ_p: Pillar load or the average pillar stress (MPa)

This theory is widely used in most of the room and pillar mining systems where pillars are left for support purposes.

The pillar load can also be expressed as a function of extraction ratio (the ratio of the mined-out area to the total area):

$$e = (A - Ap) / A = 1 - (Ap / A)$$

Where e is the extraction ratio.

Substituting the above equation in (1), we find that the pillar load or the average pillar stress is expressed as follows:

$$\sigma_p = \gamma H / (1 - e)$$

This equation gives the prediction of pillar loading by the tributary area theory and the variation of the average pillar stress with extraction at the depth of 500 meters is shown in Fig 2.4. This approach assumes that the pillar is subjected to the vertical pressure only. This is presumed to be constant over the mined area and each pillar supports the column of rock above area A. It is also assumed that stress distribution is uniform over the cross-sectional area of the pillar. Nevertheless, rock mechanics research has shown the opposite. In most cases, the maximum stress occurs at the corners formed by the sidewalls of the pillar and roof or floor.

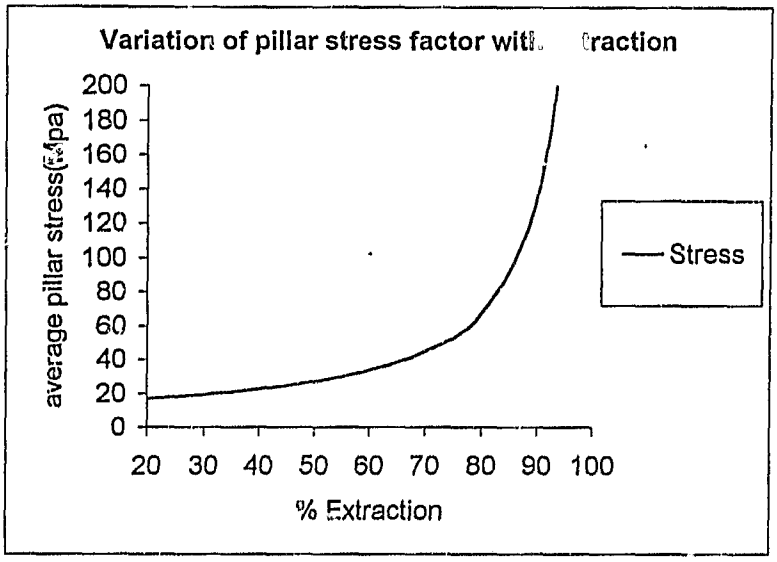

Fig.2.4 Average pillar stress vs percentage extraction at the depth of 500m.

Another approach is the theory of elastic-deflection developed by Salamon (1964, 1967), Coates (1966), and Oravecz (1977). The most important consideration is to simulate seam convergence by incrementing load due to mining, in order to obtain pillar-load distribution. Coates (1966) derived the following complicated serial formula for the plane strain case to compute incremental loading resulting from field stresses and mining:

$$S_p/S_v = (\Delta S_p/S_v) + 1$$

$$\Delta S_p = 2R \frac{-kh\,(1-w)(1-x2+h) - w\,(khn)}{hn + \pi\,(1-\nu)(1+1/N)[1+h/(1-x2)]/[2+2Rb'(1-w)\,\pi]}$$

Where S_p = total pillar load

S_v = virgin vertical stress (field stress normal to the mining zone)

ΔS_p = pillar load due to mining

$n = M / M_p$ where $M = E / (1 - \gamma^2)$ and $M_p = E_p / (1 - \gamma^2)$

E: modulus of elasticity of the medium

E_p: modulus of deformation of the pillar rock.

$w = \gamma / (1 - \gamma)$ where γ = Poisson's ratio

$k = \sigma_h / \sigma_v$ where σh and σv are respectively horizontal and vertical stresses acting on the seam.

$b' = b / L$ where b = width of the pillar and L= breadth of the mining zone.

$x = x' / \ell'$ where x'= displacement in x direction and ℓ'= pillar length

$h = h' / \ell'$ where h'= pillar length

N = number of pillars

R = radial distance from centre to the specific point

This equation might be used as a guide in planning pillar system. It has been shown that results obtained from this equation are lower than the values from the tributary area theory (Coates, 1966).

From mining observations and in situ measurement, Salamon (1983) confirmed that the magnitude of pillar load is a function of the mined area size. This means that the wider the mined area, the greater the load on the pillar as illustrated in Fig. 2.5. This is because of the load bearing ability of the abutments.

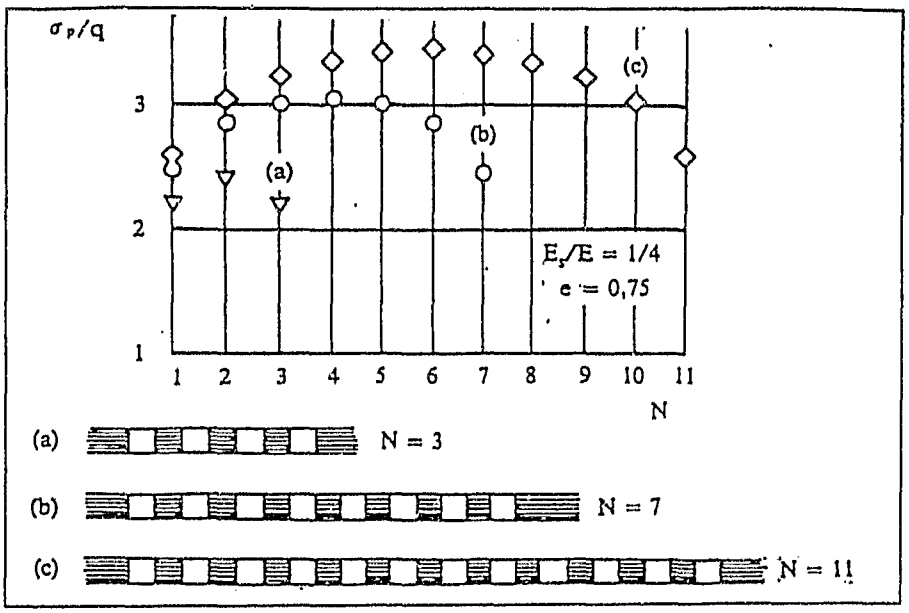

Fig.2.5 Pillar load versus mined area size

2.4 Failure Mode of Pillars

Investigations, conducted by Bieniawski (1967) have shown that above a certain stress level, which is referred to as the long-term strength, rock material fails some time under constant load. Mining observations have also shown that pillars subjected to uniaxial compressive stress can fail in one of the three main modes of failure, when stresses approach the rock mass strength. (See Fig. 2.6)

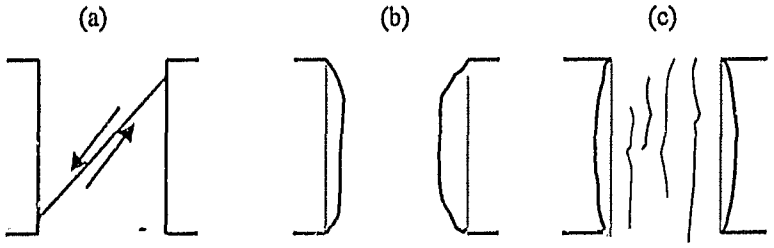

Fig. 2.6 Pillar failure modes

a) Failure by shearing along oblique planes: This results from a crushing failure when pillars are subjected to a uniaxial compressive stress (Coates, 1966). Brady and Brown (1985) found that there are kinematic factors, which promote the development of shear zones. A high height / width ratio in regularly jointed ore body rock may favour the transecting of the pillar. This has been confirmed in the model tested by Brown (1970).

b) Failure by slabbing off pillars: The central sections of the pillar start disintegrating. Brady and Brown (1985) have noticed from field observations in relatively massive rock that the generation of small surface spalls may be the first signs of local overstressing in the mine pillar.

c) Failure by lateral expanding and vertical splitting: Coates (1966) highlighted that in some cases this failure mode can be a better indication of approaching failure than some deformation or stress measurements. Brady and Brown (1985) said that this failure might occur in a stratiform ore body where soft bedding partings define the foot and hanging walls or in an ore body with highly deformable surfaces of weakness forming the interfaces between the pillar and the adjacent country rock.

According to Jaeger and Cook (1979), pillars at high stress induced by mining activity can cause violent failures, termed rockburst when it results in damage to excavations or 'bumps' when it does not necessarily generate damage in the workings.

2.4.1 Failure criteria

Jeremic (1987) suggested that for mine stability studies both tensile and shear failure criteria should be considered:

- Tensile failure criteria

a) Maximum tensile stress criterion of failure.

This criterion assumes that rock fails by brittle fracture in tension if the absolute value of minor principal stress σ_3 is equal to the uniaxial tensile strength σ_t:

$$ABS\ (\sigma_3) = \sigma_t$$

In this case, the rock splits parallel to the direction of the major principal stress and perpendicular to the direction of the maximum tensile strain.

Earlier, Stacey and Jongh (1977) used a macro - strain approach to express the failure criterion. They conclude that fracture of the rock will occur in indirect tension when the tensile strain exceeds a limit value, which is dependent on the properties of the rock:

$$\sigma_t = \sigma_3 - \nu\ (\sigma_1 + \sigma_3)$$

Where ν = Poisson's ratio

σ_1 = major principal stress

σ_3 = minor principal stress.

b) Grifffith (1924) assumed that failure takes place when the maximum tensile stress in the crack of most dangerous orientation reaches some value characteristic of the material:

$$(\sigma_1 - \sigma_3)^2 + 8T(\sigma_1 + \sigma_3) = 0 \quad \text{if} \quad (\sigma_1 + 3\sigma_3) > 0$$

$$\sigma_3 = -To \quad \text{if} \quad (\sigma_1 + 3\sigma_3) < 0$$

Where To = uniaxial tensile strength.

- Shear failure.

The Coulomb-Navier's criterion of failure postulates that failure occurs when the maximum shear stress at a point in the material reaches its shear strength (Jeremic 1987):

$$\tau = \tau_s + \mu\sigma_n$$

Where τ = shear stress acting along the plane of failure

τ_s = intrinsic shear strength or cohesion

μ = coefficient of friction

σ_n = normal stress acting on the plane of failure.

Jeremic (1987) indicated that Mohr extended the Coulomb-Navier's failure theory by postulating that a material fails when the shear stress on the failure surface has reached the shear strength of the material, which is dependent on the normal stress acting on the surface. However, in a tensile stress state the material will fail when the tensile principal stress has reached a limiting value that is experimentally determined.

- For underground excavation design, Bieniawski (1974) proposed this empirical strength failure criterion.

$$\sigma_1 / \sigma_c = 1 + A\,(\sigma_m/\sigma_c)^k \quad \text{or} \quad \tau_m / \sigma_c = 0.1 + B(\sigma_m/\sigma_c)^c$$

Where $\tau_m = (\sigma_1 - \sigma_3) / 2$

$\sigma_m = (\sigma_1 + \sigma_3) /2$

σ_c = uniaxial compressive strength

$k \cong 0.75$ and $c \cong 0.90$ for the range of rocks tested by Bieniawski.

A = from 3 to 5 and B = from 0.70 to 0.8 depending on nature of rocks.

- Another practical empirical failure criterion suggested by Hoek and Brown (1980a) has been described in section 2.3.2.

2.4.2 Pillar safety factor

a) The simplest way to express the safety factor in pillar design is that pillars will fail as soon as the applied load reaches their ultimate strength:

$$\text{Safety Factor } SF = \sigma_s / \sigma_p$$

Where σs is the pillar strength and σ_p is the pillar stress.

This approach assumes that the stress distribution is constant and uniform across the entire pillar section. Using the pillar strength and pillar stress equations described above, it can be shown that the safety factor is a function of pillar size, stope span and pillar height.

The choice of a suitable factor of safety to guard against pillar failure is based upon engineering experience and various authors recommend different safety factors for different applications:

	Safety factor (SF)
Conventional production panels	1.6
Geological disturbed areas	1.7
Competent seams	1.5
Main development layouts	2 - 2.5
Shaft bottom areas	2.5

From the back-analysis study conducted by Salamon and Munro (1967) in the South African coal mines, it has been shown that pillars in the range of safety

factor from 1.3 to 1.9 were stable. In this case, the acceptable average value of safety factor in pillar design is 1.6.

b) The Hoek - Brown failure criterion may be used to express a safety factor (SF) at a given point in the following manner:

$$SF \geq [\sigma_3 + (m\sigma_c\sigma_3 + \sigma_c^2 s)^{1/2}] / \sigma_1$$

Where σ_1 : major principal stress at the failure

σ_3 : minor principal stress or confining stress

σ_c : uniaxial compressive strength

m and s : Hoek – Brown material constants as defined in the section 2.3.2

This equation is useful for computing a safety factor in areas having a non-uniform stress distribution.

2.5 Basic Concepts of Numerical Modelling in Rock Mechanics.

The development of powerful computers observed during the two last decades has helped to improve the numerical modelling programmes in rock mechanics. Therefore, the modern trend in rock mechanics is to use more numerical modelling techniques (eg: finite element, finite difference, boundary element) than the other analytical methods such as physical models and mathematical modelling (closed-form solutions). One of the advantages of the numerical modelling in rock mechanics is to integrate some rock mass properties.

The numerical modelling techniques are well described in most rock engineering courses and various references such as Chandrakant and John (1977), Crouch and Starfield (1983), Brady and Brown (1985), Hoek et al. (1995), this literature survey will be limited to the basic concepts of these

techniques. Actually, the most common numerical modelling methods in geotechnical engineering are categorised in two distinct groups; namely Differential and Integral methods. Both recognise geologic structure as being discontinuous.

In differential methods, the entire domain of interest is discretized in subdomains or zones as shown in Fig. 2.7. This means that a complex problem of large extent can be divided into smaller equivalent units. These methods use the implicit solution scheme termed matrix solution to solve the problem. Methods, such as Finite element, Finite difference, and Distinct element, are categorised under Differential group.

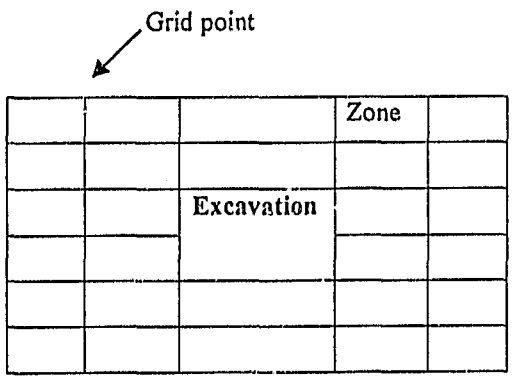

Fig.2.7 Finite difference method.

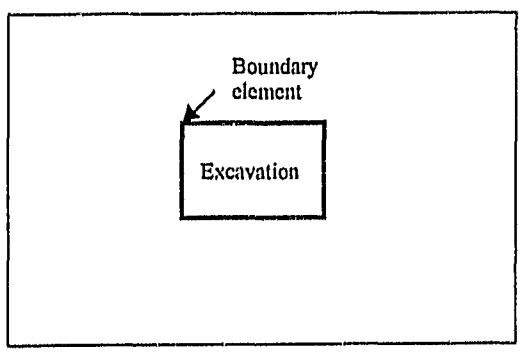

Fig.2.8 Boundary element method.

In integral or boundary methods, the contour or boundary of excavation is discretized as depicted in Fig.2.8. So, the numerical solution built on analytical solutions is found by using the explicit solution scheme in order to satisfy the specified boundary conditions at each element along the boundary. Depending on the type of formulation, the following methods have been established:

a) Indirect method, using "fictitious forces" known as Boundary element method and using fictitious "displacements" known as Displacement discontinuity method. In Boundary element method, it is assumed that fictitious unit forces applied at the centre of a segment generate forces and displacements at the centre of every other segment. In the Displacement discontinuity method, unit displacements are used across each segment.

b) Direct method, making use of Betti's reciprocal theorem that gives a set of simultaneous equations of forces (T), displacements (U), the unknown values of induced forces (t) and displacements (u) to be solved numerically.

$$\Sigma T.u = \Sigma U.t$$

The numerical solution is first obtained at the boundary, and then the solution at different points within the body is obtained from the boundary solutions. Methods, such as Indirect method, Direct method, and displacement discontinuity method, all belong to the Integral method of numerical modelling.

According to the data-limited problems in rock mechanics either in quantity or in quality, Starfield and Cundall (1988) described a methodology for rock

mechanics modelling by defining a useful set of guidelines that may be summarised in the following steps:

a) Establish the raison and objectives of numerical modelling.
b) Design a conceptual model at the earliest stage of the project.
c) Identify important mechanisms, modes of deformation and failure.
d) Think of experiments to be performed on the model and visualise what the answer might be.
e) Design or borrow the simplest model that will allow the important mechanisms to occur.
f) Implement the model, choose the simplest experiment and run it. If the model ties with the expectations, proceed to more complex. If not, identify the weaknesses in the model and remedy them before continuing.
g) If the only available model has irremediable weaknesses, make a series of simulations in order to bracket the true case.
h) Run more complex models including the geology in order to explore its aspects.

2.6 CONCLUSION

For this work, the two most recent approaches, namely the Geological Strength Index (GSI) derived from the Bieniawski (1976) rock mass classification and the Rock Mass Index from the Q-Classification, appear to offer the most effective method of evaluation of the Kamoto rock mass characteristics from the available data.

The strength of pillar will be determined using the most promising empirical formulae in hard rock engineering such as proposed by Hedley and Grant (1972) from mathematical expression derived by Salamon (1967) and Obert *et*

al. (1967). The stress on pillars will be computed by numerical modelling using an available boundary elastic code.

CHAPTER 3

KAMOTO MINING GEOLOGY

3.1 Introduction

This chapter gives a brief geological overview of the stratiform orebodies in Kamoto mine with the view of setting up the geotechnical parameters for determining rock mass strength. It summarises available information about geology, stratigraphy and mineralisation obtained from various technical documents from Kamoto mine.

3.2 Form and Structure of Ore-Body

The Kamoto Principal ore-body belongs to the Katanga copper be!. named "Serie des mines '. It is one of the biggest parts of the Kolwezi copperfield and shaped as a regular synclinal basin limited on each side by the major faults. Its mean geometrical dimensions are as follows:

- North - South extent: 1300 m
- East - West extent : 1500 m
- Depth : 0 - 535 m
- Number of ore bodies : 2
- Ore-body thickness : 12m for the upper ore body,
  14 m for the lower ore body.

On average a 15 meter-thick waste rock layer separates the two ore bodies. The dip angle changes from West to East·

Western part	Middle part	Eastern part	Far extreme part
25°-30°	30° – 40°	60° - 80°	80° – 90°

The Northern part of the ore body, where the Room and Pillar mining method had been applied, is flat dipping at an angle of between 0° and 12°.

3.3 Lithostratigraphy of the Katangan System

The lithostratigraphy of the Katangan system in Katanga (Democratic Republic of Congo) compiled from François (1973) and up-dated by Cahen (1984) is shown in table 3.1. These authors used the following abbreviations to describe rocks of the Katangan copper belt:

- R.A.T.: Argillaceous dolomitic siltstone (Roches Argilo-Talqueuses)
- S.D.B.: Lower dolomitic shales (Shales Dolomique de Base)
- R.S.F.: Sileceous laminated dolostones (Roches Silicieuses Feuilletées)
- BOMZ: Black Ore Mineralized Zone (Zone à minerais noir)
- D.Strat.: Stratified dolomite (Dolomites Stratifiées)
- S.D.: Dolomitic shales (Shales Dolomitique)
- R.S.C: Massive and sileceous dolomite (Roches Siliceuses Cellulaires)
- R.G.S: Dolomitic and argillaceous silstones (Roches Gréseuses Supérieures)
- Ks: Upper Kundelungu (Kundelungu supérieur)
- Ki: Lower Kundelungu (Kundelungu inférieur
- R: "Roan"

Table 3.1 Lithostratigraphy of the Katangan system

Pleistocene Upper Carboniferous +/- 650 Ma			KAROO and KALAHARI		
		Supergroup	Group	Formation and /or Lithologies	
		Upper Kundelungu (Ks)	Plateaux (Ks-3)	Arkoses with sandstones and shales	
			Kiubo (Ks-2)	Ks-2.2/Ks-2.1: carbonated shales,sandy and argillaceous shales,sandstones	
			Kalule (Ks-1)	Ks-1.3/Ks-1.2 : carbonated siltstones,sandy and argilleceous shales, pink limestones Ks-1.1: diamictide ('petit conglomerat')	
		Lower. Kundelungu (Ki)	Monwezi (Ki-2)	Arkosic sandstones with carbonated shales and siltstones	
	K A T A N G A N		Likasi (Ki-1)	Ki-1.3: carbonated shales and siltstones. Ki-1.2: dolomites and limestones with shales . Ki-1.1: diamictite ('grand conglomerat')	
			Mwashya	R-4.2: dolomitic shales, with sandstones or carbonaceous shales at top; 'conglomerat de Mwashya' at the base. R-4.1: dolostones, dolomitic shales, jasper, oolites, pyroclastic units, iron.	
Prote-Rozoic			Dipeta (R-3).	R-3.4/R-3.3: dolostones, limestones, shales, sandstones and arkose. R-3.2/R-3.1: dolomitic and argillaceous siltstones (R.G.S),dolostones	
		Roan (R)	Mines (R-2)	Kambove Dolomite (R-2.3)	R-2.3.2 (upper unit) R-2.3.1 (lower unit)
				Dolomitic shales (R-2.2)	R-2.2.3: SD3a/3b R-2.2.2: SD2b/2c/2d R-2.2.1:SDB/Bomz/2a
				Kamoto Dolomite (R-2.1)	R-2.1.3:R.S.C. R-2.1.1:grey R.A.T. R-2.1.2:R.S.F./D.Strat.
			R.A.T. (R-1)	R-1.3/R-1.2/R-1.1: argillaceous dolomitic siltstones and sandstones	
+/- 1050Ma		Base of the R.A.T. sequence – unknown Basal conglomerate			
+/- 2050Ma		KIBARAN and PRE – KIBARAN			

3.4 Stratigraphy of the Roan Group.

- Red R.A.T (R-1): argillaceous dolomitic siltstones and sandstones. These rocks have a red colour and essentially consist of massive detritus formations. The thickness is more than 235m. They have been fractured during the orogenic events and sometimes have no cohesion in presence of "oligiste" plates.

- Grey R.A.T. (R-2.1.1): this formation consists of around 2 meter thick chloritic and dolomitic siltstone.

- D.Strat. (R-2.1.2.1): this formation is a 4.5-meter thick stratified dolomite including a fine-grained dolostones.

- R.S.F (R-2.1.2.2): this 6.5 meter thick unit is siliceous, laminated dolostones.

- R.S.C (R-2.1.3): this formation is massive and generally stromatolitic dolostones. It is about 7 to 25 meters thick.

- S.D (R-2.2): The dolomitic shales. This 30 -110 meter thick formation consists mainly of fine clastic material cemented by a micritic dolomite. At its base, there are sedimentary rocks, which are characterised by carbonate-quartz nodules, irregular lenses and lenticular beds called Lower dolomitic shales (R-2.2.1). These rocks constitute the upper ore body.

- C.M.N: this formation forms the upper part of the Mines group and is divided into two main units:

a) The upper C.M.N; generally composed by clean dolostones containing interbedded chloritic - dolomitic siltstones.
b) The lower C.M.N; generally dark dolostones, enriched in organic matter.

3.5 Mineralisation

In Kamoto Mine, the mineralisation occurs as stratiform copper-cobalt deposits. The primary mineralisation is the disseminated sulphides of which the major minerals in association are:

- Chalcocite (Cu2S)
- Carrollite (CuCo2S4)
- Bornite and Chalcopyrite are seldom observed.

The copper and cobalt average grades are 5 % and 0.3 - 0.4 % respectively.

3.6 Geological Mining Reserves

So far, the available geological reserves for Kamoto ore body are estimated at 40.2 millions tons of ore (December 1995), which has been mined by different methods according to the geometric and geotechnic properties of each part of the main ore body. Table 3.2 displays provisional geological reserves by mining method:

Table 3.2 Geological mining reserves

Mining method	Reserves (Mtn)	%
Caving system	8.0	20%
Room and pillar	8.4	21%
Cut and fill	23.8	59%
Total :	40.2	100%

CHAPTER 4

KAMOTO ROCK MASS CLASSIFICATION AND STRENGTH

4.1 Introduction

The purpose of this section is to apply geotechnical classification to the rock mass of the Kamoto mine room and pillar area in order to estimate the strength of the in situ rock mass. It has been stated that one of the most fastidious tasks in design mining and stability analysis is the evaluation of the strength of rock mass, especially when not enough geological and geotechnical data are available at the designing stage. There are, however, many methods of expressing the strength of rock mass, which have been briefly explained in the literature survey. Unfortunately, there seems to be no exclusive parameter or index that can fully and quantitatively describe a jointed rock mass for engineering design purposes. During the past two decades, different attempts have been made to carry out in situ tests on jointed rock masses in order to predict their strength. At this stage of research, knowledge is limited to confirm their reliability.

For this work, two different systems have been used for evaluation of the rock mass classification and strength:

a) A combination of the Rock Mass Rating (RMR) system developed by Bieniawski in 1976, the modified Hoek-Brown criterion (Hoek *et al.*,1992) and the Geological Strength Index (GSI) proposed by Hoek *et al* (1995).

b) The Rock Mass Index (RMI) based on the Q-Classification developed by Palmström (1997).

These systems have been extensively used in the mining industry because they take into account some parameters that are measurable in the field and provide a

reputable systematic measure to relate to rock quality and strength. In this study, the Kamoto rock mass classification has been conducted based on information from available database.

4.2 Mechanical Properties of Kamoto Intact Rocks

The table 4.1 summarises the laboratory tests conducted on various samples of rocks at the Mining research centre of Gécamines company.

Table 4.1: Physical properties of Kamoto intact rocks

PHYSICAL PROPERTIES OF INTACT ROCKS								
Rock designation	h	ρ	UCS	Ts	ν	E	G	ϕ
	m	Kg/m^3	MPa	MPa	-	GPa	GPa	Degr.
Upper dolomite (SS)		2.79	148.7	10.5	0.3	59.5	22.9	61.8
Lower dolomite (SDB)	12	2.87	136	11.4	0.29	62.1	24.1	58.7
Massive dolostone (RSC)	15	2.68	180	10.3	0.27	79.7	31.4	61.7
Siliceous laminated dolostones (RSF)	6.5	2.66	148.3	10.7	0.22	67.6	27.7	60.4
Stratif. Dolomite (D.Strat.)	4.5	2.83	207.3	10.6	0.28	89.5	35	60.4
Grey RAT	3	2.74	77.7	9.7	0.29	50.4	19.5	59
Breach RAT (No alteration)	-	2.83	81.2	8.7	0.23	44.7	18.2	-
Red RAT	-	2.73	70.5	7.1	0.31	38.7	14.8	51.9

Where h is the layer thickness,

ρ is the density of rock,

UCS is the uniaxial compressive strength,

Ts is the tensile strength,

ν is the Poisson's ratio,

E is the elasticity modulus,
G is the rigidity modulus and
ϕ is the internal angle of friction.

4.3 Rock Mass Classification by Bieniawski's System

Hoek and Brown (1988) proposed that the 1976 version of Bieniawski's Rock Mass Rating (RMR_{76}), as shown in Appendix C, is acceptable to assess RMR values, hence the Geological Strength Index (GSI). This version assumes co. pletely dry conditions and a very favourable joint orientation. This rock mass classification is based on the following parameters:

- strength of intact rock material,
- rock quality design,
- spacing of discontinuities,
- condition of discontinuities,
- ground water condition.

4.3.1 Strength of intact rock material (IRS)

The intact rock strength is the unconfined uniaxial compressive strength (UCS) of the rock obtained mainly from the destructive laboratory tests on cores. In the present work, the UCS values are taken from the Gecamines company Geotechnical Database. Following the stratigraphy, the classification of Kamoto rocks using RMR_{76}, system is as shown in Table 4.2.

Table 4.2 UCS values

Rock designation	U C S (MPa)	Range values (Mpa)	RMR Rating
Upper Dolomite (SS)	149	100 – 200	12
Lower Dolomite (SBB)	136	100 – 200	12
Massive Dolostone (RSC)	180	100 – 200	12
Siliceous laminated dolostone (RSF)	148	100 – 200	12
Stratified Dolomite (D. Strat.)	207	> 200	15
Grey RAT	78	50 – 100	7
Breach RAT	81	50 – 100	7
Red RAT	70	50 – 100	7

4.3.2 Rock quality designation (RQD)

RQD is one of the most widely used geomechanics measurements in rock mass classification theories. Deere (1964) defined the RQD as follows:

$$RQD = 100 * (\Sigma l_i) / L$$

Where l_i are the lengths of individual pieces of core having length of 10 cm or greater, and L is the total length of the drill run.

The compilation of results coming from different drill hole RQD's (F1512, F1481, F1683, F1686) conducted in Kamoto flat ore body as shown in Table 4.3 and Fig. 4.1, gives the mean RQD values.

Table 4.3: RQD values

Rock designation	R Q D (%)	Range values (MPa)	RMR Rating
Upper Dolomite (SS)	40	25 – 50	8
Lower Dolomite (SBB)	37	25 – 50	8
Massive Dolostone (RSC)	59	50 – 75	13
Siliceous laminated dolostone (RSF)	51	50 – 75	13
Stratified Dolomite (D. Strat.)	72	50 – 75	13
Grey RAT	52	50 – 75	13
Breach RAT	50	50 – 75	13
Red RAT	41	25 – 50	8

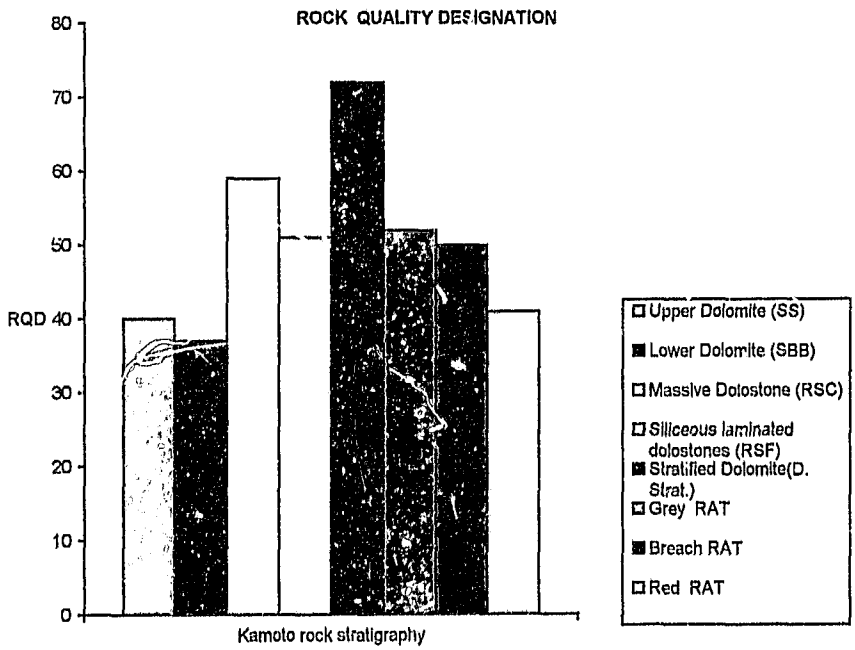

Fig 4.1 Kamoto rock quality designation

4.3.3 Spacing of joints: Js

The influence of discontinuities where an opening is driven in a jointed rock mass must be taken into account in order to adjust the laboratory values and in this special case, the rock mass strength. At Kamoto mine, some major geological structures are combined with secondary fracturating and jointing. Consequently, the spacing of joints changes from point to point along a drive and in different drives. So far, neither geostructural nor geotechnical study has been described in detail. Thus, the survey conducted by the geological department of Kamoto mine in some drifts of room and pillar workings (Tab.4.4) in the upper ore body has been examined in order to find out a mean spacing of joints.

Table 4.4 Kamoto room and pillar joint spacing

Drift number	Upper Orebody		
	L (m)	N	X
D16NE	10.9	9	1.2
D16NW	12.8	10	1.3
D16SE	14.6	23	0.6
D16SW	18.2	17	1.1
R4E/D16	34.4	42	0.8
R4W/D16	33.4	37	0.9
D12NE	17.8	21	0.8
D12NW	18.4	16	1.2
D12SE	19.3	20	1.0
D12SW	14.3	19	0.8
R4E/D12	23.7	32	0.7
R4W/D12	23.2	37	0.6
TOTAL	- 241	283	
SPACING JOINT MEAN			0.9

Where L is the drift length,

N is the number of joints and

X is the joint spacing mean.

According to RMR Classification tables (Appendix C), as the spacing joint mean is between 0.3 and 1 m, thus a rating value of 20 has been allocated to all geological layers.

4.3.4 Joint condition: Jc

Joint condition is an estimation of the frictional properties of joints. Field observations at Kamoto room and pillar area have shown that the joints roughness profiles can be categorised into three mean groups as follows:

- slightly rough surface and hard joint wall contact,
- slightly rough surface and soft joint wall contact,
- slickensided surface and continuous joint.

An adjustment rate mean of 12 has been taken to assess mechanical properties of joint.

4.3.5 Ground water condition: Gwc

According to Hoek et al. (1995) rock mass criterion, the rock mass should be assumed completely dry and a rating of 10 is assigned to the groundwater condition in the Bieniawski's (1976) Rock Mass Rating.

4.3.6 Joint orientations

In the Bieniawski's (1976) Rock Mass Rating, very favourable joint orientations should be assumed and an adjustment for joint orientation is set to zero.

4.3.7 Rock mass classification summary

Fig. 4.2 and Table 4.5 summarise the rock mass classification of Kamoto mine by using Bieniawski's 1976 Rock Mass classification. It has been noticed that there is very little variation in rock quality in terms of rock masses defined by Bieniawski (1976).

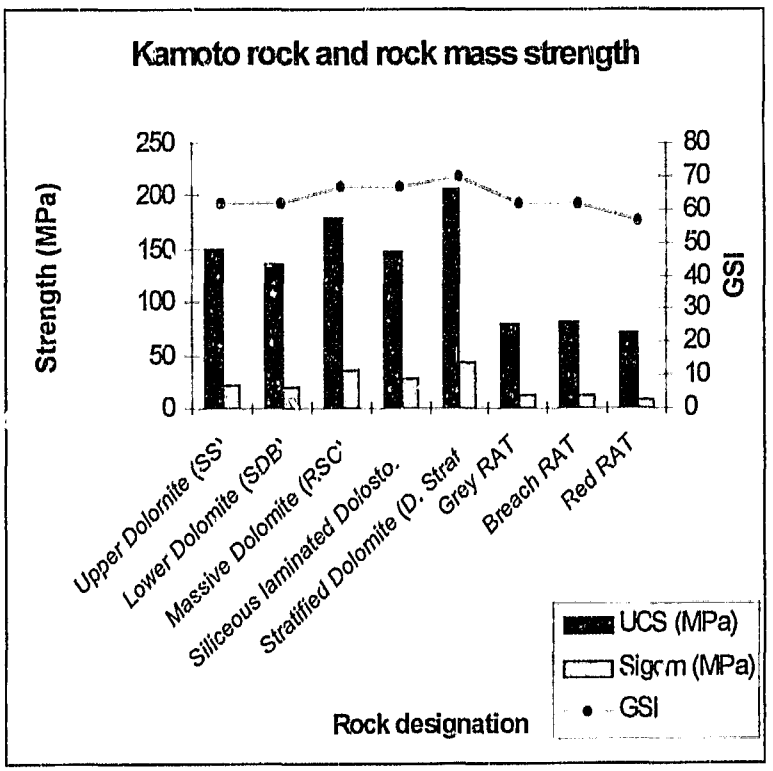

Fig.4.2 Kamoto rocks and rock mass strengths

Table 4.5: Kamoto rock mass classification

Rock designation	UCS*	RQD	Js	Gwc	Jc	RMR_{76}**	GSI***	Rock mass Class
Upper Dolomite (SS)	12	8	20	10	12	62	62	Good rock
Lower Dolomite (SBB	12	8	20	10	12	62	62	Good rock
Massive Dolostone (RSC)	12	13	20	10	12	67	67	Good rock
Silecocous laminated dolostone (RSF)	12	13	20	10	12	67	67	Good rock
Stratified Dolomite (D. Strat.)	15	13	20	10	12	70	70	Good rock
Grey RAT	7	13	20	10	12	62	62	Good rock
Breach RAT	7	13	20	10	12	62	62	Good rock
Red RAT	7	8	20	10	12	57	57	Fair rock

UCS* from Laboratory tests, RMR76** from Bieniaswki (1976) and

GSI*** from the procedure developed by Hoek *et al* (1995)

4.4 Strength of Kamoto Jointed Rock Mass by GSI approach

In spite of numerous literature on pillar strength, for most engineering and numerical modelling analysis in rock mechanics practice the Hoek-Brown criteria is used among different types of strength criterion to express the failure of isotropic rock material (Wagner 1992, Hoek et al. 1995). This criterion takes into account the characteristics of rock mass that regulate its strength and deformation behaviour once any load is applied. The most general form of Hoek-Brown failure criterion to determine the strength of jointed rock mass is:

$$\sigma'_1 = \sigma'_3 + \sigma_c \{m_b (\sigma'_3/ \sigma_c) + s\}^a$$

Where m_b is the value of the constant m for the rock mass

s and a are constants which depend upon the characteristics of the rock mass

σ_c is the uniaxial compressive strength of the intact rock

σ'_1 is the axial effective principal stress

σ'_3 is the confining effective principal stress.

Hoek, Kaiser and Bawden (1995) suggested a procedure for estimating the strength of jointed rock mass using the Hoek-Brown and Mohr-Coulomb criteria, in which the main parameters remain the geological strength index (GSI), the strength of the intact rock (σ_{ci}) and the Hoek-Brown constant of intact rock (m_i). This method based on the range of equations derived by Priest and Brown (1983) and Balmer (1952) operates as a spreadsheet computing these parameters.

According to Priest and Brown (1983) the values of the rock mass, constants m_b, s and a can be determined by the following equations:

For GSI > 25 (Undisturbed rock masses)

$m_b = m_i \exp\{(GSI-100)/28\}$

$s = \exp\{(GSI-100) / 9\}$

$a = 0.5$

For GSI < 25 (Undisturbed rock masses)

$s = 0$

$a = 0.65 - (GSI/200)$

Where GSI is the geological strength index coming from Bieniawski's 1976 rock mass rating. For RMR76'> 18, GSI = RMR76'.

m_i is the intact rockmass constant suggested by Hoek and Brown (1980b) as follows:

- $m_i \cong 7$ for carbonate rocks (dolomite, limestone, marble),
- $m_i \cong 10$ for lithifed argillaceous rocks (mudstone, siltstone, shale and slate),
- $m_i \cong 15$ for arenaceous rocks (sandstone and quartzite)
- $m_i \cong 17$ for fine-grained polyminerallic igneous crystalline rocks (andesite, dolerite, diabase, rhyolite)
- $m_i \cong 25$ for coarse-grained polyminerallic igneous and metamorphic rocks (amphibolite, gabbro, gneiss, granite, norite, quartz-diorite)

Balmer (1952) expressed the Mohr-Coulomb shear strength criterion in terms of principal stresses as follows:

$$\tau = c + \sigma n \tan\phi$$

$$\sigma_n = \sigma_3 + (\sigma_1 - \sigma_3) / ((\delta\sigma_1/\delta\sigma_3)+1)$$

$$\tau = (\sigma_n - \sigma_3) (\delta\sigma_1/\delta\sigma_3)^{0.5}$$

For GSI > 25, a = 0.5:

$$\delta\sigma_1/\delta\sigma_3 = 1 + ((m_b\sigma_c) / 2(\sigma_1 - \sigma_3))$$

For GSI < 25, s = 0

$$\delta\sigma_1/\delta\sigma_3 = 1 + a\,(m_b)\,a\,(\sigma_3/\sigma_c)^{a-1}$$

Where τ = shear strength on a plane of failure,

σ_n = normal stress acting on the plane,

c = cohesion and ϕ = angle of internal friction. These two values are carried out from the linear relations between $\sigma_1 = f(\sigma_3)$ and $\tau = f(\sigma_n)$

m_b = constant for rock mass

$\delta\sigma_1$ and $\delta\sigma_3$ are variations of principal stresses

Finally, the uniaxial compressive strength of the rock mass is related to c and ϕ by the following equation:

$$\sigma_{cm} = 2c\cos\phi/(1-\sin\phi)$$

Table 4.6 summarises some characteristics of Kamoto rock mass from the spreadsheets (Appendix D) using the above range of equations:

Table 4.6 Kamoto rock mass characteristics

Rock designation	U C S (Mpa)	Sigcm(Mpa)*	Cohesion*	Phi angle*	GSI*	E (Mpa)*	mb*	s*	a	K values (MPa)	
										**	***
Upper Dolomite (SS)	149	22.0	5.1	40.1	62	19953	2.57	0.015	0.5	–	–
Lower Dolomite (SBB)	136	20.0	4.7	40.1	62	19953	2.57	0.015	0.5	29	26
Massive Dolostone (RSC)	180	35.1	7.2	45.1	67	26607	4.62	0.026	0.5	–	–
Siliceous laminated dolostone (RSF)	148	26.7	6.2	39.9	67	26607	2.77	0.026	0.5	32	39
Stratified Dolomite (D. Strat.)	207	43.0	9.9	40.4	70	31623	3.08	0.036	0.5		
Grey RAT	78	11.5	2.7	40.1	62	19953	2.51	0.015	0.5		
Breach RAT	81	11.9	2.8	40.1	62	19953	2.51	0.015	0.5	–	–
Red RAT	70	8.8	2.0	40.9	57	14962	2.53	0.008	0.5		

UCS from Laboratory tests

* from Hoek *et al.* (1995) procedure

**K values for the ore body rock mass from RMI method (See Section 5.3.1)

*** K values for the ore body rock mass from Ryder-Ozbay procedure and Hoek et al.(1995) method (See Section 5.3.1)

4.5 Strength of Kamoto Rock Mass by RMI approach

The Rock Mass Index (RMI) explained briefly in the section 2.3.1 of the literature survey and some field observation will be used to assess the rating of the following features; JR, JA and JL, which are involved in calculation of the jointing parameter JP. This parameter expresses the rock mass classification as defined by Palmström (1997).

4.5.1 Rating of the joint roughness factor (JR)

In Kamoto mine, the joint roughness is almost slightly undulating on a large scale and between slightly rough and slickensided surface at small scale. Therefore, a value of 1.5 can be allocated.

4.5.2 Rating of the joint alteration (JA)

It has been observed in Kamoto room and pillar area that in most cases the contact between the two joint surfaces is clean and fresh. Therefore, the rating of joint alteration can be assumed to be 1.

4.5.3 Rating of the joint size and continuity factor (JL)

From observations in Kamoto room and pillar area, it has been found that joint lengths encountered during the mining process can be categorised as medium, long and very long. According to Palmström's tables (Appendix B) an average rating of 0.75 might be suitable for the joint size and continuity.

4.5.4 Strength of Kamoto jointed rock mass

Palmström (1995) suggested the use of the equations below to perform the Rock Mass Index (RMI) which reflects the strength of rock mass.

The joint condition factor: JC = JL .(JR / JA)

The jointing parameter: $JP = 0.2\ (JC)^{0.5}\ .\ V_b^{\alpha}$

Where $\alpha = 0.37JC^{-0.2}$

Rock Mass Index: $RMI = \sigma_c\ .\ JP$

Where JR is the joint roughness factor,

JA is the joint alteration factor,

JL is the joint size and continuity,

V_b is the volume of the rock block (m^3) and

σ_c is the uniaxial compressive strength of the intact rock (MPa).

The strength of a cubical specimen of rock material in each ore body is given by a simple spreadsheet carrying out the above equations in Table 4.7.

Table 4.7 RMI results on Kamoto rock mass

Ore body	Rock type	σ_c (MPa)	JC	Vb (m^3)	JP	K (Mpa)
OBS	Lower dolomite(SDB)	136	1.125	1	0.21	29
OBI	Siliceous dolostones(RSF), Stratified dolomite(D.Strat) and Grey RAT.	152	1.125	1	0.21	32

Where K is the strength of one cubic meter of the rock material.

4.6 Conclusion

The Rock Mass Rating (RMR) system is used to estimate the mechanical properties of rock masses for mining purposes. This system has been used on different types of rocks found at Kamoto mine. Despite the paucity of available

data, the Bieniawski's geotechnic classification proves that almost all Kamoto rocks are categorised in the class of "good rock" with a RMR between 62 and 70. The only exception is the red RAT rock, which is in the class of "fair rock" with a RMR equal 57. This section represents an attempt for classification of Kamoto rock mass and the starting effort for evaluation of the strength of rock by using the Geological Strength Index concept. The strength of Kamoto jointed rock mass has been assessed by using Hoek-Brown and Mohr-Coulomb failure criteria. It has been noticed that the strength of upper and lower ore bodies rock masses are 20.0 MPa and 29.8 MPa respectively. According to the rock mass conditions presented in this work, these values give an indication that the strength of the rock mass in the room and pillar area is in the range between 13% and 21% of the uniaxial compressive strength. This is mainly related to the influence of joints that reduce the compressive strength and facilitate the fracturing of mine pillars. From mining experience, Jeremic (1987) indicates that structural defects could decrease the pillar bearing capacity by up to 50 %.

From the Rock Mass Index (RMI), the jointing parameter of Kamoto rock mass was found to be 0.21 and the strengths of cubical specimen to be 29 MPa and 32 MPa for the upper ore body (OBS) and the lower ore body (OBI) respectively. These values will be used in the following chapter to compute the pillar strength.

CHAPTER 5

KAMOTO PILLAR STRESSES AND STRENGTH

5.1 Introduction

In general, Kamoto mine used rectangular pillars as integral parts of the room and pillar mining method. These pillars were left in place during the mining process in order to provide regional support to maintain ground stability in the working area. In Kamoto Mine room and pillar area, excavation of each ore body was usually carried out in three main phases due to its thickness. Figure 5.1 shows the different mining phases.

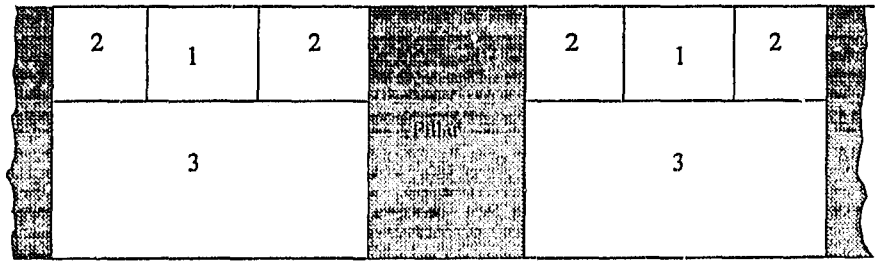

Fig. 5.1: Mining phases (section view)

The first stage (1) is the development of 6 m wide and 5 m high drifts at the top of the ore body. The second stage (2) is the drifts widening in order to have the full room span of 15 m. The third stage (3) is the benching of the bottom part of the ore body. The primary roof support during development was 2.4 meter long and 16 mm diameter mechanical bolts. After widening out stopes, a permanent support between pillars was provided by 4 meter long and 38 mm diameter cement grouted bolts. In poorer ground conditions, shotcrete and mesh could be used. The mining proceeded as a sequence of isolated blocks. A typical block had 5 rooms separated by rectangular pillars. A "barrier pillar" had been designed between different mining blocs. This variant of room and pillar mining method for Kamoto mine has been designed with a system of non-yield and barrier pillars for the two

ore-bodies. This should have provided a regional support and hence, stability of all the room and pillar area (Fig 5.2). The most important parameters of the geometry design were as follows:

For non-yield pillars:

Pillar length: 15 m

Pillar width: 10 m

Pillar height: 12 m (upper ore-body), 14 m (lower ore-body)

Room length: 100 m (Normal room)

Room width: 15 m

Room height: 12 m (upper ore-body), 14 m (lower ore-body)

For barrier pillars:

Length: 150 m (in room direction), 125 m (in transverse direction)

Width: 35 m (in room direction), 25 m (in transverse direction)

The barrier pillars were located between blocs.

This case study will be focused on the rectangular pillars within a room and pillar mining block as shown in Fig. 5.2. These pillars, classified as non-yield pillars, failed in 1990 during the mining process. However, the numerical model will integrate all pillars left during the mining process.

Kamoto mine had a computerised seismic activity recording station (Electrolab) which could capture seismic events through geophones installed in some room and pillar mining blocks. Unfortunately, this system was not always reliable because it was not properly calibrated in order to determine some specific parameters of seismic events such as the source, nature, magnitude, and frequency. In 1990, seismic events, especially rockfalls and pillar splitting, increased in exponential manner. These events have preceded the global instability in the room and pillar area in both ore bodies.

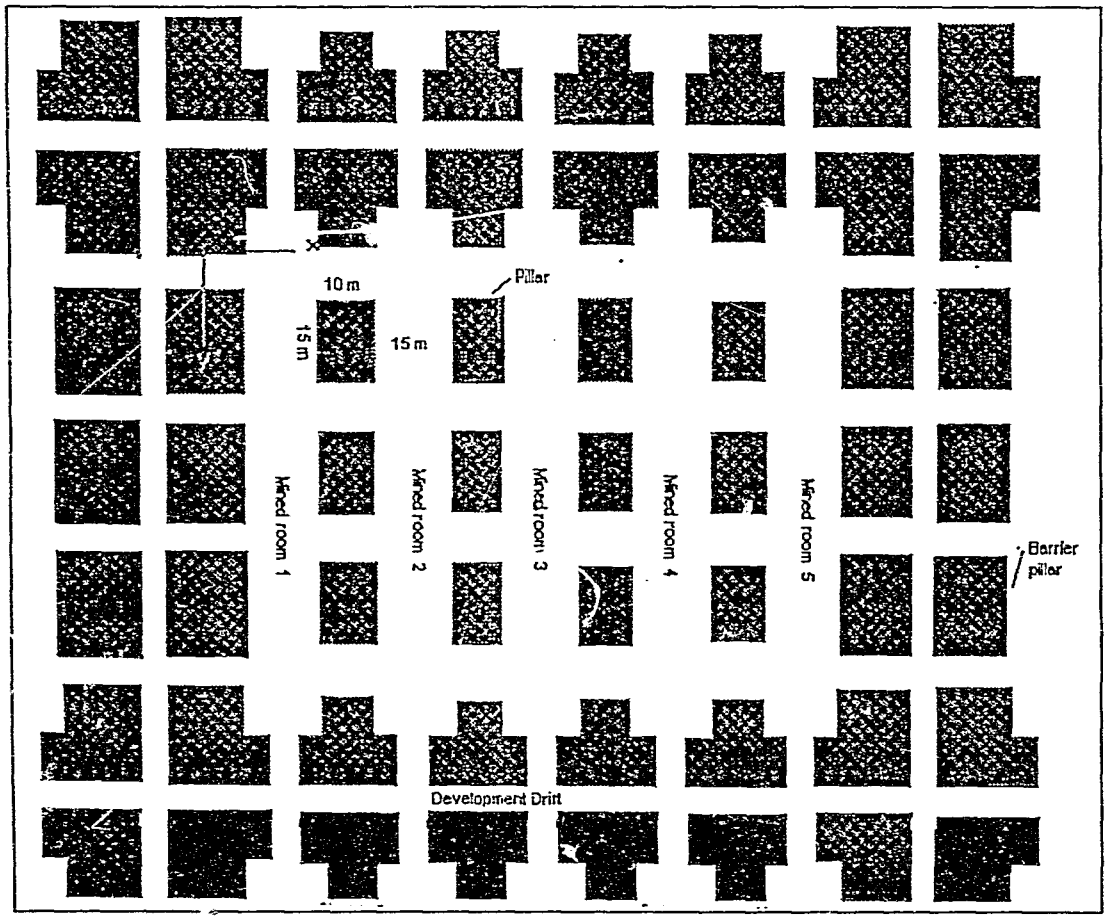

Fig. 5.2 Kamoto room and pillar design

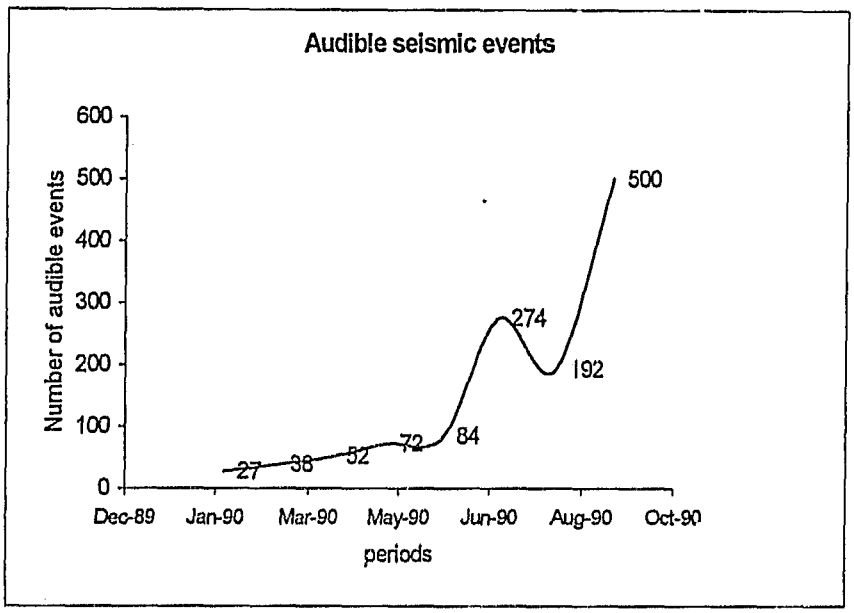

Fig. 5.3 Audible seismic events

Figure 5.3 illustrates the number of events called "Bumps" per month. These are seismic activities that were audible to the miners during eight months before the collapse. These were clear signs that the acting stress in the pillars had reached the pillar strength. Therefore, the aim of this work is to determine what the pillar strength or bearing capacity was in the Kamoto room and pillar workings by combining the classical method and numerical modelling method.

5.2 Stresses in Kamoto Pillars

5.2.1 Tributary area approach

This approach assumes that the ore body is subjected only to vertical and constant pressure from the country rock, each pillar carries the uniform load of rock over a tributary area. Consequently, pillars should be able to carry the all load of

overburden rock. In this case, the equation to compute the pillar stress has been defined in section 2.3.3 by the following mathematical expression:

$$\sigma_p = \gamma H (A / Ap) \qquad (1)$$

Where $A = Ap + Am$: Total area (m^2)

Ap: Pillar area (m^2)

Am: Mined area (m^2)

γ : Unit weight of the overburden (MN/m^3)

H: Depth below surface (m)

σ_p : Pillar load or the average pillar stress (MPa)

The typical Kamoto rectangular pillars parameters required in this formula were:

-Pillar length: 15m

-Pillar width: 10m

-Pillar height: 12 m in upper ore body

14 m in lower ore body

-Unit weight of the overburden: 0.027 MN /m^3

- Depth below surface: 465 m from the upper ore body

492 m from the lower ore body

Table 5.1 gives the average pillar stress from the formula (1) for each ore body.

Table 5.1: Average pillar stress from tributary area concept

Ore body	A(m^2)	Ap(m^2)	γ(MN/m^3)	H(m)	σ_p(MPa)
OBS*	625	150	2.7	465	52
OBI*	625	150	2.7	492	55

OBS* is the upper ore body and OBI* the lower ore body.

Recently, many researchers have shown that the assumptions made in this approach are more conservative and overestimate the pillar load because it does not consider the capacity of the abutment to carry a part of load. From measurements, Hustrulid and Swanson (1981) found that the pillar load could be overestimated by about 40%. This conservative theory may be valid only if the mined-out area, without any barrier pillar, is greater than the mining depth. In fact, the stress distribution is not uniform along the pillar section and is highly sensitive to the width/height ratio.

5.2.2 Numerical approach

5.2.2.1 Stress analysis computer programme

A large number of software packages for geotechnical-engineering purposes are available on the market. For this work, it has been mainly planned to use Minsim-W (Mine simulation). This computer program is a boundary element elastic code for the analysis of stresses and displacements around multiple arbitrarily orientated tabular excavations. The first version (1.1) was developed in 1994/95 by the CSIR's (Council for Scientific and Industrial Research) Mining Technology division. This computer code is widely used in the following mining applications:

- Modelling of changes in stress and deformation associated with incremental mining.
- Modelling of backfill and crush pillars.
- Design assistance of stope layout and support.
- Planning assistance of stope layout and support.
- Potential of fault slip analysis.

MinsimW is composed of three main parts:

1) Mine Edit; this mine plan editor helps to build or to represent a mine situation, which needs to be simulated. At this stage, mining steps, geology, off-reef workings and backfill can be the input.

2) Job set-up; this is the data preparation and processing part. During this step, we can place some on-reef or off-reef sheets in the area of interest to be analysed.

3) Post Processor; this portion of the main programme provides graphic representation of different parameters such as contour plots, stress and displacement vector plots, ERR (energy released rate).

Furthermore, it is important to point out that this programme can accommodate up to 99 reefs, 99 mining steps and 99 coarse and fine on-reef sheets.

5.2.2.2 Kamoto room and pillar model

The aim of this work is to determine the pillar strength from the collapse of room and pillar workings in Kamoto mine. In order to understand the complex mechanism of pillar loading and to determine the pillar stress values just before the collapse, a numerical modelling approach was used in this investigation. This approach would enable simulation of the situation of pillar loading in time and space from the beginning of benching to the manifestation of instability in the Kamoto room and pillar area. This model takes into account the quasi-real situation of pillars left during the mining process, mining strategy adopted at Kamoto mine and the physico-mechanical properties of rock mass as calculated in Chapter 4.

Kamoto room and pillar area has been modelled with the well-known computer code MinsimW (Mine simulation for windows) described in Section 2.5. It has been chosen because it is particularly suitable for use in design and back analysis

in room and pillar system of multiple seams. This computer code is widely used in the mining industry. The MinsimW/Mine edit program and the Summasketch 3 digitizer have been used to generate the different computer mine plans (Fig. 5.4a and 5.4b) from the real Kamoto mine plans. This model includes the mining steps based on the mining strategy that was familiar, and the approximate periods during the Kamoto room and pillar benching. Five main mining steps have been selected for the purpose of this work.

Mining step	Approximate mining period
1	1982 – 1985
2	1985 – 1987
3	1987 – 1988
4	1988 – 1989
5	1989 – 1990

5.2.2.3 Assumptions and parameters required in MinsimW

Some assumptions and parameters have been established before carrying out the MinsimW programme as follows:

a) The room and pillar area is assumed to be almost horizontal at the mining depths of 465 and 492 meters for the upper and lower ore bodies respectively.

b) The local coordinate system of Kamoto mine has been adjusted to right handed system with a positive Z down system that is stated in MinsimW.

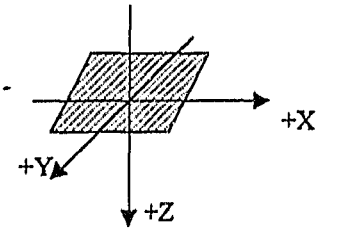

c) After running tests and according to the size of a typical pillar (15x10 m), a decision was made to select the grid element size of 6x6 m for the coarse sheets in order to improve the resolution. A coarse sheet has 64x64 square elements and covers 384x384 m^2 of mined area. For the Kamoto model, a total of 8 coarse sheets have been positioned on each ore body in order to extend over all the mined area (Fig. 5.4a and 5.4b).

d) In order to obtain a fine solution, fine sheet has been placed within a coarse on-reef sheet covered the first mining step in each ore body as the area of interest. MinsimW automatically allocate a grid element size of 1.5 x 1.5 m for these fine windows. Two and one fine sheets have been provided in this model for the upper and lower ore bodies respectively, as shown in Fig. 5.4a and 5.4b

e) From the properties of rock mass classification given in section 4.5, Table 4.6, the following parameters have been assessed for MinsimW' use, as shown in Table 5.2. Laubscher's monogram (Appendix E) has been used to estimate the strength of rock mass of the lower ore body comprising hard and soft layers.

Table 5.2 Parameters and constants used in MinsimW

Reef designation	Sigcm (MPa)	Cohesion (MPa)	Friction angle	Ore body thickness (m)	Young modulus (MPa)
Upper ore body (OBS)	20	4.7	40	12	19953
Lower ore body (OBI)	29	6.9	40	14	27320

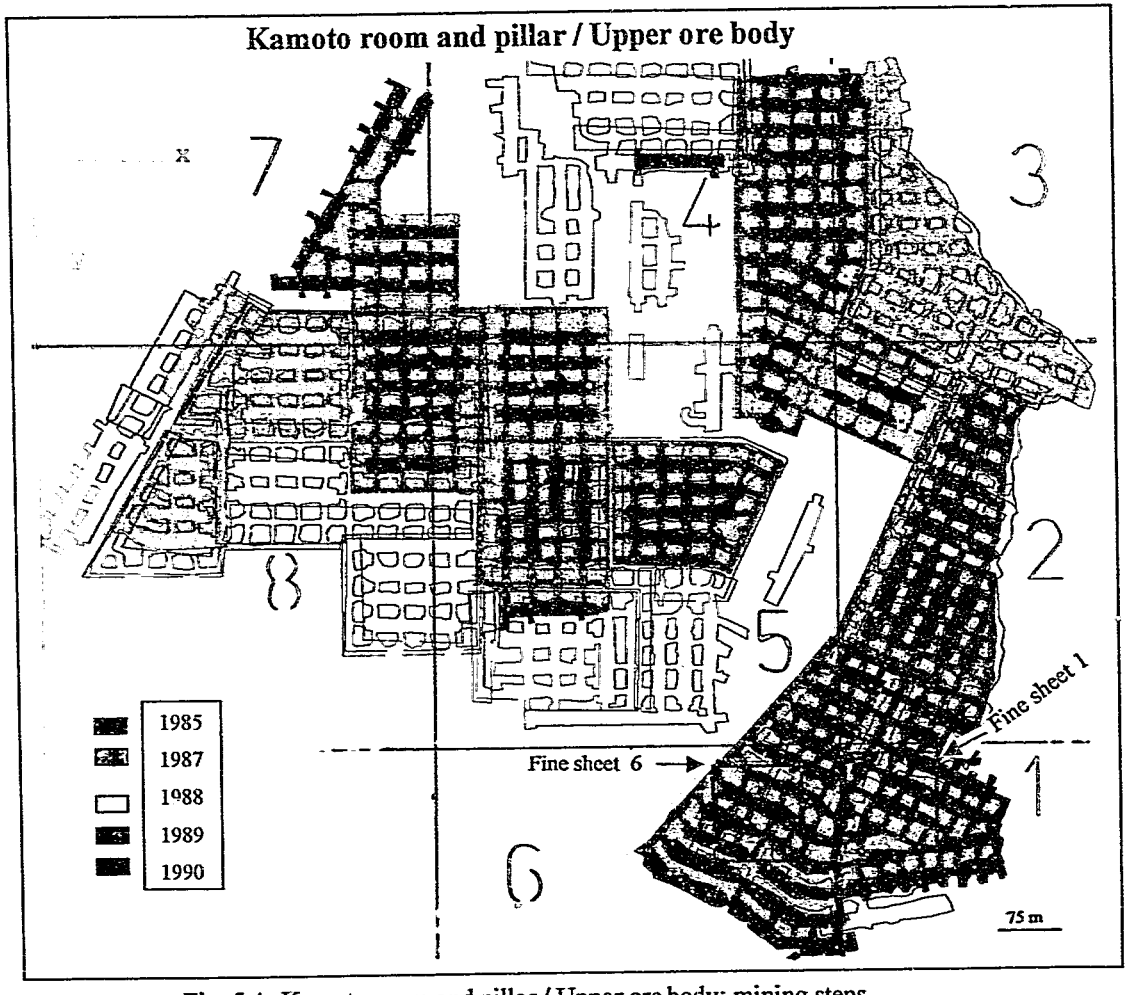

Fig. 5.4a Kamoto room and pillar / Upper ore body: mining steps

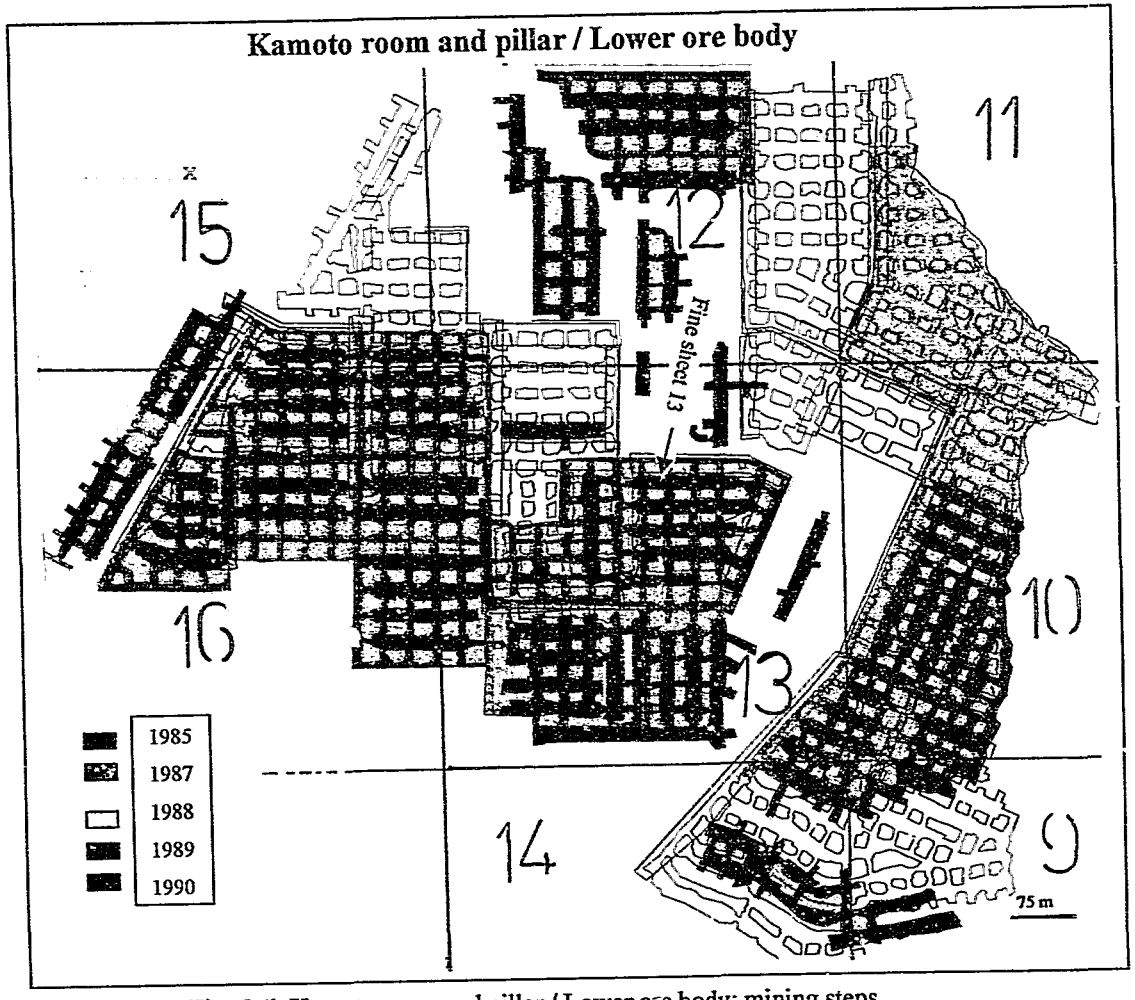

Fig. 5.4b Kamoto room and pillar / Lower ore body: mining steps

In this MinsimW version, the elasticity modulus and the Poison's ratio are assumed to be the same for host rock and the ore body. For this study, the Young modulus of 23637 MPa and the Poison's ratio of 0.29 have been used as average values between the two ore bodies.

f) The sign convention is that the compressive stresses are negative and the tensile stresses are positive.

5.2.2.4 MinsimW results

The MinsimW/Job set-up uses the Solution and Benchmark programs to compute stress and displacement values at the centre of each element for both coarse and fine sheets. After each run, the program creates various output files, which contain different rock mechanics variables. Each variable or a criterion using different variables can be displayed or plotted by using the MinsimW/Post processor programme.

Tables 5.3 to 5.14 and Figures 5.8 to 5.11 show the compilation of MinsimW output values of some rock engineering parameters for five pillars in the upper ore body and six pillars in the lower ore body which are covered by the fine sheets (Fig. 5.5a, Fig.5.5b and Appendix F). In this work, the selected rock engineering parameters are as follows:

- TZZH: Hangingwall stress in the direction normal to the ore body (MPa)
- TXXH: Hanging wall stress in ore body strike direction (MPa)
- TYYH: Hangingwall stress in ore body dip direction (MPa)
- SIG1: Major principal stress (MPa)
- SIG2: Intermediate principal stress (MPa)
- SIG3: Minor principal stress (MPa)

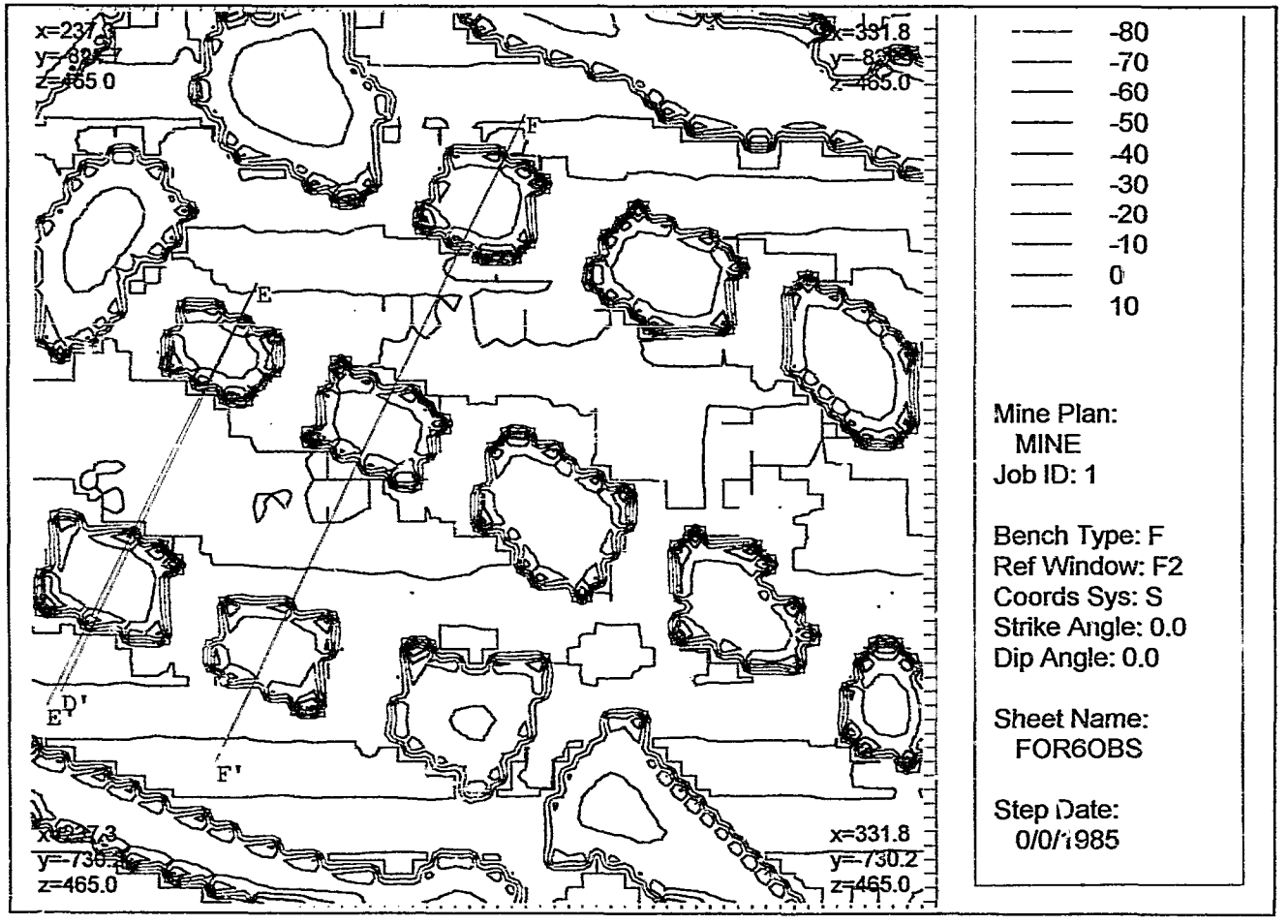

Fig. 5.5a Fine sheet 6 on the upper ore body showing vertical stress (TZZH) in MPa around unmined (pillar) ground

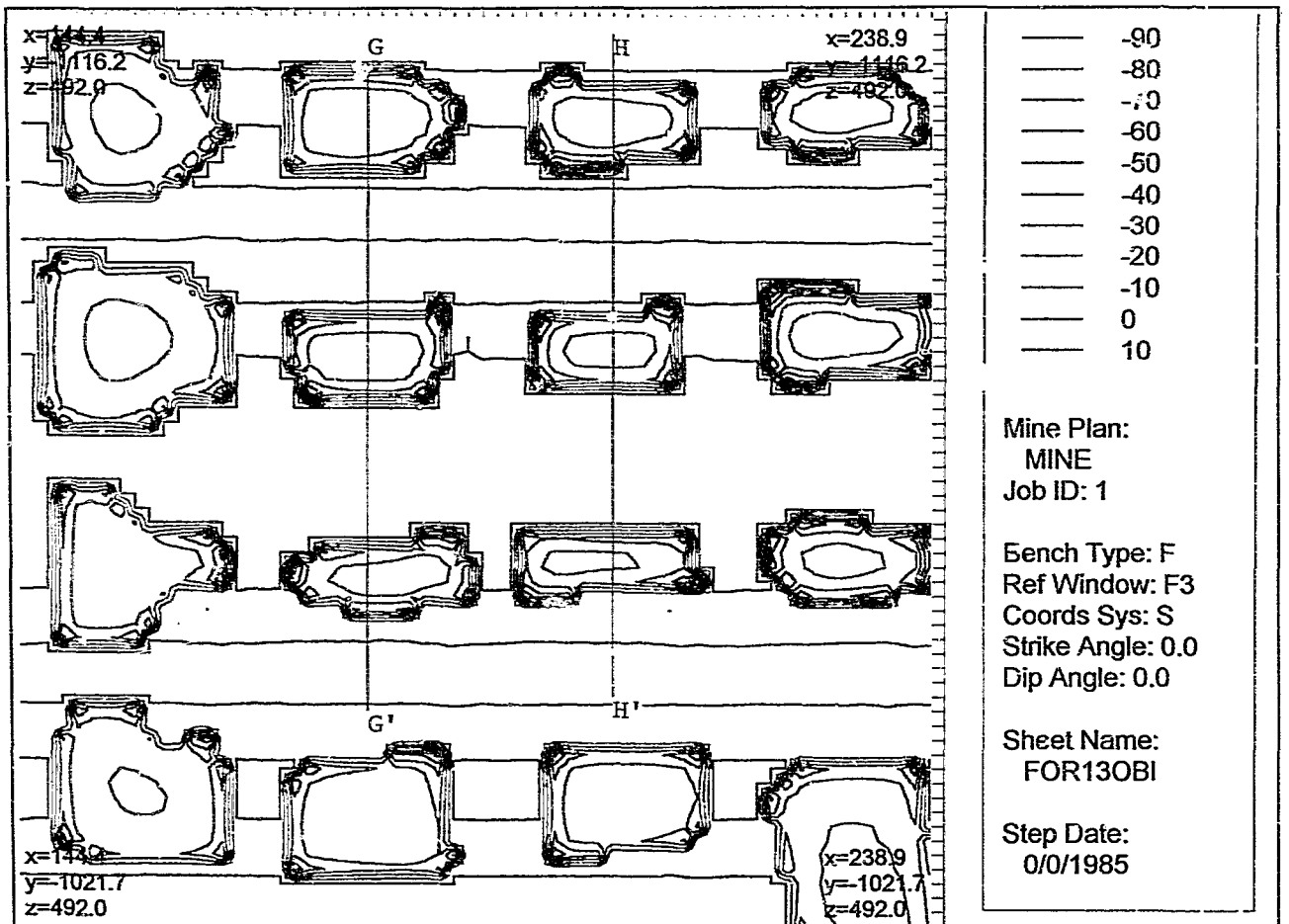

Fig. 5.5b Fine sheet 13 on the lower ore body showing vertical stress (TZZH) in MPa around unmined (pillar) ground

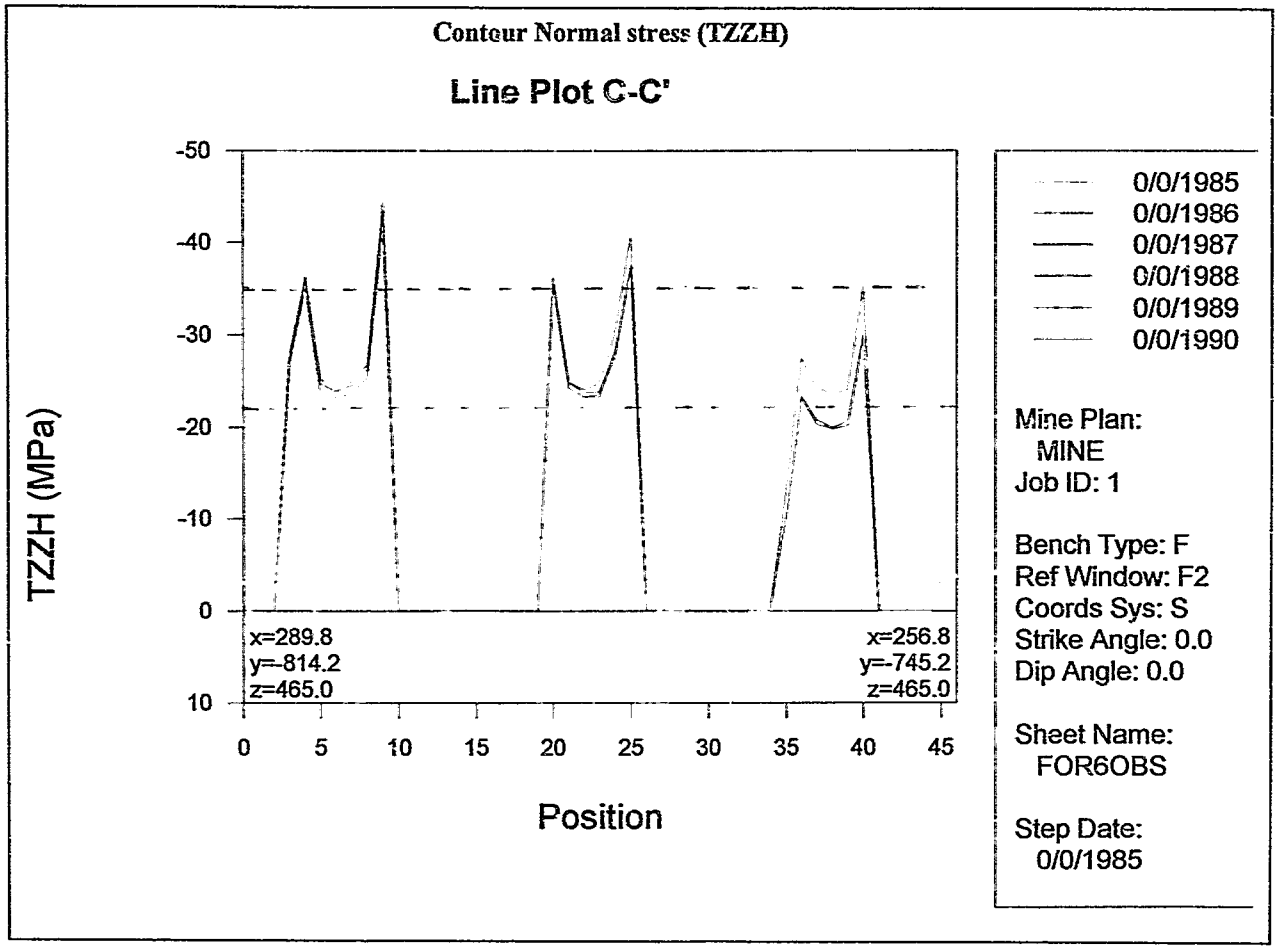

Fig. 5.6 Normal stress (TZZH) line plot in the upper ore body pillars

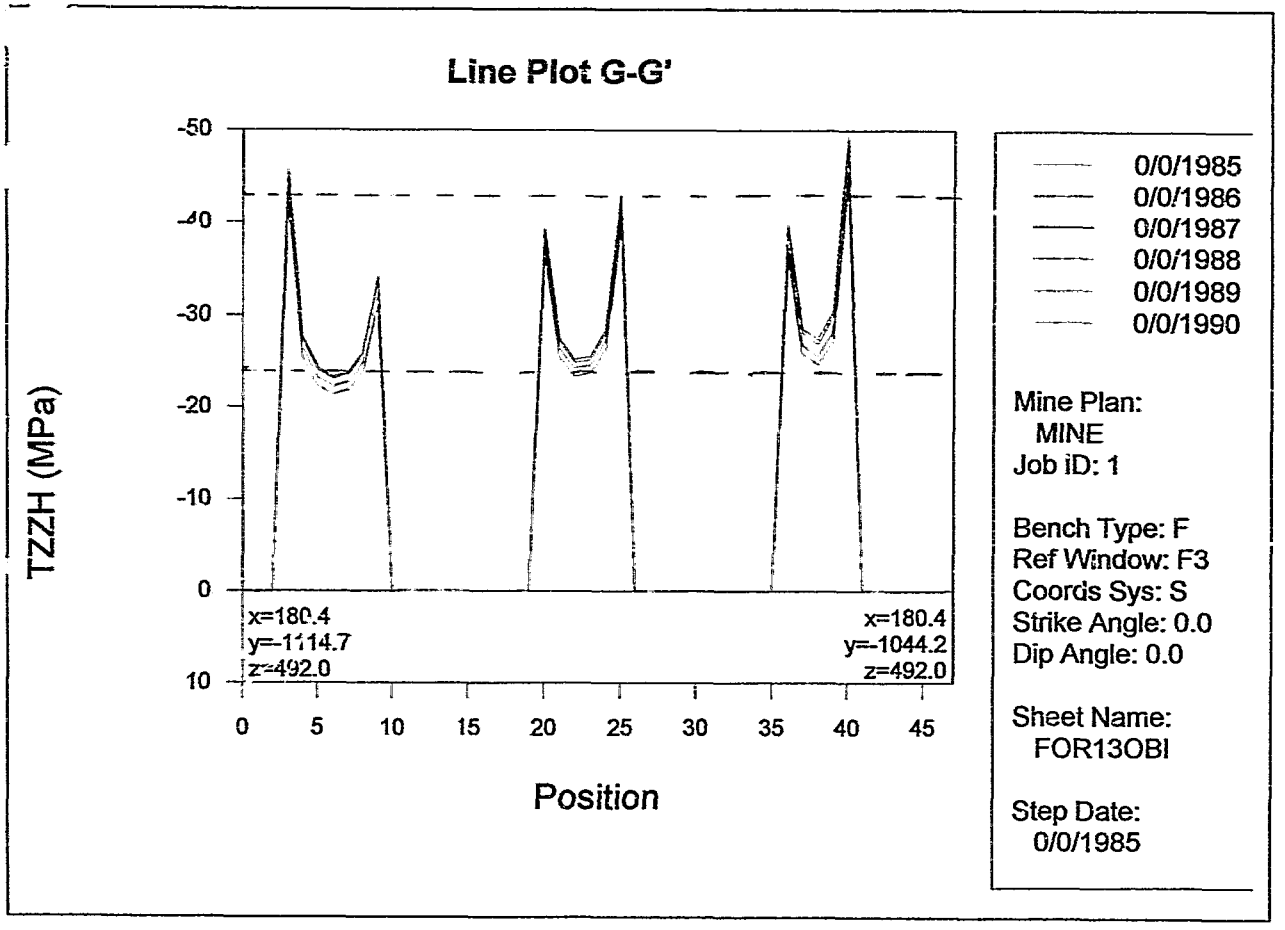

Fig. 5.7 Normal stress (TZZH) line plot in the lower ore body pillars

UPPER ORE BODY

Table 5.3 Normal stress (TZZH) in the upper ore body

	Peak abutment TZZH (Mpa)					Centre of pillar TZZH (MPa)				
	Mining steps					Mining steps				
Pillar No	1	2	3	4	5	1	2	3	4	5
1	-29	-25	-25	-25	-25	-22	-19	-19	-19	-19
2	-32	-32	-32	-32	-32	-23	-24	-24	-24	-24
3	-47	-50	-50	-50	-50	-24	-25	-26	-26	-26
4	-29	-30	-30	-30	-30	-25	-25	-24	-24	-24
5	-43	-38	-37	-37	-37	-22	-20	-19	-19	-19
Average	-36	-35	-35	-35	-35	-23	-23	-22	-22	-22

Table 5.4 Strike stress (TXXH) in the upper ore body

	Peak abutment TXXH (Mpa)					Centre of pillar TXXH (MPa)				
	Mining steps					Mining steps				
Pillar No	1	2	3	4	5	1	2	3	4	5
1	-18	-16	-16	-16	-16	-13	-12	-12	-12	-12
2	-20	-20	-20	-20	-20	-14	-14	-14	-14	-14
3	-32	-33	-33	-33	-33	-15	-15	-15	-15	-15
4	-28	-28	-28	-28	-28	-16	-15	-15	-15	-15
5	-34	-30	-30	-30	-30	-16	-14	-14	-14	-14
Average	-26	-25	-25	-25	-25	-15	-14	-14	-14	-14

Table 5.5 Dip stress (TYYH) in the upper ore body

	Peak abutment TYYH (MPa)					Centre of pillar TYYH (MPa)				
	Mining steps					Mining steps				
Pillar No	1	2	3	4	5	1	2	3	4	5
1	-23	-20	-20	-20	-20	-14	-14	-14	-14	-14
2	-25	-25	-25	-25	-25	-16	-15	-15	-15	-15
3	-38	-39	-39	-39	-39	-16	-16	-16	-16	-16
4	-27	-28	-28	-28	-28	-16	-15	-15	-15	-15
5	-34	-30	-30	-30	-30	-16	-14	-14	-14	-14
Average	-29	-28	-28	-28	-28	-16	-15	-15	-15	-15

Table 5.6 Major principal stress (SIG1) in the upper ore body

	Peak abutment SIG1 (MPa)					Centre of pillar SIG1 (MPa)				
	Mining steps					Mining steps				
Pillar No	1	2	3	4	5	1	2	3	4	5
1	-30	-25	-25	-25	-25	-22	-17	-17	-17	-17
2	-29	-30	-30	-30	-30	-23	-24	-24	-24	-24
3	-48	-52	-52	-52	-52	-24	-25	-26	-26	-26
4	-29	-29	-29	-30	-30	-25	-25	-25	-26	-26
5	-42	-38	-38	-38	-38	-22	-19	-19	-19	-18
Average	-36	-35	-35	-35	-35	-23	-22	-22	-22	-22

Table 5.7 Intermediate principal stress (SIG 2) in the upper ore body

	Peak abutment SIG 2 (MPa)					Centre of pillar SIG 2 (MPa)				
	Mining steps					Mining steps				
Pillar No	1	2	3	4	5	1	2	3	4	5
1	-25	-22	-22	-22	-22	-16	-15	-15	-15	-15
2	-27	-26	-26	-26	-26	-16	-15	-15	-15	-15
3	-31	-32	-32	-32	-32	-14	-15	-15	-15	-15
4	-23	-22	-22	-22	-22	-18	-17	-17	-17	-17
5	-36	-32	-32	-32	-31	-16	-15	-15	-15	-15

Table 5.8 Minor principal stress (SIG 3) in the upper ore body

	Peak abutment SIG 3 (MPa)					Centre of pillar SIG 3 (MPa)				
	Mining steps					Mining steps				
Pillar No	1	2	3	4	5	1	2	3	4	5
1	-17	-15	-15	-15	-15	-13	-12	-12	-12	-12
2	-18	-18	-18	-18	-18	-14	-14	-14	-14	-14
3	-37	-38	-38	-38	-38	-15	-16	-16	-16	-16
4	-17	-17	-17	-17	-17	-14	-14	-14	-14	-14
5	-25	-22	-22	-22	-22	-13	-12	-11	-11	-11
Average	-23	-22	-22	-22	-22	-14	-14	-13	-13	-13

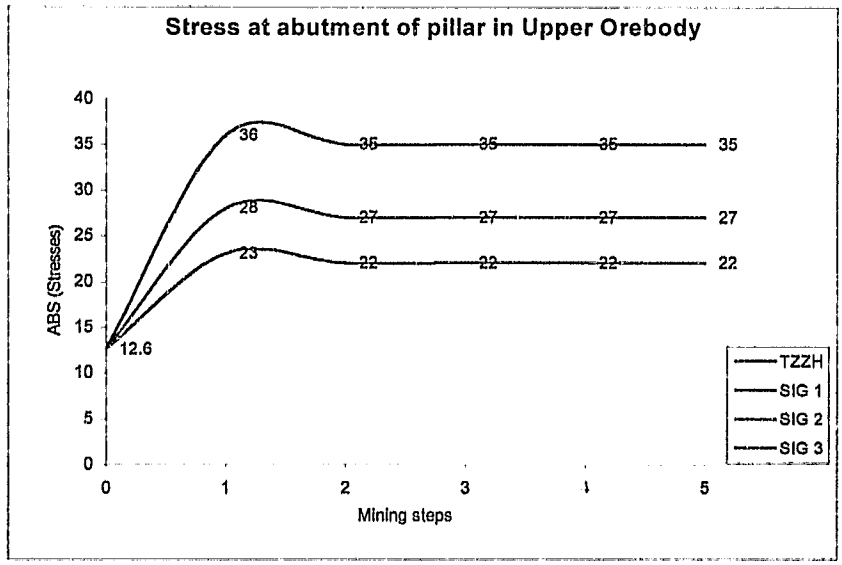

Fig.5.8 Stress at abutment of pillar in upper ore body

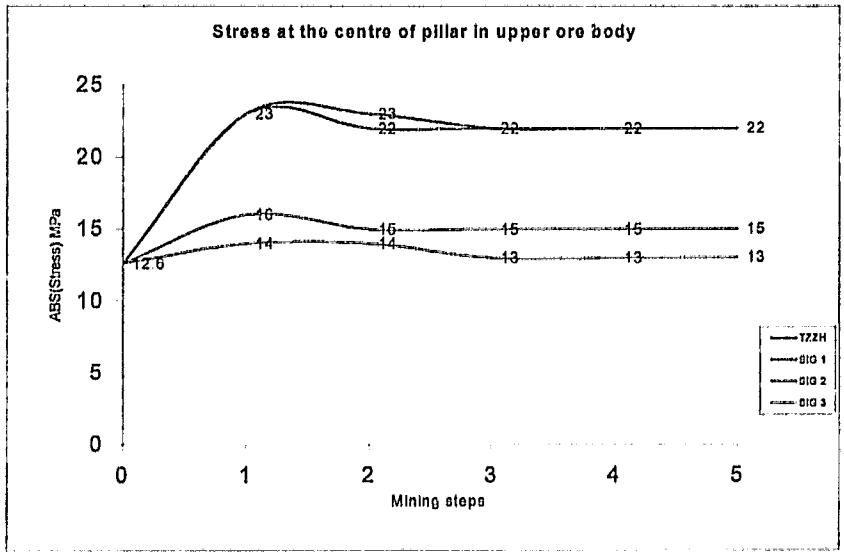

Fig.5.9 Stress at the centre of pillar in upper ore body

LOWER ORE BODY

Table 5.9 Normal stress (TZZH) in the lower ore body

	Peak abutment TZZH (MPa)					Centre of pillar TZZH (MPa)				
	Mining steps					Mining steps				
Pillar No	1	2	3	4	5	1	2	3	4	5
1	-45	-46	-44	-44	-44	-23	-23	-22	-21	-21
2	-43	-42	-43	-42	-42	-25	-25	-25	-24	-23
3	-47	-48	-48	-45	-45	-27	-27	-26	-25	-25
4	-52	-52	-52	-49	-49	-25	-25	-24	-24	-22
5	-39	-39	-38	-38	-36	-26	-27	-25	-24	-24
6	-43	-44	-44	-40	-40	-29	-30	-30	-27	-27
Average	-45	-45	-45	-43	-43	-26	-26	-25	-24	-24

Table 5.10 Strike stress (TXXH) in the lower ore body

	Peak abutment TXXH (MPa)					Centre of pillar TXXH (MPa)				
	Mining steps					Mining steps				
Pillar No	1	2	3	4	5	1	2	3	4	5
1	-27	-26	-26	-26	-26	-14	-13	-13	-13	-13
2	-27	-28	-27	-27	-27	-14	-15	-14	-14	-14
3	-28	-27	-27	-27	-27	-15	-15	-15	-14	-14
4	-31	-31	-30	-30	-30	-14	-14	-14	-14	-14
5	-23	-23	-22	-22	-22	-16	-17	-14	-14	-14
6	-24	-24	-23	-23	-23	-16	-16	-16	-16	-15
Average	-27	-27	-26	-26	-26	-15	-15	-14	-14	-14

Table 5.11 Dip stress (TYYH) in the lower ore body

	Peak abutment TYYH (MPa)					Centre of pillar TYYH (MPa)				
	Mining steps					Mining steps				
Pillar No	1	2	3	4	5	1	2	3	4	5
1	-39	-39	-39	-38	-38	-16	-16	-16	-15	-15
2	-34	-35	-34	-33	-32	-17	-17	-17	-16	-16
3	-39	-40	-39	-39	-39	-20	-20	-19	-18	-18
4	-31	-32	-31	-30	-30	-15	-15	-14	-14	-14
5	-23	-23	-22	-22	-22	-16	-16	-15	-15	-15
6	-24	-24	-23	-23	-23	-16	-16	-15	-15	-15
Average	-32	-32	-31	-31	-31	-17	-17	-16	-16	-16

Table 5.12 Major principal stress (SIG1) in the lower ore body

	Peak abutment SIG1 (Mpa)					Centre of pillar SIG1(MPa)				
	Mining steps					Mining steps				
Pillar No	1	2	3	4	5	1	2	3	4	5
1	-36	-36	-36	-34	-34	-18	-18	-18	-17	-17
2	-33	-34	-34	-32	-31	-20	-20	-20	-19	-19
3	-37	-38	-38	-36	-36	-21	-21	-21	-20	-20
4	-52	-51	-51	-50	-49	-25	-25	-25	-24	-23
5	-39	-40	-38	-38	-37	-26	-27	-27	-25	-24
6	-43	-44	-44	-42	-40	-29	-30	-30	-27	-27
Average	-40	-41	-40	-39	-38	-23	-24	-24	-22	-22

Table 5.13 Intermediate principal (SIG 2) in the lower ore body

	Peak abutment SIG 2 (Mpa)					Centre of pillar SIG 2 (MPa)				
	Mining steps					Mining steps				
Pillar No	1	2	3	4	5	1	2	3	4	5
1	-37	-38	-37	-37	-36	-16	-16	-16	-15	-15
2	-35	-35	-35	-35	-34	-17	-18	-18	-17	-16
3	-40	-41	-41	-39	-39	-20	-20	-20	-19	-18
4	-44	-45	-45	-44	-43	-18	-18	-17	-17	-17
5	-32	-32	-32	-31	-30	-19	-19	-19	-18	-18
6	-34	-35	-35	-34	-34	-22	-22	-22	-21	-21
Average	-37	-38	-38	-37	-36	-19	-19	-19	-18	-18

Table 5.14 Minor principal stress (SIG 3) in the lower ore body

	Peak abutment SIG 3 (Mpa)					Centre of pillar SIG 3 (MPa)				
	Mining steps					Mining steps				
Pillar No	1	2	3	4	5	1	2	3	4	5
1	-26	-26	-26	-25	-25	-13	-12	-12	-13	-12
2	-25	-25	-24	-24	-23	-14	-15	-15	-14	-14
3	-28	-29	-29	-27	-26	-15	-15	-15	-15	-14
4	-31	-32	-32	-31	-30	-14	-14	-14	-14	-13
5	-23	-23	-22	-22	-21	-16	-16	-16	-15	-15
6	-24	-25	-23	-23	-22	-16	-16	-16	-15	-15
Average	-26	-27	-26	-25	-25	-15	-15	-15	-14	-14

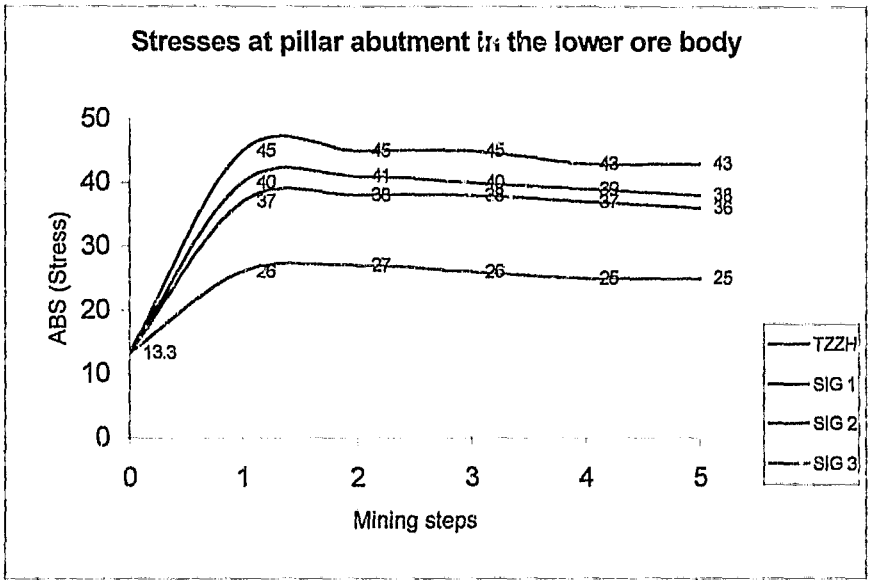

Fig. 5.10 Stress at pillar abutment in lower ore body

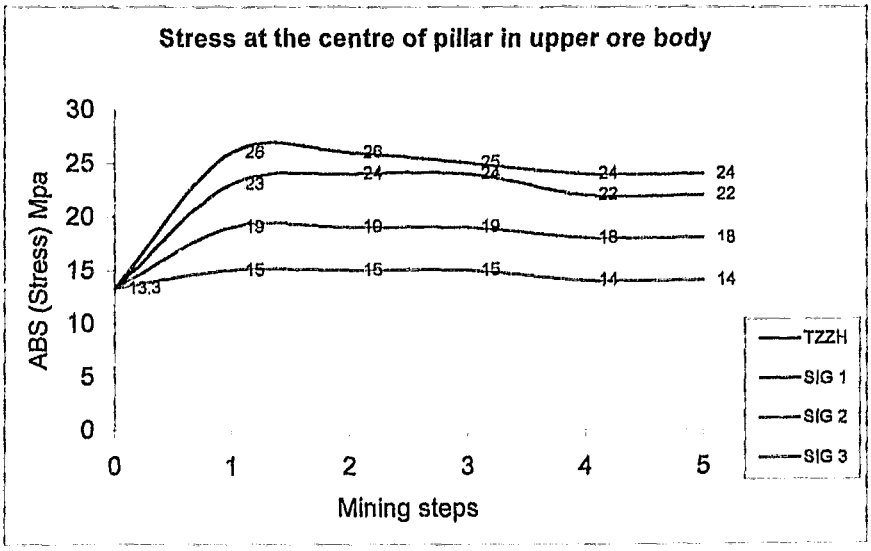

Fig.5.11 Stress at the centre of pillar in the lower ore body

5.3 Kamoto Pillar Strength

The strength of rock pillars is the ultimate stress at which failure occurs. This value may be assessed either by extrapolation of the uniaxial compressive strength from laboratory tests or based on a rock mass classification system in combination with some pillar strength formulae. In some cases, the back analyses of mining histories have been used. In this work, empirically based formulae used in hard rock pillar design and numerical modelling results have been employed to evaluate the strength of Kamoto rectangular pillars left in the room and pillar area.

5.3.1 Cubical strength of rock mass or K value

The cubical strength of rock mass or the K value is the critical data involved in pillar strength formulas. The literature survey has shown that the K value is subject to much discussion in the field of rock engineering. This is confirmed by the existence of several methods of its estimation. However, in this work, the first K values have been assessed from the RMI system in Section 4.5:

- For the upper ore body pillars, K = 29 MPa
- For the lower ore body pillars, K = 32 MPa

Ryder and Ozbay (1990) suggested another procedure in which a factor of 1.3 is used to adjust the difference in shape between a standard cylindrical core and a cube of rock. From the strength of Kamoto rock mass obtained by using Hoek *et al.*(1995) method in the Section 4.4, K values or the strength of a unit cube of the pillar material for each ore body can be calculated as follows:

- For the upper ore body pillars, K = 20.0 x 1.3 = 26 MPa
- For the lower ore body pillars, K = 29.8 x 1.3 = 39 MPa

5.3.2 Pillar strength by Salamon's formula

Salamon (1967) expressed the strength of rectangular pillars by the following equation:

$$\sigma_s = K (w^{\alpha} / h^{\beta}) \qquad (1)$$

Where σ_s is the pillar strength

h is the pillar height

w is the equivalent pillar width that is calculated after Wagner (1980) by this equation $w = 4A/C$, where A is the plane area and C the perimeter of pillar.

α and β are constants. For pillars in hard rock, Hedley and Grant (1972) suggested the values of 0.5 and 0.75 for α and β respectively.

K is the strength of one cubic meter of pillar material.

Knowing the mechanical properties of the rock, the strength of the pillar depends on the pillar size; width and height. For w = 12 m and h = 12 and 14 m in the upper and lower ore bodies respectively, the strength of pillars in Kamoto room and pillar should have been as follows:

a) With K values from the RMI system,

- $\sigma_p = 29 (w^{0.5}/h^{0.75}) = 16$ MPa for the upper ore body pillars
- $\sigma_p = 32 (w^{0.5}/h^{0.75}) = 15$ MPa for the lower ore body pillars

d) With K values from the combination of Ryder and Ozbay's procedure and Hoek *et al.*(1995) method,

- $\sigma_p = 26 (w^{0.5}/h^{0.75}) = 14$ MPa for the upper ore body pillars
- $\sigma_p = 39 (w^{0.5}/h^{0.75}) = 19$ MPa for the lower ore body pillars

5.3.3 Pillar strength by Obert-Duvall formula

Obert and Duvall (1967) derived the following pillar strength formula from laboratory tests on hard rock and elasticity for width-height ratio of 0.25 to 4.0:

$$\sigma_p = K\ (0.778 + 0.222\ w/h)$$

Where σ_p is the pillar strength,

K is the uniaxial compressive strength of a cubical specimen and

w and h are pillar dimension.

For the same width and height, the pillar strength formula becomes:

a) With K values from the RMI system,

- $\sigma_p = 29\ (0.778 + 0.222\ w/h) = 29$ MPa for the upper ore body pillars
- $\sigma_p = 32\ (0.778 + 0.222\ w/h) = 31$ MPa for the lower ore body pillars

b) With K values from the combination of Ryder and Ozbay's procedure and Hoek *et al.*(1995) method,

- $\sigma_p = 26\ (0.777 + 0.222\ w/h) = 26$ MPa for the upper ore body pillars
- $\sigma_p = 39\ (0.777 + 0.222\ w/h) = 38$ MPa for the lower ore body pillars

Figures 5.12 and 5.13 illustrate the comparison between the pillar strengths from Salamon's formula and Obert *et al.* formula with the same K value (K=26 MPa for the upper ore body and K=39 MPa for the lower ore body). These two cases indicate the variation of pillar strength with the pillar width and the mining height:

a) $\sigma_p \rightarrow f(w)$: the pillar strength with a constant mining height (h) of 14 m in the lower ore body and a variable pillar width is as follows:

$\sigma_p = 5.39\ W^{0.5}$ (Salamon's formula)

$\sigma_p = 30.34 + 0.62\ w$ (Obert-Duvall formula)

b) $\sigma_p \rightarrow f(h)$: the pillar strength with constant width (w) of 12m in the lower ore body and a variable mining heig as follows:

$\sigma_p = 90 / h^{0.75}$ (Salamon's formula)

$\sigma_p = 30.34 + 103.9 / h$ (Obert-Duvall formula)

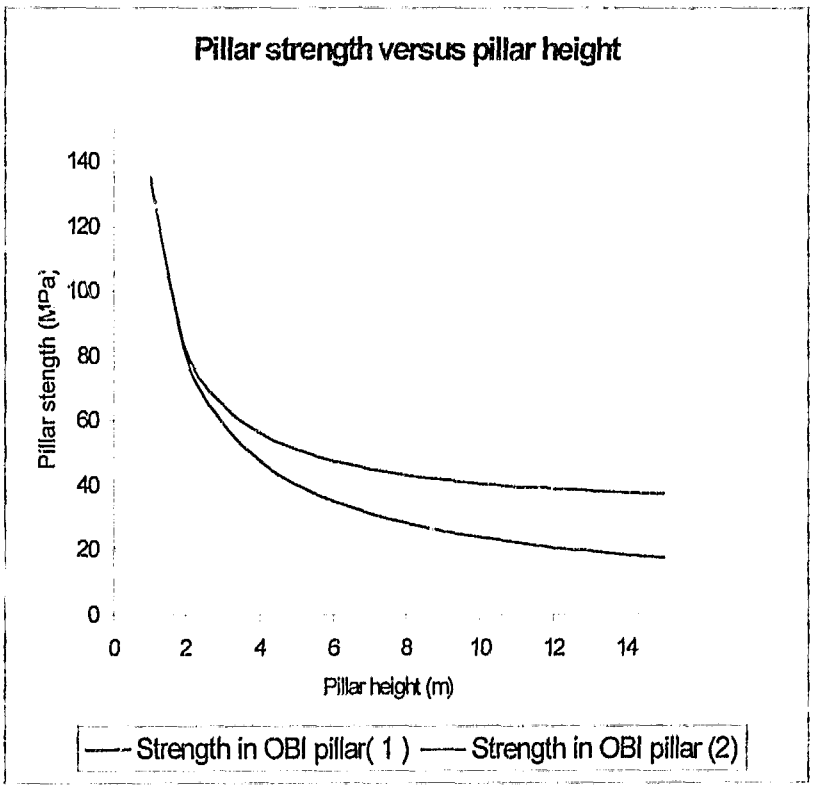

Fig.5.12 The relationship between pillar strength and pillar height by Salamon's formula (1) and Obert-Duvall formula (2)

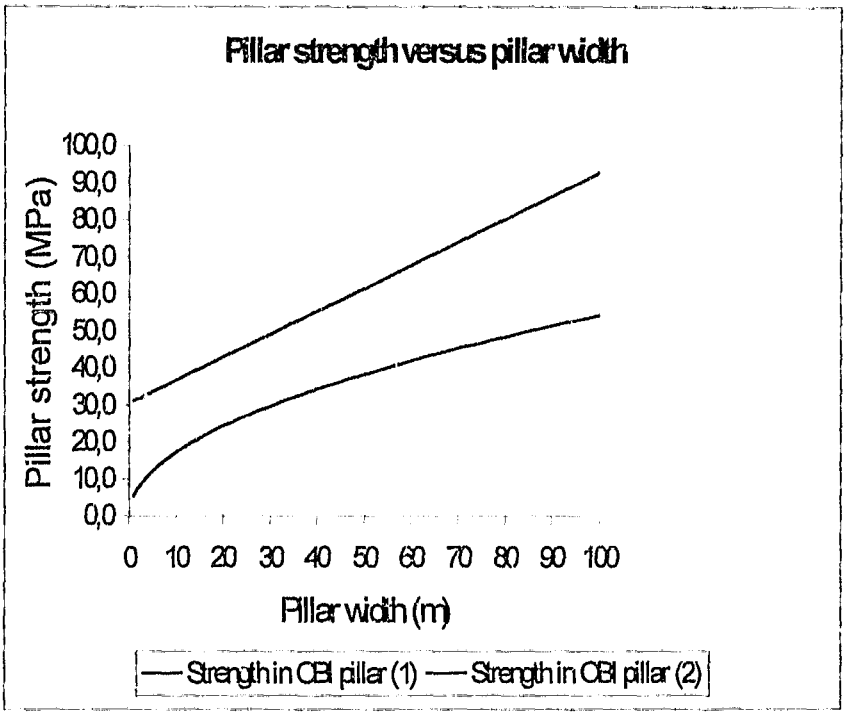

Fig.5.13 The relationship between pillar strength and pillar width by Salamon's formula (1) and Obert-Duvall formula (2)

5.3.4 Pillar strength from MinsimW results

From a back analysis of stresses in Kamoto room and pillar by a boundary elastic code in section 5.2.2.4, it has been stated that at the time approaching the collapse the average stresses in the direction normal to the pillars were as follows:

- 35 MPa and 22MPa at the abutment and the centre of pillar in the upper ore body respectively.
- 43 MPa and 24 MPa at the abutment and the centre of pillar in the lower ore body respectively.

These results confirm that the edge of pillar is subjected to a much higher stress than the centre of pillar. Herget (1988) defined a critical field stress as the stress at which a break down of rock or an extensive failure on excavation walls occurs in the field. This happen when the stresses at the pillar edge exceed the strength of the pillar material and the failure mechanism can migrate to the pillar centre and destroy the pillar. This is similar to what it has been observed in the Kamoto room and pillar area before the large-scale instability. Therefore, the rectangular pillar strength may be derived from these ultimate pillar edge stresses as follows:

- The pillar strength of 35 MPa for the upper ore body pillars
  The pillar strength of 43 MPa for the lower ore body pillars

5.4 Admissible Pillar Stress

Taking into account a factor of safety (SF) of 1.6 in Kamoto room and pillar conditions, the average acting stress on rectangular pillars designed should not exceed 22 MPa and 27 MPa respectively in the upper and lower ore bodies. According to stress values either from the tributary area theory or from numerical modelling, the pillars in Kamoto mine room and pillar workings were unstable structures.

5.5 Conclusion

From these analyses and results obtained throughout this chapter, the following conclusions may be drawn:

a) The pillar stress predicted from the tributary area is higher than that computed by numerical modelling.

b) The strengths of one cubic meter of ore body rock material using separately the RMI method and the combination of Ryder-Ozbay procedure and Hoek *et al.* (1995) method are as follows:

Ore body	K values (Mpa)	
	RMI method	Ryder-Ozbay procedure and Hoek et al. method
Upper	29	26
Lower	32	39

c) Figures 5.12 and 5.13 show that for a constant pillar width and a constant height, Salamon's pillar strength formula is more conservative than the Obert-Duvall formula.

d) This back-analysis has shown that the Kamoto pillars in room and pillar area were subjected to high stress since they were isolated. It is probably that the failure mechanism was delayed due to the presence of barrier pillars.

e) The numerical modelling of Kamoto room and pillar reveals that the stresses' limit corresponding to the rectangular pillar strengths were 35 MPa and 43 MPa respectively in the upper and lower ore bodies.

f) The low pillar width/height ratios between 0.8 and 1 had played an unfavourable role in the strength of rectangular pillars in Kamoto room and pillar.

g) The MinsimW run with backfill has not given a significant difference. This confirms that the uncemented backfill in its passive role could not carry any load. However, it could improve the pillar sidewall confinement in order to reduce the spalling.

CHAPTER 6

DISCUSSION OF RESULTS

6.1 Introduction

This chapter will focus on the analysis and interpretation of the different results presented in the previous chapters, namely the Kamoto rock mass classification, pillar stress and strength, in order to evaluate their reliability and validity in the context of Kamoto room and pillar.

6.2 Rock Mass Classification Results

The input data for rock mass classification have been compiled from the company's available geotechnical database. All geotechnical classification systems are subjective and do not lead to the same results if applied on the same rock mass. The main reason for choosing the Bieniawski's geotechnical rating system and the Rock Mass Index (after Palmström) to classify the rocks of Kamoto has been clearly explained in Section 4.1.

Bieniawski's classification has shown that the Rock Mass Rating system (RMR), which defines the Geological Strength Index (GSI), is between 57 for Red RAT rock and 70 for the stratified dolomite. From this method, different types of Kamoto rocks are classified as " Good rock", except Red RAT, which is the group of "Fair rock". Although the data size is limited, the Geological Strength Index gives a relatively good idea about the effects of properties of rock mass on its strength.

From the procedure suggested by Hoek et al. (1995) using the relationship between the Hoek-Brown and the Mohr-Coulomb failure criteria and the GSI concept, it was possible to determine different parameters that define the properties of Kamoto jointed rock mass. In terms of this concept, the different

spreadsheets as shown in Appendix D compute the elasticity modulus, strength, friction angle, cohesion and constants mb and s required in the Hoek-Brown equation. Results in Section 4.4 show that the mechanical properties of rock mass depend on the Geological Strength Index (GSI) values.

An additional rock mass classification by the Rock Mass Index (RMI) method, developed by Palmström (1995), has evaluated the jointing parameter or the reduction factor of the intact rock compressive strength at 0.21 (21%). Therefore, the strengths of a cubic meter of Kamoto rock mass are 29 MPa and 32 MPa for the upper and lower ore bodies respectively. Table 6.1 summarises the values of rock mass strength obtained from the two procedures.

Table 6.1: comparison between intact rock and rock mass strengths

Ore body	Intact rock strength (Mpa)	Mix system*		RMI system
		Rockmass strength (MPa)	K value (MPa)	K value (MPa)
Upper	136	20.0	26.0	29.0
Lower	152	29.8	39.0	32.0

* The mix system is a combination of RMR system, GSI approach, Hoek-Brown failure criterion and Ryder-Ozbay procedure.

According to these results, the uniaxial compressive strength of rock mass in Kamoto room and pillar area represents between 15 and 21 % of the uniaxial compressive strength of the intact rock. The strength of a unit cube of rock

material or K value is in the range of 20 to 26 % of the uniaxial compressive. These results reveal that the two methods of estimating K value are relevant because the standard deviation in the Kamoto case is between 1.5 and 3.5 MPa (5 to 10 % of the mean value). They are significant because they show clearly that rock mass classification is, to date, the best way to express the rock mass properties in rock engineering. However, detailed research needs to be undertaken in this field in order to provide a useful and adequate tool to mining engineers to select one of the different classification systems encountered in underground engineering.

6.3 Pillar Stress and Strength

Under conditions assumed during the design of the Kamoto model and the use of the elastic boundary element code MinsimW, the following observations can be made concerning stress and strength analysis:

a) The average pillar stress calculated from the tributary area theory is greater by between 29% and 49% higher than those coming from the numerical modeling. This confirms that the tributary area approach overestimates the pillar load when the mined area length is smaller than the mining depth or limited by the existence of barrier pillars within the mining area. This latter case reflects the Kamoto situation.

b) The stress distribution shown in different figures (5.5, 5.6 and appendix F) illustrates that the distribution of stress in the pillar is not uniform. The contours of stresses show that compressive stresses at the abutment are higher than at the centre of the pillar. In the upper ore body, the hangingwall stress in the direction normal to the ore body (TZZH) has the same magnitude as the major principal stress (σ_1). The horizontal stresses (TXXH and TYYH) are about 0.6 times the vertical stress (TZZH) at the center in the upper and lower ore bodies.

c) Figure 5.8 to 5.11 show that, from the earlier stage of benching, the average vertical stress in the rectangular pillar increases from 12.6 MPa (in situ stress) to 22 MPa at the pillar center and to 35 MPa at the pillar border in the upper ore body. It changes from 13.3 MPa to 24 MPa at the center of pillar and to 43 MPa at the pillar board in the lower ore body. Consequently, the pillar edge was subjected to high stress once a pillar was isolated. This confirms that the Kamoto room and rectangular pillar mining system was an unstable structure and apparently the zone of potential rock failure.

d) The different pillar strengths calculated from hard rock pillar design formulae and numerical modelling are recapitulated in Table 6.2.

Table 6.2 Pillar strength values

Method used	Pillar stength (MPa)	
	Upper ore body UCS = 136 MPa	Lower ore body UCS = 152 MPa
Salamon's formula	14 – 16	15 – 19
Obert-Duvall's formula	26 – 29	31 – 38
MinsimW	35	43

This table illustrates that the average strength of the rectangular pillars left during the mining, derived from the numerical analysis of the Kamoto room and pillar collapse, represent 26 % and 28 % of the uniaxial compressive strength of the intact rock respectively in the upper and lower ore bodies. These values are more than twice and about 1.2 times more than those predicted respectively by Salomon's formula and Obert-Duvall's formula. Figures 5.12 and 5.13 show that Salamon's formula is more conservative than the Obert-

Duvall formula for the same width-to-height ratio. The relative difference between the numerical modelling and Salamon's formula is about 59 % while it is 21 % with Obert-Duvall's formula. It is apparent from these figures that for lower width-to-height ratios the Salamon's formula predicts the lowest pillar strength, which is out of the range of pillar strengths from the back analysis, due to the influence of the increase of pillar volume in the formula. For future pillar design at Kamoto mine and in the absence of numerical modelling the Obert-Duvall might be recommended. In fact, doing a cross-checking by using other pillar strength formulas, field instrumentation and engineering judgement must be considered.

Field observations have confirmed that the pillar edge failure by spalling or shearing was observed during the mining of stopes within some blocs, just after pillars have been formed at their final size. Furthermore, The haulage sidewall in the barrier pillar around a mining block, which showed stable conditions during the mining period, started showing intensive fracturation about four months before the large-scale instability. This implies that the overloading mechanism of pillars should have been initiated at the earlier stage of mining and the pillar failure mechanism at Kamoto room and pillar was progressive in time and space, by gradual deterioration of the rock mass. Potvin, Hudyma and Miller (1989) defined this pillar failure as "stable (progressive) pillar failure." the rectangular pillars were likely conveying a part of their load to the barrier pillars around a mining bloc till when the barrier pillars strength has been also exceeded.

CHAPTER 7

CONCLUSIONS AND RECOMMENDATIONS

7.1 Conclusions

From the rock mass classification, empirical method for determination of pillar strength, numerical modeling, field observations and the assumptions made in previous chapters, the following main conclusions are drawn:

a) The Geological Strength Index (GSI) or the Rock Mass Rating (RMR_{76}) is in the range of 57 for the Red RAT' (Fair rock) and 70 for the Stratified Dolomite (Good rock) in the stratigraphic column.

b) The strength of rock mass in the area of interest before the collapse, as computed by Hoek-Brown failure criterion for jointed rock mass (Hoek et al.1995), is 20.0 MPa in the upper ore body and 29.8 MPa in the lower ore body.

c) The strength values of a cubic meter of the pillar material derived from a combination of the Rock Mass Rating (Bieniawski's RMR_{76}), the Geological Strength Index (GSI) from Hoek *et al.* (1995) and the Ryder-Ozbay procedure are 26 MPa and 39 MPa respectively for the upper and lower ore bodies. From the Rock Mass Index (RMI) developed by Palmström in 1995, these values are 29 MPa for the upper ore body and 32 MPa for the lower ore body. It has been stated in this work that these two methods are relevant and can be used in the future design at Kamoto mine to assess the K values.

d) The average modelled stresses by a boundary elastic code (MinsimW) acting on the edge of pillar at the time approaching the large scale failure mechanism were 35 MPa and 43 MPa respectively in the upper and lower ore bodies. The spalling observed on the surface of pillars in the two ore bodies was initiated by these stresses. The mechanism of pillar disintegration was progressive, probably due to the existence of some barrier pillars within the mined area. The pillars of 15 m long, 10m wide and 12 m high in the upper ore body or 14 m high in the lower ore body high could not bear more than these loads. Therefore, the average pillar strengths in the Kamoto room and pillar area were 35 MPa (26 % of the UCS) for the upper ore body pillars and 43 MPa (28 % of the UCS) for the lower ore body pillars. These values are more than twice the magnitude of those predicted by Salamon's formula and 1.2 times greater than those assessed by the Obert-Duvall equation.

7.2 Recommendations

a) Despite the research that has been carried out in the last two decades, the determination of pillar strength in hard rock, taking into account the properties of rock, is subject to controversial debate in rock engineering and mine design. This implies that research must continue in order to provide a reliable tool to the mining industry. This should include the use of rock mass classification and numerical modelling on different case histories involving pillar failure in order to improve knowledge of pillar strength estimation in rock engineering. The reliability and relevance of the modified Salamon's strength pillar formula need to be confirmed in different types of hard rock, in terms of the constant values (α =0.5 and β= 0.75) suggested by Hedley and Grant (1972).

b) Even if the most promising concepts in rock engineering have been practised in this work, the available geotechnical data was limited. However, this work represents the beginning of a complete and complex study of Kamoto room and pillar collapse. Therefore, from the rock-engineering point of view, it is important to analyse this case because it is a rare application of the room and pillar block system with pillar barrier. This was applied simultaneously in two thick (12 and 14 meters) and superimposed sedimentary ore bodies at shallow depth.

c) It has been pointed out that not only was the geotechnical data insufficient at the designing stage, but also and above all, it was not sufficiently updated, analysed and interpreted by a multidisciplinary team. Therefore, the understanding of pillar stability might be ambiguous. In order to avoid what happened in the past, the following points are recommended:

- Kamoto mine, Geological Department, Mining research Department and eventually some good external experts should up-date and complete the existing geotechnical database with the rock mass classification, in situ measurements and some important field observations in order to set up a rational engineered approach for design and stability analysis.

- In the light of the conclusion drawn in this work, a mining system suited to sedimentary and flat ore bodies must be investigated and redesigned for the remaining flat parts of Kamoto ore bodies. The objective of the design should be the maximum extraction of ore compatible with safe working conditions.

REFERENCES

Barton et al. (1978) *Suggested Methods for the Quantitative Description of Discontinuities in Rock Masses*, International Journal of Rock Mechanics and Mining Sciences & Geomechanics Abstracts, Vol.15, No. 6. pp.319-368.

Bawden W.F. *et al.* (1989) *Practical rock engineering stope design case histories from Noranda Minerals Inc.* CIM Bulletin, July 1989, Vol 82.No 927. Pp. 37-45

Bieniawski Z. T. (1967) *Mechanism of Brittle Fracture of Rock.* Dr.Sc(Eng.), University of Pretoria, 226p.

Bieniawski Z.T. (1974) *Estimating the Strength of Rock materials.* Journal of the S.A. Inst. of Mining and Metallurgy, March, 1974, pp.395-423.

Bieniawski, Z. T. and Van Heerden, W. L. (1975) *The significance of in situ tests on large rock specimens*, International Journal on Rock Mechanics, Mining Science, Vol. 12, pp.101-113.

Bieniawski Z.T. (1976) *Rock mass classification in rock engineering.* Proc. Symposium on Exploration for Rock engineering, Johannasburg A.A. Balkema, Vol, 1, 97-106.

Bieniawski Z.T. (1984) *Rock Mechanics Design in Mining and Tunnelling*, A.A Balkema, Rotterdam, pp.272.

Brady B.H.G. and Brown E.T. (1985) *Rock mechanics for underground mining*, George Allen & Unwin. London, 527p.

Brown, E. T. (1970) *Strength of models of rock with intermittent joints.* Journal Soil Mech. Found. Div., Am. Soc. Civ. Engrs 96, 1935-49.

Budavari S. (1983) *Rock Mechanics in Mining Practice,* SAIMM, Johannesburg, 282p.

Cahen, L. et al (1984) *The geochronology and evolution of Africa,* Clarendon Press, Oxford, 512 p.

Cailteux J. (1994) *Lithostratigraphy of the Neoproterozoic Shaba-type (Zaire) Roan Supergroup and metallogenesis of associated stratiform mineralization,* Journal of African Earth sciences, vol.19, No. 4, pp.279-301.

Cameron-Clarke I. S. (1978) *An evaluation of the reliability of borehole core data in engineering rock mass classification systems.* MSc Thesis, Johannesburg, 381 p.

Chandrakant, S.D. and John, T. C. (1977) *Numerical Methods in Geotechnical Engineering,* McGraw-Hill, New York.

Coates, D.F. (1966) *Pillar loading – a new hypothesis.* Canada Department of Mines and Technical Surveys, Mines Branch Research reports R168/170/180, February 1966.

Coates D. F. (1970) *Rock Mechanics Principles,* Mining Research Centre / Mines Branch Department of energy, mines and resources. Ottawa,

Crouch S.L. and Starfield (1983) *Boundary element methods in solid mechanics,* 1st ed. George Allen & Unwin . London, 322p.

Deere, D.U. (1964) *Technical description of rock cores for engineer-purpose.* Rock Mechanics and Engineering Geology. Vol. 1, Number 1, p 17-22

Desai C. S. (1977) *Numerical Methods in Geotechnical Engineering,* McGraw-Hill, New York, 783 p.

Esterhuizen G.S. (1993) *Variability considerations in hard rock pillar design,* Proceedings of the symposium Rustenburg 4-5 March 1993, SANGORM, Johannesbourg, pp 48 - 54.

ETI U.S.,Inc. (1983) *Kamoto – Mine Stability analysis plateure,* Technical report No.93, Part 1 Tucson, Az , 80 p.

ETI U.S.,Inc. (1987) *Standardization of Geostructural Evaluation of Kamoto - Plateure,* Technical report No.47 , Tucson , Az , 81 p.

Evans, I., Pomeroy, C.D. (1958) The strength of cubes of coal in uniaxial compression, in Mechanical Properties of Non-metallic and Brittle materials, W.H. Walton, London, Butterworths, p5-28.

Evans, I., Pomeroy, C. D. and Berenbaum, R , (1961) *The compressive strength of coal.* Colliery Engineering, Vol.38, pp 126-128.

Fairhurst, C. (1967) *Failure and breakage of rock,* proceedings of the 8th Symposium on Rock Mechanics, AIME, New York, 377 p.

Francois, A. P. (1973) *L'extremité occidentalee de l'Arc cuprifère shabien.* Bureau d'etudes geologiques, Gecamines , 65p.

Gash Peter J.S. (1986) *Geotechnical evaluation for open-pit planning.* The Planning and Operation of Open-Pit and Strip Mines. ed. Deetlefs. J.P. Johannesburg. SAIMM. pp. 23-36.

Geomines, Inc. (1984) *Kamoto plateure / Backfilling and pillar recovery Part 2,* Technical Report No.135, Tucson, AZ, 1984, 96 p.

Geomines, Inc. (1984) *Kamoto plateure / Classification of cracks,* Technical Report No. 124, Tucson, Arizona, 26p.

Griffith, A., (1924) *Theory of rupture,* Proc.First International Congr. Applied Mechnics, J. Waltman, Jr. Press, Delft, pp. 53-66.

Hardy, M.P. and Agapito, J. (1977) *Pillar Design in Underground Oil shale Mines,* Proceedings 16th US Rock Mechanics Sympos, University of Minnesota, Minneapolis, pp.257-266.

Hedley, D.G.F and Grant, F. (1972) *Stope and pillar design for Elliot Lake uranium mines,* CIM Bulletin, July 1972. Vol. 65, pp.37-44.

Herget G. (1988) *Stresses in rock,* A. A. Balkema, Rotterdam, 179 p.

Hoek, E. (1968) *Brittle fracture of rock,* Rock Mechanics in Engineering Practice, John Wiley and Sons, London, pp. 93-124.

Hoek, E. and Brown, E.T. (1980a) *Empirical strength criterion for rock masses, Journal of Geotechnical Engineering,* ASCE, Vol.106, No. GT9, Sept.1980, pp.1013 – 1035.

Hoek, E. and Brown, E.T. (1980b) *Underground Excavations in Rock.* Institution of Mining and Metallurgy. London, 527 p.

Hoek, E. and Brown, E.T. (1988) *The Hoek-Brown failure criterion – a 1988 update. In Rock engineering for underground excavations*, Proceedings 15th Canadian Rock Mech. Symposium, J.C Curran, pp31-38.

Hoek, E., Wood, D. and Shah, S. (1992) *A modified Hoek – Brown criterion for rock masses.* Proc. Rock characterization Symposium, Int. Soc. Rock Mech. London: Brit. Geol. Soc., p 209 – 214.

Hoek E., Kaiser P.K. and Brawden W.F. (1995) *Support of Underground Excavations in Hard Rock.* A.A Balkema Rotterdam, pp 20-98

Holland, C.T. (1962) *Design of pillars for overburden support* Mining Congress Journal, Part 1 March 1962, pp24 –32.

Hustrulid, W. A and Swanson, S.R. (1981) *Field verification of coal pillars strength prediction formulas*, Final report to U.S Bureau of Mines, April 1981.

Jaeger, J.C. and Cook, N.G.W. (1979) *Fundamentals of Rock Mechanics*, 3th ed. Chapman and Hall. London, 593 p.

Jeremic M.L. (1987) *Ground Mechanics in Hard Rock Mining*, A.A Balkema, Rotterdam, 533 p.

Laubscher, D.H. (1990) *A geomechanics classification system for the rating of rock mass in mine design*, Journal of the S.A. Inst. of Mining and Metallurgy, vol. 90, no. 10. South Africa, Oct.1990, pp.257-273.

Laubscher, D.H. (1977) *Geomechanics classification of jointed rock masses – mining applications.* Trans. Inst. Min. Metall. 86, A1-8.

Murrell, S. A. F. (1965) *The effect of triaxial stress systems on the strength of rocks at atmospheric temperatures*, Geophys. J., 10, 231-81.

Obert, L. and Duvall, W.I. (1967) *Rock Mechanics and the Design of structures in rocks*, John Wiley & sons, New York, pp.542-545.

Oravecz, K. (1977) *Analogue modelling of stresses and displacements in bord and pillar workings in coal mines.* International Journal of Rock Mechanics and Mining Sciences, Vol.14, No.1, pp. 7-23.

Ozbay M. U. (1987) *Design considerations for Mining of hard-rock tabular deposits situated at moderate depths*, PhD Thesis, Johannesburg, 203 p.

Ozbay, M.U. et al. (1994) *A literature and mine survey on the design of pillar systems in tabular hard rock mines*, Project report for SIMRAC project GAP 027/026, Johannesburg.

Palmström A. (1997), *Collection and use of geological data in Rock Engineering*, News Journal, International Society for Rock Mechanics, Vol. 4, No 2, pp 21-25.

Potvin Y., Hudyma M. and Miller H.D.S. (1989), *Rib pillar design in open mining*, CIM Bulletin, July 1989, pp 31-36.

Priest, S.D. and Brown, E.T. (1983). *Probabilistic stability analysis of variable rock slopes.* Trans. Inst. Min. Metall. 92. Jan.1983, A1-A12

Protodiakonov, M.N. (1964). *Methods for evaluation of cracks and strength of rock systems in depth*, 4th Int. Conf. Strata Control and Rock Mechs., Henry Crumb School of Mines, Columbia University, New York, Addendum.

Robert M.K.C. and Jager A. J. (1993) *Pillars as stope support in shallow mining of tabular deposits – a review,* Proceedings of the symposium Rustenburg 4-5 March 1993, SANGORM, Johannesbourg, pp 76 - 84.

Ryder J. A. and Ozbay M.U. (1990) *A methodology for designing pillar layout for shallow mining,* Proc. Static and dynamic considerations in rock engineering, Brummer (ed.) Balkema, pp 273-286.

Salamon, M.D.G. (1964) *Elastic analysis of displacements and stresses induced by the mining of seam or reef deposits.* Journal of the S.A. Inst. of Mining and Metallurgy, Vol.65, pp.319-338.

Salamon M.D.G. and Munro, A.H. (1967) *A study of the strength of coal pillars,* Journal of the S.A. Inst. of Mining and Metallurgy, Johannesburg, Vol. 68. 55-67.

Salamon, M.D. G. (1967) *A method of designing bord and pillar workings.* Journal of the S.A. Inst. of Mining and Metallurgy, 68. pp 68 - 78.

Salamon M.D.G. and Oravecz K.I. (1976) *Rock Mechanics in coal mining.* Chamber of Mines of S.A. Johannesburg, 119p.

Salamon M.D.G. (1983) *The role of Pillars in Mining,* SAIMM, Monograph series No 3, p.173 - 200.

SANGORM, (1993) *Rock-engineering problems related to hard rock mining at shallow intermediate depth,* Proceedings of the symposium Rustenburg 4-5 March 1993, SANGORM, Johannesbourg, 103p.

Stacey, T.R. and Jongh C.L. (1977). *Stress fracturing around a deep-level cored tunnel.* Journal of the S.A. Inst. of Mining and Metallurgy, December, pp124-234.

Starfield A. M. and Cundall P. A.(1988) *Towards a Methodology for Rock Mechanics Modelling.* International Journal of Rock Mechanics and Mining Sciences, Vol.25, No.3, pp. 99-106.

The University of Witwatersrand, Mining Department, *Rock Mechanics Post-graduate Courses,* 1996-1997.

Wagner H. (1980) *Pillar design in coal mines,* Journal of S.A. Inst. of Mining and Metallurgy, Vol.79, pp 83-90.

Wagner H. (1992) *Some Rock – mechanics Aspects of Massive –mining Methods at depth,* MASSMIN 92, Johannesburg, Journal of the S.A. Inst. of Mining and Metallurgy, pp 49-54.

APPENDICES

Appendix A

Appendix A1 Production by mining method

	PRODUCTION BY MINING METHOD			METHOD (Ktn)	
YEARS	SLC	CAF	RAP	OTHER	TOTAL
1970	170,4	25,6	0	0	196
1971	351,2	523,6	0	0	874,8
1972	653	973,6	0	0	1626,6
1973	863,9	1288	0	0	2151,9
1974	850,5	1690,9	0	0	2541,4
1975	1149,3	1451,2	0	0	2600,5
1976	1462,1	1327,1	0	0	2789,2
1977	1388,3	1351,3	0	99,1	2838,7
1978	1519,1	1179	29,8	65,2	2793,1
1979	1434,5	1438,3	111,5	71,8	3056,1
1980	1316,5	1230,4	169,6	333,5	3050
1981	1581 5	692,2	384,7	56,3	2714,7
1982	1379	532,1	794,4	21,6	2727,1
1983	1385,1	336,3	1115,8	11,9	2849,1
1984	1035,4	158	1693,4	0	2886,8
1985	576	333,7	2213,2	14,5	3137,4
1986	558,3	308	2341,2	0,5	3208
1987	425,2	264,9	2597,5	0	3287,6
1988	481,4	294,8	2361,5	5,6	3143,3
1989	603	159,1	2526,3	1,3	3289,7
1990	432,2	295,7	1838,8	64,4	2631,1
1991	417	309,1	68,1	3,5	797,7
1992	336,6	406,1	325,4	0	1068,1
1993	132,7	231	65,2	58,2	487,1
1994	97,4	175,2	0,7	34,3	307,6

Appendix B

Table B1 Rock Mass Index tables (after Palmström, 1997); ratings of the factors represented in the joint condition factor (JC)

Ratings of the joint roughness factor (jR)[*]

Small scale *smoothness of* joint surface	Large scale waviness of joint plane				
	Planar	Slightly undulating	Strongly undulating	Stepped	Interlocking (large scale)
Very rough	3	4	6	7.5	9
Rough	2	3	4	5	6
Slightly rough	1.5	2	3	4	4.5
Smooth	1	1.5	2	2.5	3
Polished	0.75	1	1.5	2	2.5
Slickensided	0.6 - 1.5	1 - 2	1.5 - 3	2 - 4	2.5 - 5

*) For filled joints $jR = 1$

Ratings of the joint alteration factor (jA)

1. CONTACT BETWEEN THE TWO JOINT WALLS		
Joint wall character	Description	Rating of jA
CLEAN JOINTS:		
Healed or welded joints	Non-softening, impermeable filling (quartz, epidote, etc.)	0.75
Fresh joint walls	No coating or filling in joint, except from staining (rust)	1
Altered joint walls:		
1 grade higher	One grade higher alteration of wall rock than else	2
2 grades higher	Two grades higher alteration of wall rock than else	4
COATING OR THIN FILLING OF:		
Friction materials	Material of sand, silt calcite, etc. without content of clay	3
Cohesive materials	Material of clay, chlorite, talc, etc.	4

2. FILLED JOINTS WITH PARTLY OR NO JOINT WALL CONTACT		Partly wall contact	No wall contact
Type of joint filling	Description	Thin filling (approx. < 5 mm)	Thick filling or gouge
		Rating of jA	Rating of jA
Friction materials	Sand, silt calcite, etc. without content of clay	4	8
Hard cohesive materials	Compact filling of clay, chlorite, talc, etc.	6	10
Soft cohesive materials	Medium to low overconsolidated clay, chlorite, talc, etc.	8	12
Swelling clay materials	Filling material exhibits swelling properties	8 - 12	12 - 20

Ratings of the joint size and continuity factor (jL)

Joint length	Term	Type	Continuous joints[*]	Discontinuous joints
			Rating of jL	Rating of jL
< 0.5 m	Very short	Bedding or foliation partings	3	6
0.1 - 1 m	Short or small	Joint	2	4
1 - 10 m	Medium	Joint	1	2
10 - 30 m	Long or large	Joint	0.75	1.5
> 30 m	Very long or large	(Filled) joint, seam or shear	0.5	1

*) Discontinuous joints end in massive rock

Table B2 Q-Classification parameters (after Barton *et al.*, 1974)

DESCRIPTION	VALUE	NOTES
1. ROCK QUALITY DESIGNATION	*RQD*	
A. Very poor	0-25	1. Where *RQD* is reported or measured as ≤ 10 (including 0),
B. Poor	25-50	a nominal value of 10 is used to evaluate *Q*.
C. Fair	50-75	
D. Good	75-90	2. RQD intervals of 5, i.e. 100, 95, 90 etc. are sufficiently
E. Excellent	90-100	accurate.
2. JOINT SET NUMBER	J_n	
A. Massive, no or few joints	0.5-1.0	
B. One joint set	2	
C. One joint set plus random	3	
D. Two joint sets	4	
E. Two joint sets plus random	6	
F. Three joint sets	9	1. For intersections use $(3.0 \times J_n)$.
G. Three joint sets plus random	12	
H. Four or more joint sets, random,	15	2. For portals use $(2.0 \times J_n)$.
heavily jointed, 'sugar cube', etc.		
J. Crushed rock, earthlike	20	
3. JOINT ROUGHNESS NUMBER	J_r	
a. Rock wall contact		
b. Rock wall contact before 10 cm shear		
A. Discontinuous joints	4	
B. Rough and irregular, undulating	3	
C. Smooth undulating	2	
D. Slickensided undulating	1.5	1. Add 1.0 if the mean spacing of the relevant joint set is
E. Rough or irregular, planar	1.5	greater than 3 m.
F. Smooth, planar	1.0	
G. Slickensided, planar	0.5	2. $J_r = 0.5$ can be used for planar, slickensided joints having
c. No rock wall contact when sheared		lineations, provided that the lineations are oriented for
H. Zones containing clay minerals thick	1.0	minimum strength.
enough to prevent rock wall contact	(nominal)	
J. Sandy, gravely or crushed zone thick	1.0	
enough to prevent rock wall contact	(nominal)	
4. JOINT ALTERATION NUMBER	J_a	ϕr degrees (approx.)
a. Rock wall contact		
A. Tightly healed, hard, non-softening,	0.75	1. Values of ϕr, the residual friction angle,
impermeable filling		are intended as an approximate guide
B. Unaltered joint walls, surface staining only	1.0	25-35 to the mineralogical properties of the
C. Slightly altered joint walls, non-softening	2.0	25-30 alteration products, if present.
mineral coatings, sandy particles, clay-free		
disintegrated rock, etc.		
D. Silty-, or sandy-clay coatings, small clay-	3.0	20-25
fraction (non-softening)		
E. Softening or low-friction clay mineral coatings,	4.0	8-16
i.e. kaolinite, mica. Also chlorite, talc,		
gypsum and graphite etc., and small		
quantities of swelling clays. (Discontinuous		
coatings, 1-2 mm or less in thickness)		

Table B2 : (continued)

DESCRIPTION	VALUE	NOTES	
4, JOINT ALTERATION NUMBER	J_a	ϕr degrees (approx.,	
b. Rock wall contact before 10 cm shear			
F. Sandy particles, clay-free, disintegrating rock etc.	4.0	25-30	
G. Strongly over-consolidated, non-softening clay mineral fillings (continuous < 5 mm thick)	6.0	16-24	
H. Medium or low over-consolidation, softening clay mineral fillings (continuous < 5 mm thick)	8.0	12-16	
J. Swelling clay fillings i.e. montmorillonite, (continuous < 5 mm thick). Values of J_a depend on percent of swelling clay-size particles, and access to water,	8.0-12.0	6-12	
c. No rock wall contact when sheared			
K. Zones or bands of disintegrated or crushed	6.0		
L. rock and clay (see G, H and J for clay	8.0		
M. conditions)	8.0-12.0	6-24	
N. Zones or bands of silty- or sandy-clay, small clay fraction, non-softening	5.0		
O. Thick continuous zones or bands of clay	10.0-13.0		
P. & R. (see G,H and J for clay conditions)	6.0-24.0		
5. JOINT WATER REDUCTION	J_w	approx. water pressure (kgf/cm^2)	
A. Dry excavation or minor inflow i.e. < 5 l/m locally	1.0	< 1.0	
B. Medium inflow or pressure, occasional outwash of joint fillings	0.66	1.0-2.5	
C. Large inflow or high pressure in competent rock with unfilled joints	0.5	2.5-10.0	1. Factors C to F are crude estimates; increase J_w if drainage installed.
D. Large inflow or high pressure	0.33	2.5-10.0	
E. Exceptionally high inflow or pressure at blasting, decaying with time	0.2-0.1	> 10	2. Special problems caused by ice formation are not considered.
F. Exceptionally high inflow or pressure	0.1-0.05	> 10	
6. STRESS REDUCTION FACTOR		*SRF*	
a. Weakness zones intersecting excavation, which may cause loosening of rock mass when tunnel is excavated			
A. Multiple occurrences of weakness zones containing clay or chemically disintegrated rock, very loose surrounding rock any depth)		10.0	1. Reduce these values of *SRF* by 25-50% if the relevant shear zones only influence but do not intersect the excavation
B. Single weakness zones containing clay, or chemically disintegrated rock (excavation depth < 50 m)		5.0	
C. Single weakness zones containing clay, or chemically disintegrated rock (excavation depth > 50 m)		2.5	
D. Multiple shear zones in competent rock (clay free), loose surrounding rock (any depth)		7.5	
E. Single shear zone in competent rock (clay free). (depth of excavation < 50 m)		5.0	
F. Single shear zone in competent rock (clay free). (depth of excavation > 50 m)		2.5	
G. Loose open joints, heavily jointed or 'sugar cube', (any depth)		5.0	

Table B2 : (continued)

DESCRIPTION			VALUE	NOTES
6. STRESS REDUCTION FACTOR			*SRF*	
b. Competent rock, rock stress problems				
	σ_c/σ_1	σ_t/σ_1		2. For strongly anisotropic virgin stress field
H. Low stress, near surface	> 200	> 13	2.5	(if measured): when $5 \leq \sigma_1/\sigma_3 \leq 10$, reduce σ_c
J. Medium stress	200-10	13-0.66	1.0	to $0.8\sigma_c$ and σ_t to $0.8\sigma_t$. When $\sigma_1/\sigma_3 > 10$,
K. High stress, very tight structure	10-5	0.66-0.33	0.5-2	reduce σ_c and σ_t to $0.6\sigma_c$ and $0.6\sigma_t$, where
(usually favourable to stability, may				σ_c = unconfined compressive strength, and
be unfavourable to wall stability)				σ_t = tensile strength (point load) and σ_1 and
L. Mild rockburst (massive rock)	5-2.5	0.33-0.16	5-10	σ_3 are the major and minor principal stresses.
M. Heavy rockburst (massive rock)	< 2.5	< 0.16	10-20	3. Few case records available where depth of
c. Squeezing rock, plastic flow of incompetent rock				crown below surface is less than span width.
under influence of high rock pressure				Suggest *SRF* increase from 2.5 to 5 for such
N. Mild squeezing rock pressure			5-10	cases (see H).
O. Heavy squeezing rock pressure			10-20	
d. Swelling rock, chemical swelling activity depending on presence of water				
P. Mild swelling rock pressure			5-10	
R. Heavy swelling rock pressure			10-15	

ADDITIONAL NOTES ON THE USE OF THESE TABLES

When making estimates of the rock mass Quality (Q), the following guidelines should be followed in addition to the notes listed in the tables:

1. When borehole core is unavailable, *RQD* can be estimated from the number of joints per unit volume, in which the number of joints per metre for each joint set are added. A simple relationship can be used to convert this number to *RQD* for the case of clay free rock masses: $RQD = 115\text{-}3.3\ J_v$ (approx.), where J_v = total number of joints per m^3 ($0 < RQD < 100$ for $35 > J_v > 4.5$).

2. The parameter J_n representing the number of joint sets will often be affected by foliation, schistosity, slaty cleavage or bedding etc. If strongly developed, these parallel 'joints' should obviously be counted as a complete joint set. However, if there are few 'joints' visible, or if only occasional breaks in the core are due to these features, then it will be more appropriate to count them as 'random' joints when evaluating J_n.

3. The parameters J_r and J_a (representing shear strength) should be relevant to the weakest significant joint set or clay filled discontinuity in the given zone. However, if the joint set or discontinuity with the minimum value of J_r/J_a is favourably oriented for stability, then a second, less favourably oriented joint set or discontinuity may sometimes be more significant, and its higher value of J_r/J_a should be used when evaluating Q. The value of J_r/J_a should in fact relate to the surface most likely to allow failure to initiate.

4. When a rock mass contains clay, the factor *SRF* appropriate to loosening loads should be evaluated. In such cases the strength of the intact rock is of little interest. However, when jointing is minimal and clay is completely absent, the strength of the intact rock may become the weakest link, and the stability will then depend on the ratio rock-stress/rock-strength. A strongly anisotropic stress field is unfavourable for stability and is roughly accounted for as in note 2 in the table for stress reduction factor evaluation.

5. The compressive and tensile strengths (σ_c and σ_t) of the intact rock should be evaluated in the saturated condition if this is appropriate to the present and future in situ conditions. A very conservative estimate of the strength should be made for those rocks that deteriorate when exposed to moist or saturated conditions.

Appendix C

Table C1 Rock Mass Rating system (after Bieniawski, 1976)

(a) Classification parameters and their ratings

Parameter		Ranges of values						
1 strength of intact rock material	point-load strength index (MPa)	>8	4–8	2–4	1–2	for this low range, uniaxial compression test is preferred		
	uniaxial compressive strength (MPa)	>200	100–200	50–100	25–50	10–25	3–10	1–3
rating		15	12	7	4	2	1	0
2 drill core quality *RQD* (%)		90–100	75–90	50–75	25–50	<25		
rating		20	17	13	8	3		
3 joint spacing (m)		>3	1–3	0.3–1	0.05–0.3	<0.05		
rating		30	25	20	10	5		
4 *condition of joints*		very rough surfaces, not continuous, no separation, hard joint wall rock	slightly rough surfaces, separation <1 mm, hard joint wall rock	slightly rough surfaces, separation <1 mm, soft joint wall rock	slickensided surfaces or gouge <5 mm thick or joints open 1–5 mm, continuous joints	soft gouge >5 mm thick or joints open >5 mm, continuous joints		
rating		25	20	12	6	0		
5 groundwater	inflow per 10 m tunnel length (l min^{-1})	none		<25	25–125	>125		
	or joint water pressure	0		0.0–0.2	0.2–0.5	>0.5		
	major principal stress or general conditions	completely dry		moist only (interstitial water)	water under moderate pressure	severe water problems		
rating		10		7	4	0		

(b) Rating adjustment for joint orientations

Strike and dip orientations of joints		very favourable	favourable	fair	unfavourable	very unfavourable
Ratings	tunnels	0	−2	−5	−10	−12
	foundations	0	−2	−7	−15	−25
	slopes	0	−5	−25	−50	−60

(c) Rock mass classes determined from total ratings

Ratings	100 – 81	80 – 61	60 – 41	40 – 21	<20
Class no.	I	II	III	IV	V
Description	very good rock	good rock	fair rock	poor rock	very poor rock

(d) Meaning of rock classes

Class no.	I	II	III	IV	V
average stand-up time	10 years for 5 m span	6 months for 4 m span	1 week for 3 m span	5 hours for 1.5 m span	10 minutes for 0.5 m span
cohesion of the rock mass (kPa)	>300	200–300	150–200	100–150	<100
friction angle of the rock mass	>45°	40°–45°	35°–40°	30°–35°	<30°

Appendix D

SPREADSHEETS FOR THE CALCULATION OF HOEK-BROWN AND MOHR-COULOMB PARAMETERS (after Hoek et al., 1995)

Table D1 UPPER DOLOMITE (SS), Dolomitic shales

	GSI = 62		Sigci =149		mi =10			
		Sig3	Sig1	Ds1ds3	Sign	Tau	Signtau	Signsq
mb/mi =	0.26	0.15	19.68	10.82	1.80	5.44	9.77	3.23
mb =	2.57	0.29	21.20	10.17	2.16	5.97	12.91	4.68
s =	0.015	0.58	24.01	9.19	2.88	6.97	20.09	8.31
a =	0.5	1.16	28.95	7.90	4.29	8.77	37.60	18.37
Em=	19953	2.33	37.23	6.49	6.99	11.87	82.93	48.81
		4.66	50.61	5.17	12.10	16.93	204.84	146.40
		9.31	71.74	4.07	21.62	24.84	537.01	467.48
		18.63	105.05	3.22	39.11	36.75	1437.33	1529.54
				Sums =	90.94	117.54	2342.49	2226.81
Phi =	**40.1**							
Coh =	**5.1**							
Sigcm =	**22.0**							

Table D2 LOWER DOLOMITE (SBB), Dolomite shales

	GSI = 62		Sigci = 136		mi = 10			
		Sig3	Sig1	ds1ds3	Sign	Tau	Signtau	Signsq
Mb/mi =	0.26	0.13	17.96	10.82	1.64	4.96	8.14	2.69
mb =	2.57	0.27	19.35	10.17	1.97	5.45	10.76	3.90
s =	0.015	0.53	21.91	9.19	2.63	6.36	16.74	6.92
a =	0.5	1.06	26.42	7.90	3.91	8.01	31.33	15.30
Em =	19953	2.13	33.99	6.49	6.38	10.83	69.09	40.66
		4.25	46.19	5.17	11.04	15.45	170.66	121.97
		8.50	65.48	4.07	19.73	22.67	447.40	389.46
		17.00	95.88	3.22	35.70	33.55	1197.46	1274.29
				Sums =	83.01	107.28	1951.57	1855.19
Phi =	40.1							
Coh =	4.7							
Sigcm =	20.0							

Table D3 MASSIVE DOLOSTONE (RSC) Dolostone

	GSI = 167		Sigci = 180		Mi = 15			
		Sig3	Sig1	Ds1ds3	Sign	Tau	Signtau	Signsq
Mb/mi =	0.31	0.18	31.39	14.31	2.21	7.71	17.08	4.90
mb =	4.62	0.35	33.82	13.41	2.67	8.51	22.74	7.15
s =	0.026	0.70	38.28	12.05	3.58	10.00	35.80	12.83
a =	0.5	1.41	46.09	10.30	5.36	12.69	68.05	28.75
Em =	26607	2.81	59.07	8.38	8.81	17.36	152.88	77.57
		5.63	79.80	6.60	15.38	25.07	385.70	236.66
		11.25	112.12	5.12	27.74	37.30	1034.57	769.34
		22.50	162.22	3.97	50.59	56.00	2833.37	2559.84
				Sums =	116.36	174.64	4550.21	3697.04
Phi =	**45.1**							
Coh =	**7.2**							
Sigcm =	**35.1**							

Table D4 SILICEOUS LAMINATED DOLOSTONE (RSF)

	GSI = 67		Sigci = 148		mi = 9			
		Sig3	Sig1	Ds1ds3	Sign	Tau	Signtau	Signsq
mb/mi =	0.31	0.14	25.03	9.24	2.58	7.39	19.03	6.63
mb =	2.77	0.29	26.33	8.87	2.93	7.86	23.02	8.58
s =	0.026	0.58	28.81	8.26	3.63	8.76	31.77	13.15
a =	0.5	1.16	33.31	7.37	5.00	10.43	52.09	24.96
Em =	26607	2.31	41.14	6.28	7.65	13.37	102.24	58.49
		4.63	54.18	5.14	12.70	18.30	232.47	161.32
		9.25	75.21	4.11	22.17	26.18	580.25	491.37
		18.50	108.74	3.27	39.63	38.21	1514.20	1570.31
				Sums =	96.27	130.49	2555.06	2334.81
Phi =	39.9							
Coh =	6.2							
Sigcm =	26.7							

Table D5 STRATIFIED DOLOMITE (D. Strat.)

	GSI =	70	Sigci =	207	mi =	9		
		Sig3	Sig1	Ds1ds3	Sign	Tau	Signtau	Signsq
Mb/mi =	0.34	0.20	40.92	8.84	4.34	12.30	53.41	18.85
mb =	3.08	0.40	42.67	8.55	4.83	12.94	62.53	23.34
s =	0.036	0.81	46.03	8.06	5.80	14.17	82.22	33.66
a =	0.5	1.62	52.22	7.31	7.71	16.47	126.96	59.44
Em =	31623	3.23	63.17	6.32	11.42	20.58	235.01	130.39
		6.47	81.68	5.24	18.52	27.59	510.81	342.88
		12.94	111.85	4.23	31.67	38.91	1239.96	1015.48
		25.88	160.19	3.38	56.57	56.40	3190.47	3200.34
				Sums =	141.06	199.36	5501.38	4824.38
Phi =	**40.4**							
Coh =	**9.9**							
Sigcm =	**43.0**							

Table D6 GREY RAT, Argillaceous rock

	GSI = 62		Sigci = 78		mi = 10			
		Sig3	Sig1	Ds1ds3	Sign	Tau	Signtau	Signsq
mb/mi =	0.26	0.08	10.30	10.82	0.94	2.85	2.68	0.89
mb =	2.57	0.15	11.10	10.17	1.13	3.12	3.54	1.28
s =	0.015	0.30	12.57	9.19	1.51	3.65	5.51	2.28
a =	0.5	0.61	15.15	7.90	2.24	4.59	10.30	5.03
Em =	19953	1.22	19.49	6.49	3.66	6.21	22.73	13.38
		2.44	26.49	5.17	6.33	8.86	56.14	40.12
		4.88	37.55	4.07	11.32	13.00	147.16	128.11
		9.75	54.99	3.22	20.47	19.24	393.89	419.16
				Sums =	47.61	61.53	641.94	610.24
Phi =	40.1							
Coh =	2.7							
Sigcm =	11.5							

Table D7 BREACH RAT

	GSI = 62		Sigci = 81		mi = 10			
		Sig3	Sig1	Ds1ds3	Sign	Tau	Signtau	Signsq
mb/mi =	0.26	0.08	10.70	10.82	0.98	2.95	2.89	0.96
mb =	2.57	0.16	11.53	10.17	1.18	3.25	3.82	1.38
s =	0.015	0.32	13.05	9.19	1.57	3.79	5.94	2.45
a =	0.5	0.63	15.74	7.90	2.33	4.77	11.11	5.43
Em =	19953	1.27	20.24	6.49	3.80	6.45	24.51	14.42
		2.53	27.51	5.17	6.58	9.20	60.54	43.27
		5.06	39.00	4.07	11.75	13.50	158.70	138.15
		10.13	57.11	3.22	21.26	19.98	424.77	452.02
				Sums =	49.44	63.90	692.27	658.08
phi =	**40.1**							
Coh =	**2.8**							
Sigcm =	**11.9**							

Table D8 RED RAT, Dolomitic siltstones and sandstones

	GSI = 57		Sigci = 70		mi = 1[illegible]			
		Sig3	Sig1	Ds1ds3	Sign	Tau	Signtau	Signsq
mb/mi =	0.22	0.07	7.39	13.35	0.58	1.86	1.08	0.33
mb =	2.58	0.14	8.26	12.13	0.76	2.15	1.63	0.57
s =	0.008	0.27	9.80	10.50	1.10	2.68	2.96	1.21
a =	0.5	0.55	12.38	8.64	1.78	3.61	6.41	3.15
Em =	14962	1.09	16.55	6.85	3.06	5.16	15.79	9.39
		2.19	23.09	5.33	5.49	7.62	41.87	30.15
		4.38	33.23	4.13	9.99	11.43	114.20	99.90
		8.75	49.05	3.24	18.24	17.10	311.99	332.86
				Sums =	41.00	51.62	495.93	477.56
phi =	40.9							
coh =	2.0							
Sigcm =	8.8							

Appendix E

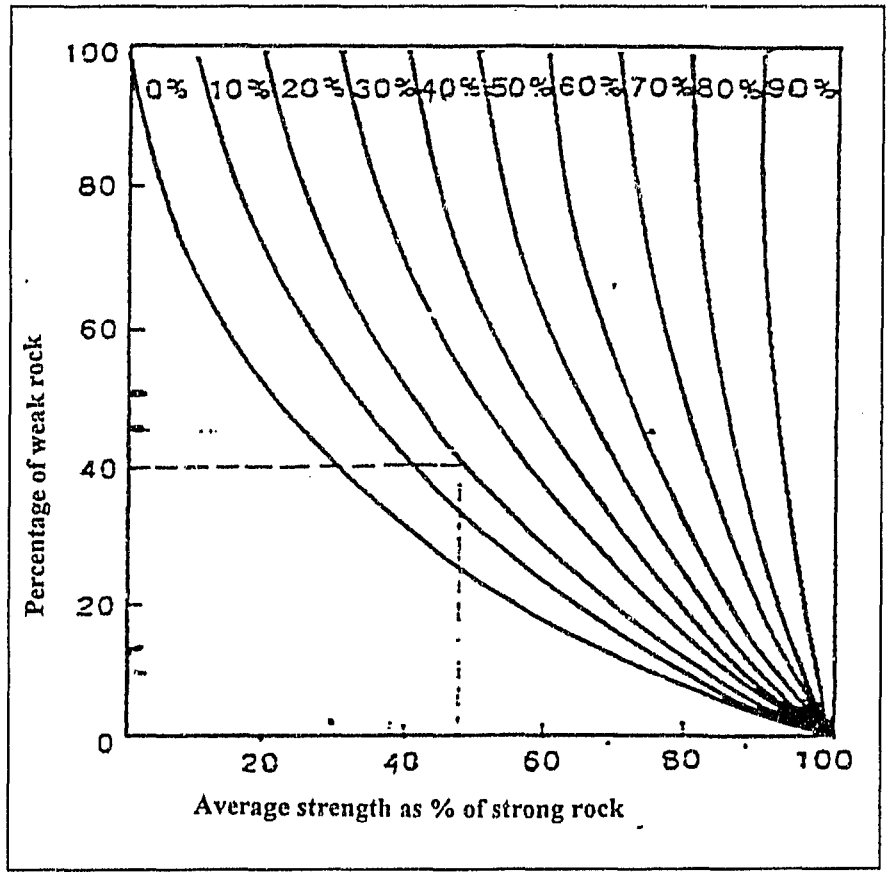

Fig. E1 Laubscher's monogram (Effect of weak rock layers on the strength of a stratified rockmass)

Appendix F

A sample of MinsimW results

Fig. F1 Fine sheet 1 on the upper ore body showing vertical stress (TZZH) in Mpa around unmined (pillar) ground

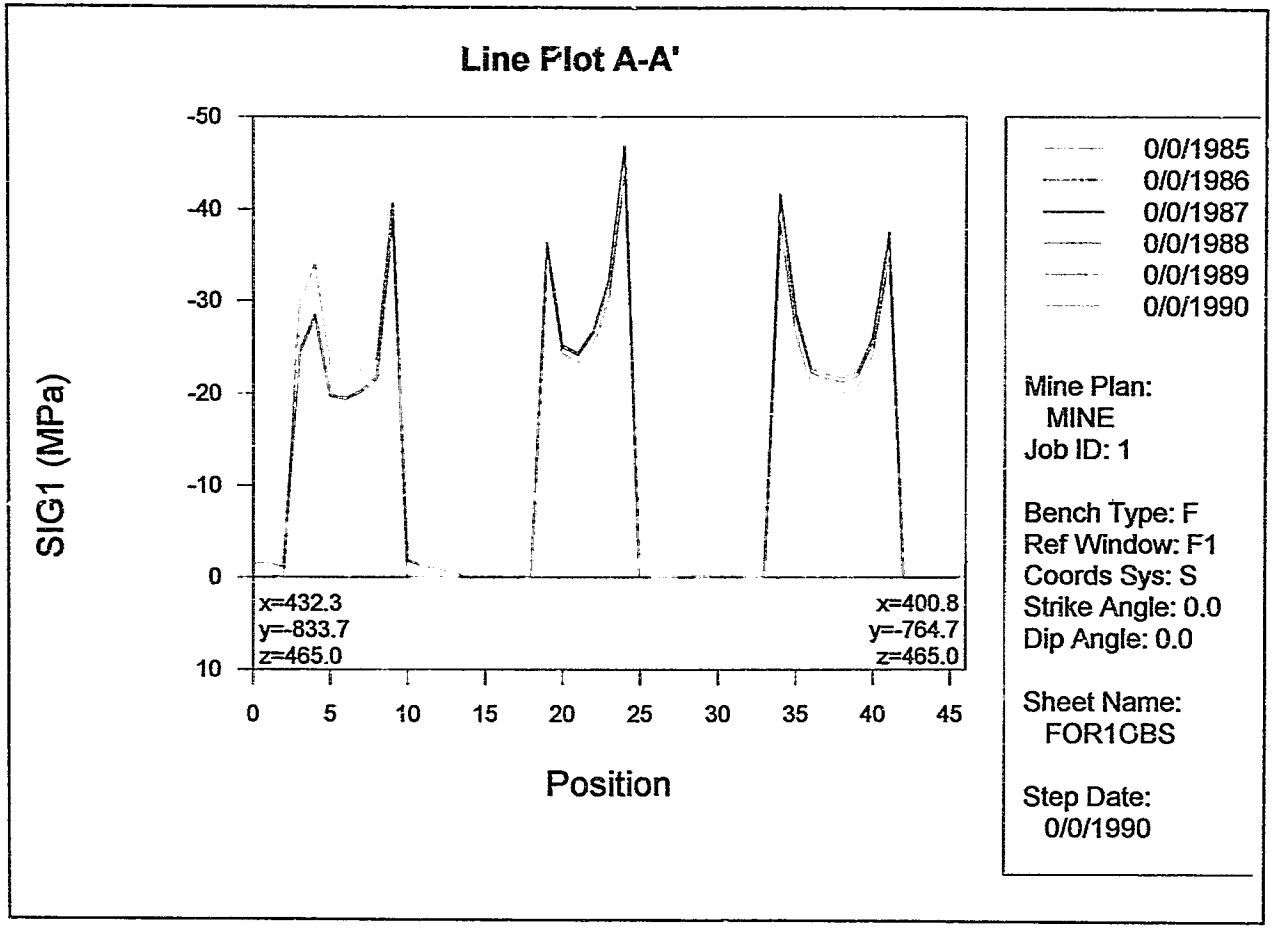

Fig. F2 Major principal stress (SIG 1) line plot in the upper ore body pillars

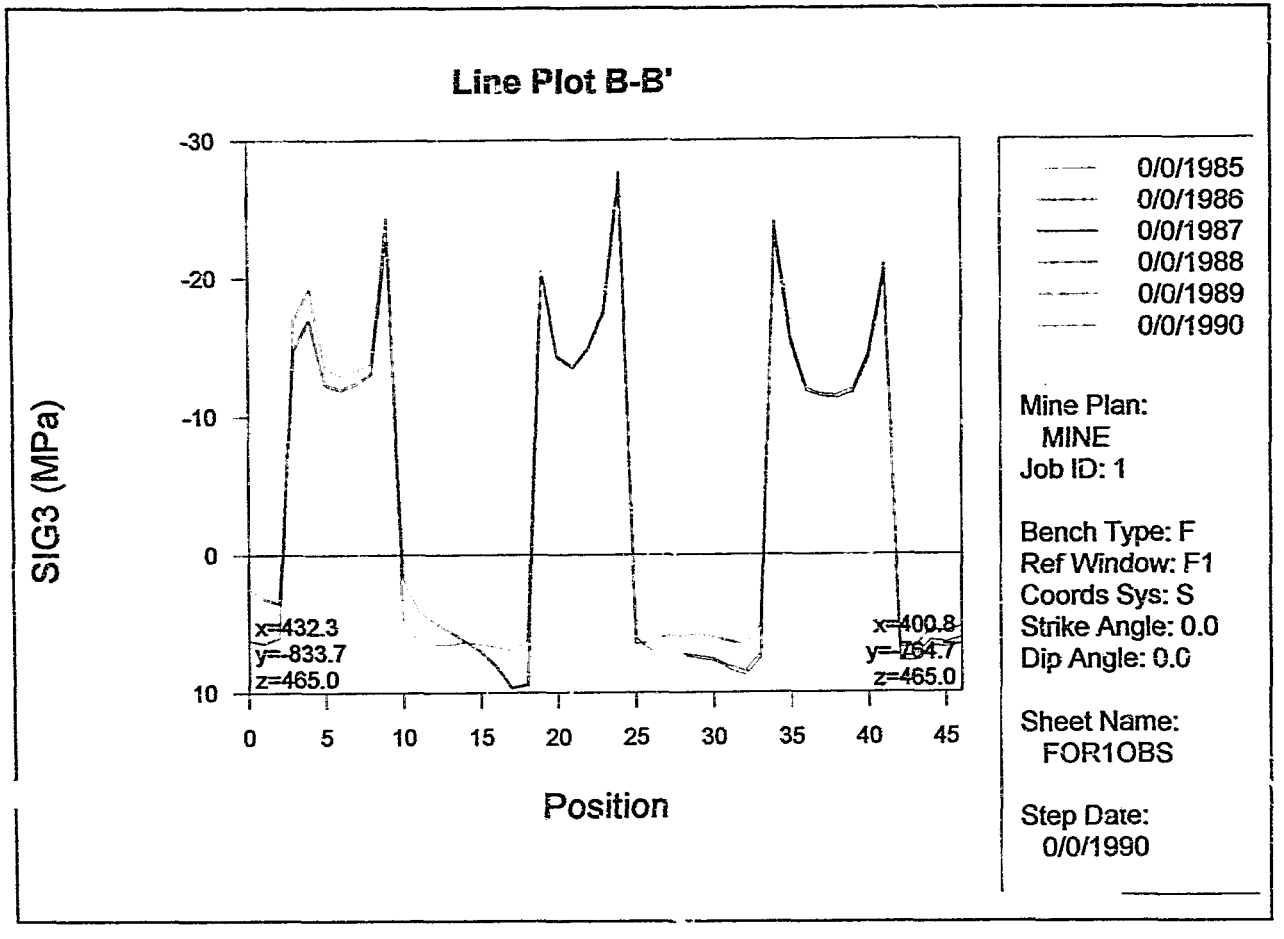

Fig. F3 Minor principal stress (SIG 3) contour plot in the upper ore body pillars

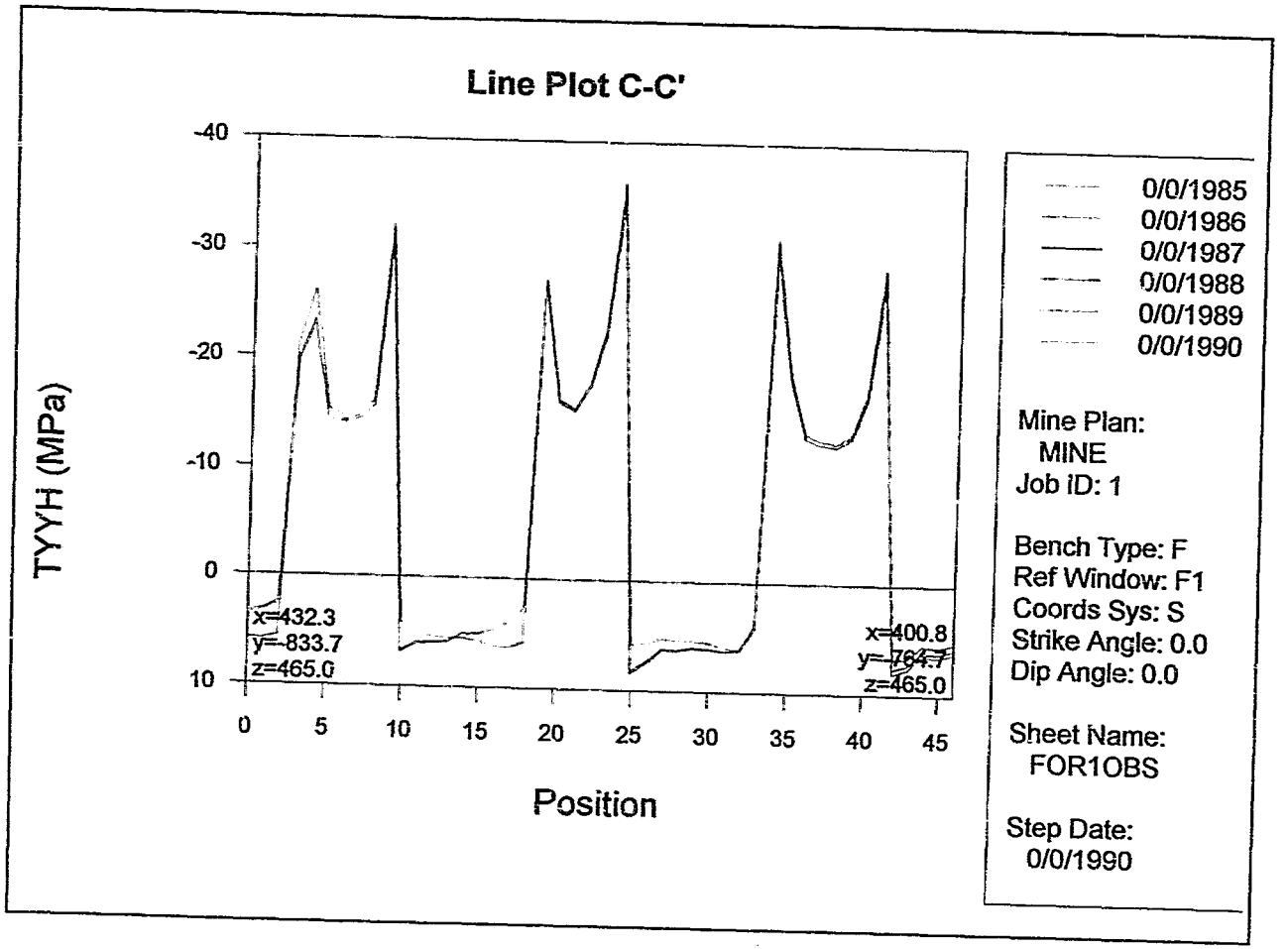

Fig. F4 Dip stress (TYYH) line plot in the upper ore body pillars

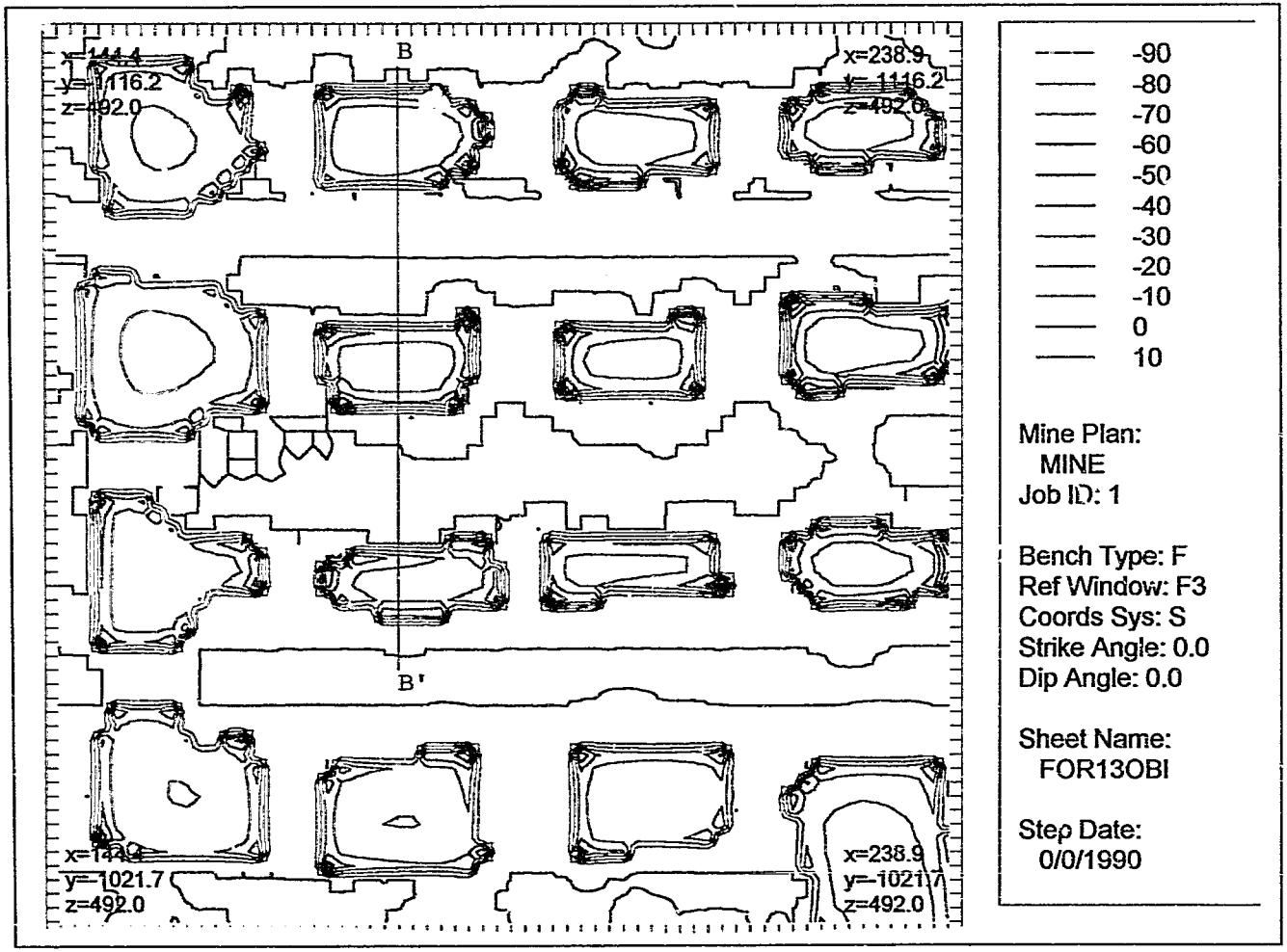

Fig. F5 Fine sheet 13 on the lower ore body / Contour Major principal stress (SIG1)

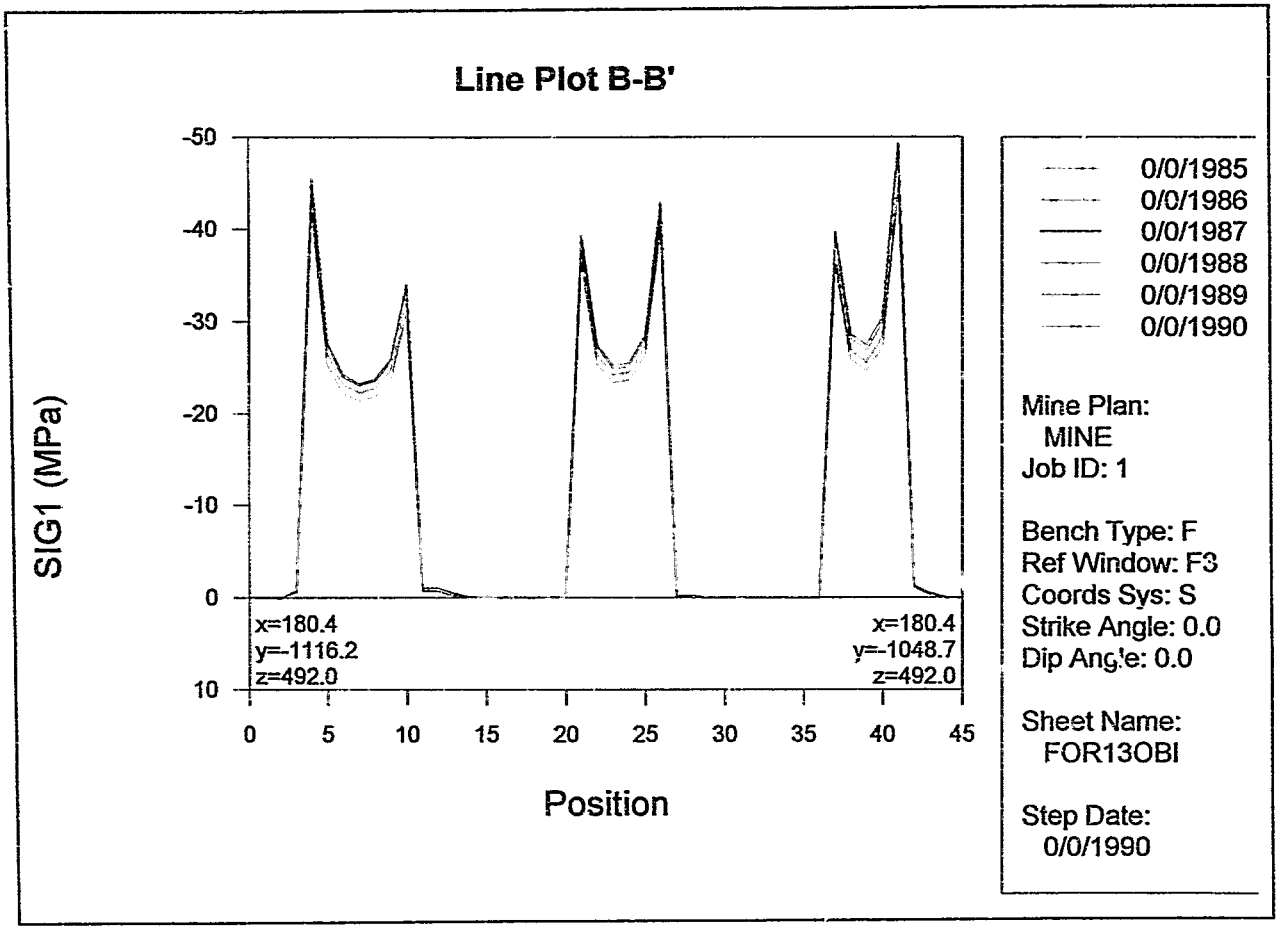

Fig. F6 Major principal (SIG1) line plot on the lower ore body pillars

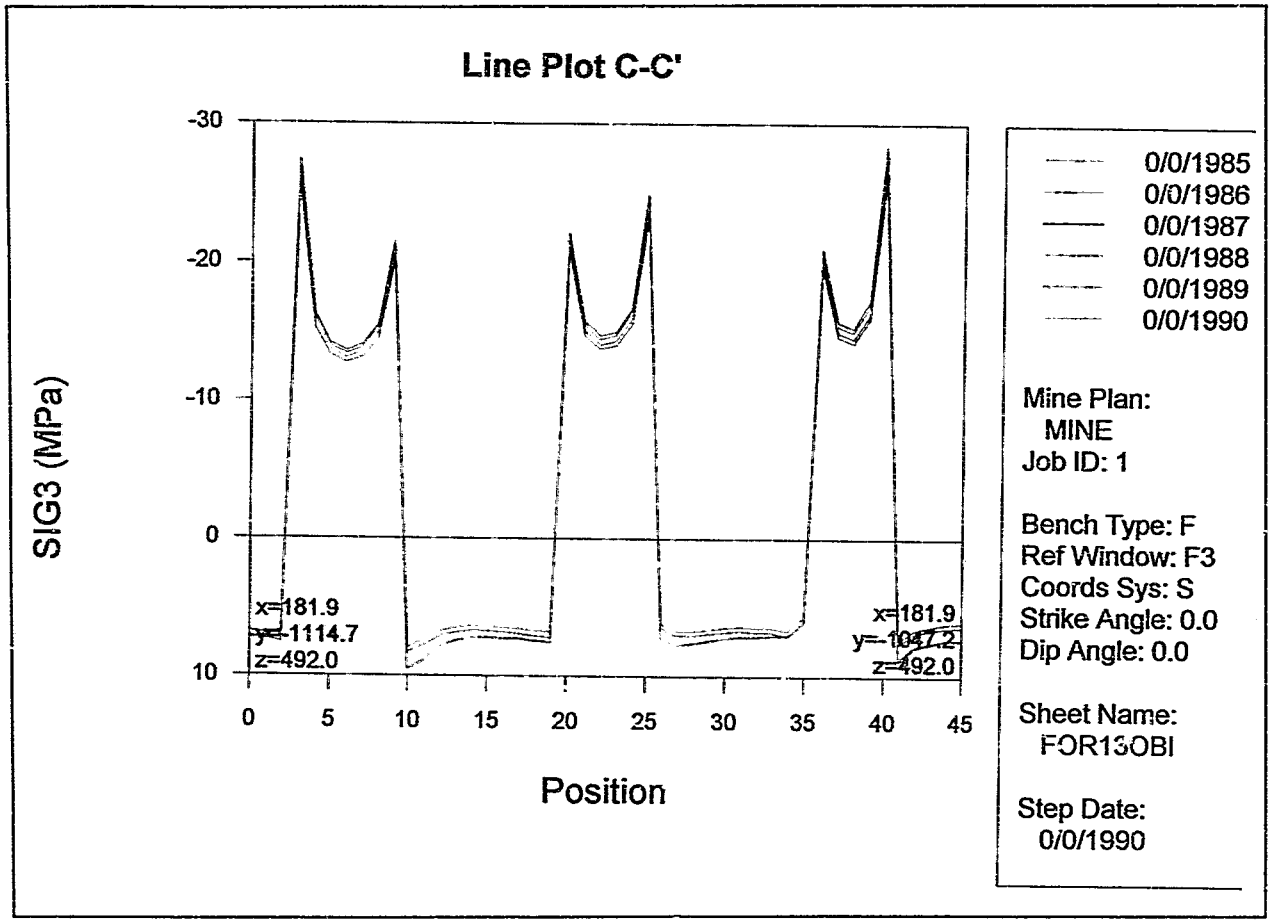

Fig. F7 Minor principal (SIG3) line plot in the lower ore body pillars

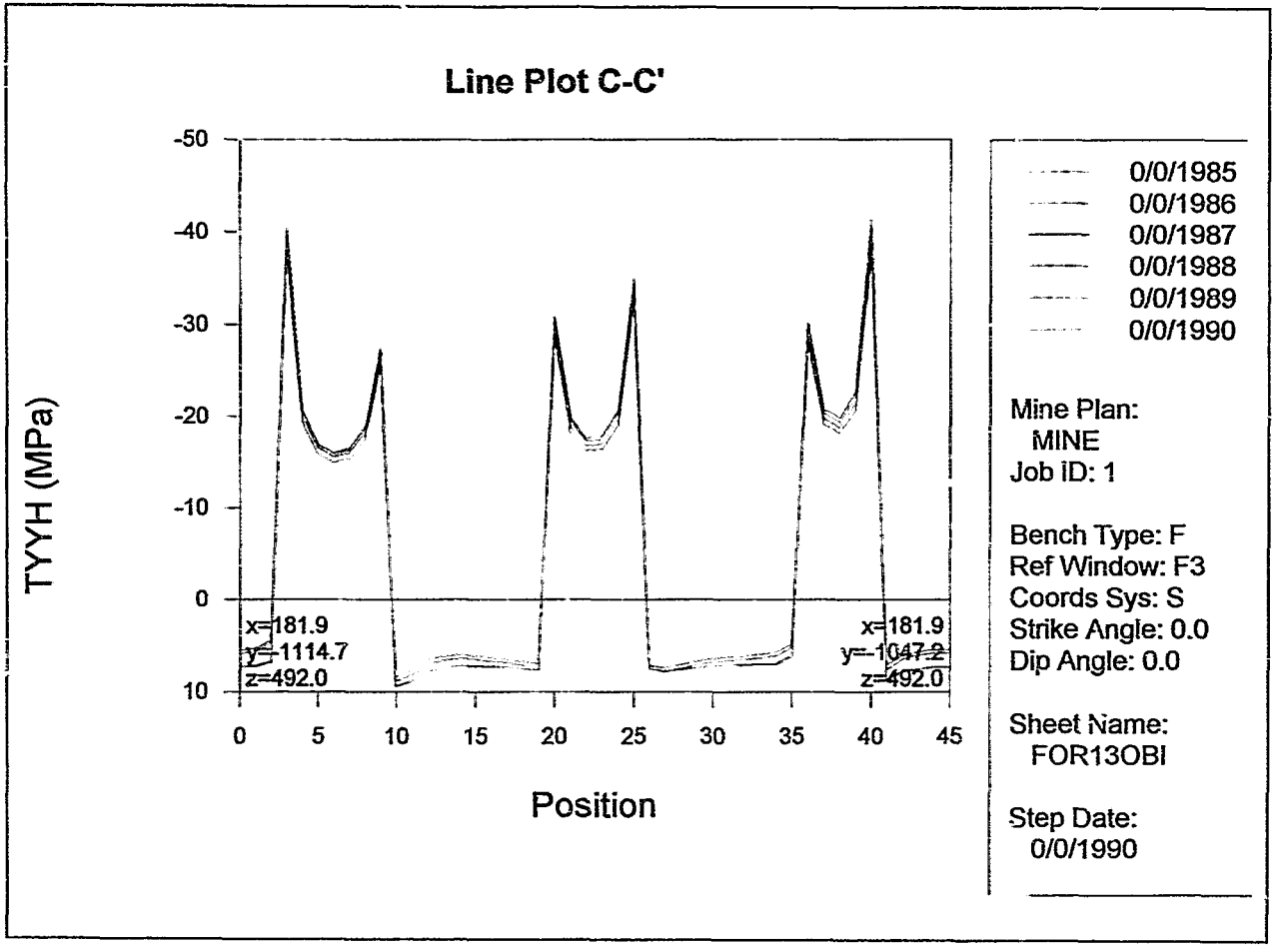

Fig. F8 Dip stress (TYYH) line plot in the lower ore body pillars